AN ABSTRACT OF THE THESIS OF

Joseph Reed Glasmann for the degree of Doctor of Philosophy

in Soil Science presented on January 28, 1982.

Title: Soil Solution Chemistry, Profile Development, and Mineral Authigenesis in Several Western Oregon Soils.

Abstract approved: Redacted for Privacy

Dr. Gerald H. Simonson

Clay mineral genesis was studied in soils representative of several different geomorphic surfaces in western Oregon, ranging in age from Pliocene-early Pleistocene to late Pleistocene. Soil solution studies, clay mineralogy, and soil micromorphology were employed to provide evidence of clay mineral synthesis and interpret soil genesis.

Soils at each study area were characterized by distinct differences in soil solution chemistry, clay mineralogy, plasmic fabric, and genetic history, although parent material compositions between sites were often similar. Soil solution studies suggested that clay mineral synthesis from solution does not occur in soils representing the oldest geomorphic surface. The oxic soil properties at this location were developed during a prior weathering cycle and the soils are at a genetic endpoint in the present environment.

Soil solutions from Ultisols on remnants of Pleistocene surfaces in the Oregon Coast Range were in equilibrium with respect to kaolinite in the solum, but stable with respect to Mg-montmorillonite in the zone characterizing active bedrock weathering. Micromorphological, clay mineralogical, and chemical evidence suggested that alteration of Mg-chlorite in sedimentary rocks leads to smectite genesis in the Cr

horizon of the Ultisols, followed by conversion of smectite to halloysite and chloritic intergrade in the solum. Alteration of basalt in these soils also leads to the formation of smectite, which is unstable with respect to halloysite in well-drained microenvironments within soil profiles.

Soil solutions from soils characteristic of silt-mantled late Pleistocene surfaces on the western margins of the Willamette Valley showed compositional variation from pedon to pedon and horizon to horizon within individual pedons, reflecting the influence of soil parent material compositional variation. Soil solutions were generally in equilibrium with respect to kaolinite, although solutions from horizons developed in tuffaceous sediments were in equilibrium with Mg-montmorillonite. Both kaolinite and smectite were observed as products of mineral authigenesis in these soils. Authigenic clay showed delicate honeycomb or hexagonal morphology in contrast to the parallel oriented appearance of illuvial clays.

Andesite alteration in wet, unstable soils of Oregon's western Cascades also resulted in the formation of smectite. The sequence of mineral alteration in andesites is similar to that described for basalts; however, the final products of mineral authigenesis are distinctly microenvironment dependent. Morphologic evidence suggests that chemical properties of bulk soil solutions can not always be considered to represent the solution conditions at the site of mineral authigenesis. In the absence of reliable <u>in situ</u> micro-chemical analytical techniques, detailed micromorphological studies can aid in interpreting soil micro-chemical properties at weathering surfaces by revealing the identity of neoformed secondary phases.

Soil Solution Chemistry, Profile Development, and Mineral Authigenesis in Several Western Oregon Soils

by

Joseph Reed Glasmann

A THESIS

submitted to

Oregon State University

in partial fulfillment of
the requirements for the
degree of

Doctor of Philosophy

Completed January 28, 1982

Commencement June 1982

APPROVED:

Redacted for Privacy

Professor of Soil Science in charge of major

Redacted for Privacy

Head of Department of Soil Science

Redacted for Privacy

Dean of Graduate School

Date thesis is presented January 28, 1982

Typed by Sally Quinn for Joseph Reed Glasmann

ACKNOWLEDGEMENTS

I greatfully acknowledge the support I have received from the Oregon Agricultural Experiment Station. Electron microscope time, which quickly passes by, does not come cheap, and the many detailed micrographs presented in this study came at considerable expense.

I would also like to express thanks to the following individuals:

Dr. G. H. Simonson for his friendship, encouragement, and "loose rein" philosophy, which occasionally allowed me to get in over my head, leading to helpful bail-out bull sessions; Dr. J. Baham for helpful insights into solution chemical problems; Dr. Kermit Cromack for leading me to Woods Creek watershed and encouraging SEM study of whole soil samples; Dr. Ed Taylor, for accepting me as one of the "guys" during my brief stint as a geology professor.

Special thanks go to Al Soeldner and the O.S.U. Botany Department Electron Microscope Laboratory for providing friendship and excellent technical assistance. Mr. Ruth Lightfoot helped in preparation of many thin sections. Thanks also go to the many students on third floor Ag Hall who occasionally had to live with the smell of resin in the air.

My deepest thanks go to my wife and children. Without their constant love and support, none of this wrok would have been possible. But since it was possible, I'd also like to thank Sally Quinn for typing the manuscripts, as well as those who reviewed initial drafts for publication.

TABLE OF CONTENTS

TABLE OF CONTENTS (Continued)

LIST OF FIGURES

LIST OF TABLES

LIST OF PLATES

LIST OF PLATES (Continued)

LIST OF PLATES (Continued)

SOIL SOLUTION CHEMISTRY, PROFILE DEVELOPMENT, AND MINERAL AUTHIGENESIS IN SEVERAL WESTERN OREGON SOILS

INTRODUCTION

Clay minerals are a ubiquitous feature of most western Oregon soils. Certain clay mineral assemblages in soils can severely affect soil management and land use decisions because of the influence clay minerals have on soil physical and chemical properties. Recently, several studies have demonstrated a relationship between clay mineralogy and landscape stability in western Oregon (Istok, 1981; Taskey, 1978; Paeth, et al., 1971; Youngberg, et al., 1971). Clay mineral assemblages have also been considered for their economic value, as in the ferruginous bauxite deposits in the Salem Hills area (Cocoran and Libbey, 1956). Clayey weathering products strongly affect soil hydrologic properties (Lowrey, 1981) and clayey soil profiles are a major factor in the development of perched water tables in many soils in the Willamette Valley area. Saturated soil conditions strongly affect both the frequency and mangitude of erosive runoff-producing events from cultivated lands (Lowrey, et al., 1981) and can lead to severe public health problems (Hammermeister, 1978; Rahe, 1978). Thus, clay minerals, either directly or indirectly, influence our ability to use and appreciate the earth on which we dwell. A better understanding of the genesis and characteristics of clay minerals in western Oregon soils can only strengthen our ability to manage our soil resources.

Detailed clay mineral genesis studies in Oregon soils are few and have largely been concerned with alteration of pumiceous deposits which blanket large areas of the state (Dudas and Harward, 1975). The large

geographic area mantled by Mazama tephra created an opportunity to study alteration of fairly homogeneous material of known age under a variety of climatic conditions. While the deposition of Mazama tephra has widely influenced Oregon soils, this deposit is but one of many volcanogenic deposits that occur in the state. Volcanic rocks, in all their genetic categories (Fisher, 1966), are the predominant parent materials of many Oregon soils. The process of clay mineral genesis in these often complex volcanogenic parent materials is the subject with which this study is concerned.

The primary objectives of this study were: 1) To characterize authigenic clays is several western Oregon soils; 2) To determine the genesis of clays in these soils; and 3) To relate clay genesis to the conditions of the soil weathering microenvironment. Realizing the first two objectives was greatly aided by detailed micromorphological observations made possible by scanning electron microscopy (SEM). Chapters 2, 3, and 4 report largely observational results of clay genesis during alteration of volcanogenic parent materials under differing geomorphic and environmental conditions. These chapters also allude to the importance of soil chemical microenvironment in determining the course of clay mineral genesis during weathering reactions. Microenvironmental conditions which affect clay genesis are discussed in greater detail in chapter 1, which deals with the problem of relating soil solution chemistry to clay mineral genesis. Chapter 1, hopefully, sets the stage whereupon succeeding chapters may act in providing background information on the nature of soil chemical environments in relation to landscape age and stability, and parent material composition in soils of western Oregon.

The term "microenvironment" is somewhat difficult to precisely define, since "micro" is relative to something one considers "macro". It is possible to discuss microenvironmental conditions relative to soil horizons, peds within a particular horizon, pores within a particular ped, skeletal grains exposed on the pore walls, crystal dislocations within a particular skeletal grain, or stressed chemical bonds within a zone of dislocation. Where weathering reactions are concernred, chemical properties on the scale of crystal dislocations are often the initial factor influencing the formation of secondary clays (Berner and Holdren, 1977; DeVore, 1956). This portion of the real world reveals its secrets grudgingly, but is probably the key to understanding processes of clay mineral genesis.

CHAPTER I

INTERRELATIONSHIPS OF CLAY MINERALOGY, SOIL SOLUTION CHEMISTRY, AND LANDSCAPE AGE IN SOILS OF WESTERN OREGON

J. R. Glasmann and G. H. Simonson

Department of Soil Science

Oregon State University

INTERRELATIONSHIPS OF CLAY MINERALOGY, SOIL SOLUTION CHEMISTRY, AND LANDSCAPE AGE IN SOILS OF WESTERN OREGON[1]

J. R. Glasmann and G. H. Simonson[2]

ABSTRACT

Clay mineral genesis was studied in soils representing three different geomorphic surfaces in western Oregon, ranging in age from Pliocene-early Pleistocene to late Pleistocene. Soil solution studies, clay mineralogy, and soil micromorphology were employed to provide evidence of clay mineral synthesis and interpret soil genesis.

Soils at each of the three study areas are characterized by distinct differences in soil solution chemistry, clay mineralogy, plasmic fabric, and genetic history. the oldest geomorphic surface is characterized by deep, red kaolinitic soils which are underlain by thick, halloysitic basaltic residuum. Soil solution studies suggest that clay mineral synthesis from solution does not occur in these soils, although kaolinitization of feldspar and formation of chloritic intergrade occur in loess contaminated A horizons. Transition from hydrated halloysite to kaolinite occurs in the lower solum, but is not accompanied by diagnostic solution chemical fingerprints. The oxic soil properties at this location were

---

[1]Oregon Agricultural Experiment Station Technical Paper No. _____. Contribution of the Dept. of Soil Science. Received _____.

[2]Graduate research assistant and professor of soil science, respectively, Oregon State University, Corvallis, OR 97331.

developed during a prior weathering cycle and the soil is at a genetic endpoint in the present environment.

Ultisols on remnants of Pleistocene surfaces in the Oregon Coast Range have mixed mineralogy, with chloritic intergrade, mica, and kaolinite occurring in the upper solum, transitional to smectite and halloysite with depth. Soil solutions are undersaturated with respect to quartz and in equilibrium with respect to kaolinite in the solum, but are stable with respect to Mg-montmorillonite in the zone of active bedrock weathering. Sharp differences between soil and stream water chemistry result from lateral movement of soil water across the active zone of weathering prior to surfacing as stream flow. Micromorphological, clay mineralogical, and chemical evidence suggests that alteration of Mg-chlorite to smectite occurs during rock weathering, followed by conversion of smectite to halloysite and chloritic intergrade in the solum.

Soil solutions from Alfisols on late Pleistocene surfaces at the western margins of the Willamette Valley show compositional variation from pedon to pedon and horizon to horizon within pedons, arising in part from the influence of compositional variations in soil parent materials. Solutions generally plot in the kaolinite stability field in the region above quartz saturation, although evidence presented suggests that saturated soil solutions are not in equilibrium with neighboring solid phases. Solution composition is related to colloid composition, modified by the relative residence time of a volume of solution in a particular horizon. Kaolinite forms during feldspar alteration and smectite genesis is related to alteration of volcanic sedimentary materials.

Additional Index Words: Soil solution chemistry, clay mineral genesis, soil micromorphology, smectite, chloritic intergrade, kaolinite, hydrated halloysite, soil genesis, weathering, Ultisols, Alfisols.

INTRODUCTION

Remnants of old erosion surfaces exist in western Oregon which are underlain by soil materials having complex weathering histories. In the Willamette Valley, the Eola geomorphic unit, which represents remnants of the oldest stable geomorphic surfaces in the area, is underlain by soils which have probably been developing since early or middle Pleistocene time (Balster and Parsons, 1968). These soils have been subjected to several changes in climate and vegetation during their period of development (Hansen, 1947). Ferruginous bauxite deposits are associated with the deeply weathered soils of the Eola unit and are believed to have formed during late Miocene or Pliocene time under conditions of tropical weathering (Corcoran and Libbey, 1956). The next youngest geomorphic surface below the Eola unit is the Dolph unit (Balster and Parsons, 1968; Parsons et al., 1970), which is probably middle Pleistocene in age. The soils of this unit often have A and B horizons formed in a more recent silty mantle over the remnant of a mid to late Pleistocene paleosol (Glasmann et al., 1980; Parsons et al., 1970). Due to the stratified nature of soil parent materials on the Dolph unit, different parts of the sola have been subjected to different weathering environments, ranging from warm, moist interglacial periods to the present cool, seasonally dry climate (Hansen, 1947; Heusser, 1966).

Clay mineral genesis studies on these old landscapes are complicated by climatic fluctuations and by changes in pedologic environment which have been induced by such factors as uplift and erosion, incision of drainages, burial by colluvium or other sediment, and the periodic addition of unweathered material (e.g. volcanic ash) to the soil surface. Clay minerals have been considered to represent "reactive responses of

"geologic materials to energies characterizing certain geochemical and geologic (pedologic) environments through time" (Keller, 1970). And while time is important, the "energies" characterizing pedologic environments also vary in space, or with position in the weathering profile (Glasmann, 1982; Eswaran, 1979). Under a given set of macroclimatic conditions, clay mineral genesis will be determined soley by the chemistry of the weathering microenvironment, which may change considerably over short distances in the soil (Glasmann, 1982; Glasmann and Simonson, 1982a; Eswaran, 1979; Eswaran and Won Chaw Bin, 1978), as well as with time, such as in response to wetting and drying cycles. Kittrick (1971) has suggested that the composition of montmorillonites formed in the soil represents the most stable composition for the soil solution conditions under which the particular mineral formed. It seems reasonable to extend this logic to the genesis of other secondary minerals in the soil.

the soil solution-mineral system is a two-way street, where minerals help determine the composition of the soil solution, and the composition of the soil solution determines the course of mineral formation in the soil (Kittrick, 1969). This logic forms the basis for "dynamic pedology" (Singer et al., 1978), where the composition of the soil solution is monitored over time and solution compositions used to deduce processes of soil formation. In mixed mineral systems, such soil solution data often provide clues to the direction of mineral genesis that may be difficult to interpret based on analyses of bulk mineralogical data alone (Sevink and Verstraten, 1978; Miller and Drever, 1977; Coen and Arnold, 1972).

This paper reports the results of clay mineral genesis research in soils from different weathering environments in western Oregon. The objectives of this research were: 1) to determine the silicate

geochemistry of the soil solution in soils developed from materials of different composition on landscapes of different age and geomorphic position, 2) to relate soil solution chemistry to soil mineralogy, and 3) to determine the course of clay mineral genesis in the present soil weathering environment.

Traditional (or "static", Singer et al., 1978) pedological investigative techniques, as well as "dynamic" and micromorphological techniques were applied to the study of clay mineral genesis. Soil micromorphology can serve as a useful tool in relating soil mineralogy to soil solution chemistry by revealing the microscopic components of the large picture of soil genesis that are measured by bulk soil properties. In the absence of micro-analytical techniques which permit in situ study of water chemistry at the mineral-soil solution interface, soil micromorphology can help in interpreting such microchemical conditions by indicating the nature of authigenic minerals formed during weathering and their position in the weathering profile (Brewer, 1976). Portions of this study are reported in subsequent papers (Glasmann and Simonson, 1982a, b).

MATERIALS AND METHODS

Description of Study Area

Clay mineral genesis was studied at three locations in western Oregon. Site 1 is located southwest of the town of Philomath in the Oregon Coast Range (SE 1/4, NW 1/4, Sec. 30, T. 12 S., R. 6 W.) at an elevation of approximately m (800') above sea level. Annual precipitation averages 1400-1500 mm annually, most of which falls during the winter as rain. The soil moisture regime is xeric and the soil

temperature regime is mesic. The landscape consists of a moderately dissected interfluve underlain by basalts of the Eocene Siletz River Volcanics (Vokes et al., 1954). The area was clear-cut in 1977, having formerly been covered with a dense stand of old growth Douglas fir. The soils of the area are predominantly deep red Ultisols (Xeric Haplohumults) formed in basaltic residuum or colluvium. The combined thickness of soil and basaltic residuum often exceeds 5 m, suggesting that these well developed soils formed during an extended period of weathering and landscape stability. More recently, drainage incision has lead to the development of oversteepened slopes, resulting in local areas characterized by slope instability and soil mass movement. Other studies in the Coast Range (Parsons and Balster, 1966) have shown that deep red soils having a B+ horizon occur primarily on stable ridgetops and pediment remnants characteristic of the Eola geomorphic unit. Site 1 apparently represents a relict Eola landscape in decay, being encroached upon by unstable landforms of a younger geomorphic surface.

Site 2 also occurs in the Oregon Coast Range in the Corvallis Watershed in an area characterized by a broad ridgetop of moderately undulating topography intersected by steep walled valleys (SE 1/4, SW 1/4, Sec. 11, T. 12S., R. 7W., south of Old Peak Road; sites H13, H14, Glasmann and Simonson, 1982a). The area lies approximately 381 m (1250') above sea level and averages 1600-1700 mm precipitation annually. Precipitation falls mainly during the winter months as rain; however, the soil moisture regime is udic and the soil temperature regime is mesic. The soils are dominantly deep red Ultisols (Typic Haplohumults) formed in residuum or colluvium of basaltic composition. The Siletz River Volcanics underlie the study area, but differ from the basalts at

site 1 by the presence of interbedded tuffaceous siltstone which occurs in the western section of site 2. These tuffaceous sediments represent a late stage of volcanic activity that produced the Siletz River Volcanics (Snavely et al., 1968) and are termed the Kings Valley Siltstone Member (Vokes et al., 1954). The siltstone is composed of fine-grained basaltic pyroclastic material, as well as sediment eroded from basaltic highlands which were exposed during Eocene time. The eastern part of site 2 is underlain by basalts (Glasmann and Simonson, 1982a). The landforms of the study area also show evidence of Holocene slope instability and soil mass movement in the vicinity of drainage heads, but the rounded hill and valley topography and the well developed soils of the more stable ridgetop are characteristic of the Eola geomorphic surface. The depth to bedrock is not as great in the soils of site 2 as it is at site 1, and in addition, stone lines were observed at site 2, suggesting that the soils of this area have been influenced by several cycles of erosion.

Site 3 lies in the foothills of the Coast Range on the western margin of the Willamette Valley. Upper Eocene sedimentary rocks of the Spencer Formation underlie the study area (Baldwin, 1964) which occurs in a 1.4 ha subwatershed in the eastern section of Elkins Road Watershed (Lowrey et al., 1981). The subwatershed lies approximately 85 m above sea level in an area characterized by high soil variability (see transect B-B', Glasmann et al., 1980). Soils are predominantly Haploxeralfs and Xerochrepts, representative of the Brateng geomorphic surface, which consists of mid-Pleistocene Dolph landscapes that have been modified by late Pleistocene deposition of Greenback Member silts of the Willamette Formation (Glasmann et al., 1980). Annual precipitation at site 3

averages about 1000 mm with a pronounced winter distribution. The soil moisture regime is xeric and the soil temperature regime is mesic.

Field and Laboratory Methods

Thirty-four profiles were described and sampled: two from site 1, 13 from site 2, and 19 from site 3. Bulk and undisturbed soil samples were taken from major soil horizons at each site and sealed in plastic containers to prevent moisture loss. Bulk soil samples were subsampled for clay mineral analyses (Glasmann and Simonson, 1982a), solution-equilibrium experiments, cation exchange and exchangeable base determinations (Berg and Gardner, 1978), pH determination (2:1 H_2O, KCl), and particle size analyses. Based on initial analysis of soil morphological and clay mineralogical data, undisturbed soil samples were selected from a limited number of profiles for detailed micromorphological characterization. The profiles selected were representative of the dominant soil series at each site, or where soil variability was high, samples were selected to represent the range of soil materials encountered. Portions of undisturbed soil samples were used for scanning electron microscope (SEM) analyses of fractured soil clods which were selected after careful study under a binocular microscope to characterize major surface features. The clods were mounted onto metallic stubs and coated with approximately 20-nm of gold in a vaccum evaporator prior to SEM analysis. Remaining undisturbed soil material was oven dried and impregnated with resin and thin sections were prepared for petrographic analysis (Eswaran, 1968). Additional samples representing lithorelicts from site 2 were also subjected to clay mineral, SEM, and petrographic characterization (Glasmann and Simonson, 1982a).

Soil solution data were obtained by two different methods. One method involved the equilibration of 20 g of soil with 40 ml DDW in capped 50 ml polyethylene centrifuge tubes for a period of four weeks at ambient room temperature. The samples were agitated daily for 15 minutes on a reciprocating shaker. The solutions thus generated were displaced from the soil by immiscible displacement (Mubarak and Olsen, 1976) using CCl_4 as the displacement medium. Following solution separation, the soil solution was filtered through a 0.45-μm Nuclepore filter and centrifuged at high speed until clear to a Tyndall beam prior to chemical analysis.

The second method used to obtain soil solutions involved field sampling of saturated soils using a network of shallow wells and piezometers at each study site. The wells and piezometers were constructed of polyvinyl chloride (PVC) pipe as reported in Lowrey et al. (1981) with a few minor deviations. These deviations consisted of increasing the length of the PVC pipe to allow for deeper wells in the sites with two deep Ultisols and modifying the piezometers to contain a water storage reservoir of approximately 100 ml in volume. While this study was not directly concerned with the occurrence of positive pore water pressure heads, the ability to sample soil water from specific soil horizons was of value and was inherent in the design and placement of the piezometers. The piezometers were located in specific soil horizons by augering to the required depth and then sealing the access hole from surface water percolation with alternating layers of bentonite and soil. Soil solution was pumped from the access tubes into duplicate 50 ml polyethylene centrifuge tubes using a portable vacuum pump constructed of Tygon tubing. Additional solution was pumped into a third centrifuge

tube and solution temperature and pH were measured in the field immediately after sampling using a Sargent Model PBL portable pH meter with a Sargent combination pH electrode.

Laboratory analyses of soil solution samples were performed within a day of sampling after filtration through a 0.6-μm Nuclepore filter and high speed centrifugation until clear to a Tyndall beam. Aliquots for ion analyses were removed by pipette, with pH again being measured on the remaining solution. Laboratory measured pH values were consistently 0.5-1.0 pH units higher than field measured counterparts, probably due to solution equilibration with atmospheric CO_2. Because of this difference in pH caused by solution handling, only field measured pH values are used when data are plotted on predominance diagrams.

Silica was determined colorimetrically with reduced molybdate (Amer. Pub. Health Assn., 1976). Calcium and Mg were determined by atomic absorption using 0.1% Sr^{2+} to eliminate interferences from Si and P. Sodium and K were determined by flame photometry in the presence of 0.1% Li. Initial calculations of ionic strength were made using the Davies equation (Davies, 1962), assuming HCO_3^- was the charge balancing anion. These calculations indicated that the difference between species activity and concentration was less than 2%; therefore, concentrations are used in the data presentation. Solution compositions were plotted on predominance diagrams calculated from idealized mineral reactions (Stumm and Morgan, 1980).

RESULTS AND DISCUSSION

Site 1

Soil Solution Chemistry

Piezometers were placed in the Bt and 2C horizons of a profile mapped as Jory silty clay, 10-20% slope (Xeric Haplohumult, clayey, mixed, mesic; Knezevich, 1975) at depths of 90 and 230 cm, respectively. Although this soil is very deep, well-drained, and occurs in sloping terrain, perched water tables were measured on several occasions during and immediately following major winter storms. Such conditions are common in western Oregon soils (Lowrey et al., 1981; Harr, 1977). Subsequent to a major storm in early December, 1980, Bt and 2C horizon piezometers showed positive pressure heads of 38 and 54 cm, respectively, placing the phreatic surface about 30 cm below ground level (calculations after Richards et al., 1973). The phreatic surface dropped rapidly following storm cessation and was absent from the upper 230 cm of the profile within 24 hours.

The results of chemical analyses of soil solutions obtained during periods of temporary soil saturation are listed in Table 1 and plotted on predominance diagrams in Fig. 1. The data representing site 1 (samples 1 and 2, Table 1) plot in the kaolinite stability field close to the kaolinite/gibbsite boundary, having silica concentrations well below quartz solubility (pH_4SiO_4 = 3.74). Several factors may explain such low solution concentrations: 1) the mineral system is highly weathered and consists of only the most stable weathering products, 2) lack of equilibrium between soil minerals and surrounding solutions, or 3) dilution by rain water seeping down around the sides of piezometers. Dilution by rain water is not likely, since the piezometers were sealed from

Table 1. Solution chemistry of soil and surface waters from soils in western Oregon.

	Site 1		Site 2							
	JL-1	J1-2	H6-1	H6-3	H5-1	H5-3	H1-2	H1-5	HSC	H7-1
	-log concentration ($mol \cdot l^{-1}$)									
pH	5.3	4.9	5.1	5.5	5.4	5.6	5.0	5.5	6.7	6.3
pH_4SiO_4	4.49	4.54	4.10	3.98	4.05	4.23	4.21	4.13	3.35	3.32
pK	5.25	5.50	5.11	5.32	4.98	5.20	5.15	5.13	4.75	4.83
pNa	4.85	4.97	4.48	4.30	4.48	4.28	4.55	4.28	3.98	3.94
pCa	5.73	5.45	5.30	5.12	5.30	5.24	5.15	5.12	3.49	3.53
pMg	5.33	5.40	5.08	5.14	5.10	5.21	5.06	5.15	4.04	4.22

	Site 3								
	ET	E4-4	E7-3	E7-4	E3-3	E3-4	E4-2	E4-3	E4-4
	-log concentration ($mol \cdot l^{-1}$)								
pH	5.4	5.9	6.1	6.5	6.6	6.3	5.7	5.8	6.5
pH_4SiO_4	3.65	3.50	3.80	3.26	3.74	3.15	3.77	3.80	3.45
pK	4.92	4.69	4.00	3.93	3.79	3.92	4.13	4.12	4.34
pNa	3.71	3.81	3.66	3.47	3.13	3.41	3.42	3.13	3.27
pCa	3.24	3.74	3.40	3.10	2.83	3.21	2.95	2.98	3.66
pMg	3.33	3.79	3.50	3.63	3.28	3.69	3.20	3.16	3.85

Figure 1. Predominance diagrams illustrating the stability relations of ideal mineral phases (after Stumm and Morgan, 1980). Solid star represents soil solution from site 1, solid circle represents solutions from site 2, and open square represents solutions from site 3. G = gibbsite; K = Kaolinite.

Figure 1.

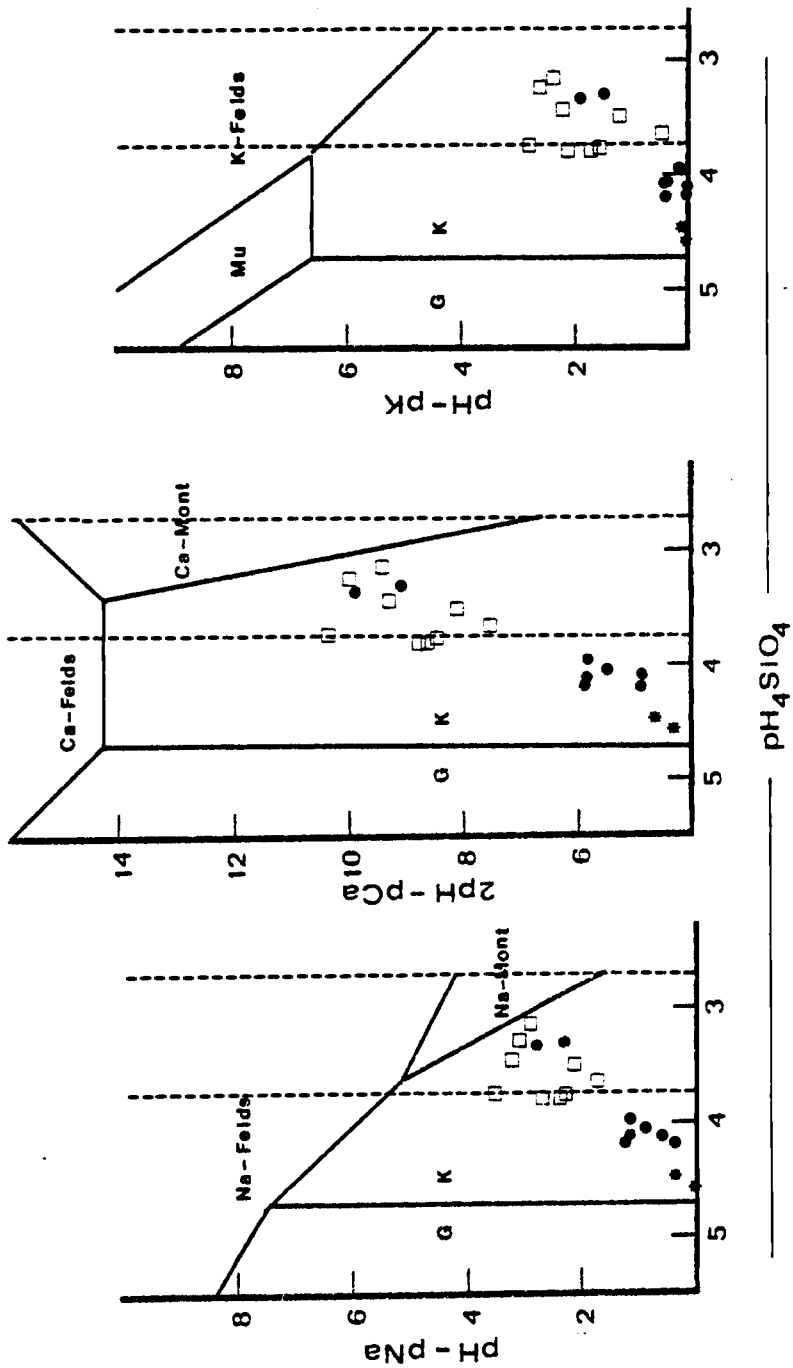
K-Felds
Mu
K
G
pH - pK
Ca-Mont
Ca-Felds
K
G
2pH - pCa
Na-Mont
Na-Felds
K
G
pH - pNa
pH4SiO4

surface leakage using several layers of bentonite. Lack of equilibrium may be important, especially since conditions of soil saturation are very short lived; however, equilibrium may be reached quickly in mineral-solution systems where the ratio of mineral surface area to solution volume is high (Miller and Drever, 1977; Bricker et al., 1968).

Clay Mineralogy

The clay mineralogy of the <2-μm fraction of bulk soil samples from major soil horizons at the piezometer station at site 1 is presented in Fig. 2. Kaolinite, mica, and chloritic intergrade are present in the clay fraction of A horizon soil material (Fig. 2a). The chloritic intergrade shows resistance to expansion with Mg-saturation and solvation, as well as considerable heat stability, evidenced by resistance to collapse with K-saturation and heating to 300°C. The intensity of mica and chloritic intergrade diffraction peaks decreases sharply with depth in the soil profile and diffraction patterns from B horizon samples indicate that the <2-μm fraction consists predominantly of kaolinite and iron oxides (Fig. 2b, c; oxide diffraction peaks not shown). The asymmetry of the 7.4 Å diffraction peak in Fig. 2b is characteristic of poorly crystalline kaolinite or dehydrated halloysite. Transmission electron microscope (TEM) analyses of B horizon clay show the presence of hexagonal platy forms which are partially coated by small, electron dense iron oxides (Plate 1a). The hexagonal plates are characteristic of kaolinite and the electron dense materials show morphologic similarities to goethite and hematite present in other highly weathered soils (Eswaran and Wong Chaw Bin, 1978).

The halloysitic component of the clay fraction is more evident in XRD patterns representing colloidal material from the Bt and 2C horizons

Figure 2. XRD patterns of <2-μm material from a deep, red, Jory profile at site 1. (a) Sample J1-1, A horizon. (b) Sample J1-2, AB horizon. (c) Sample J1-3, Bt2 horizon. (d) Sample J1-5, 2C horizon. Numbers refer to clay characterization treatments: 1, Mg-saturated, 54% RH; 2, Mg-saturated, ethylene glycol solvated; 4, K-saturated, 110°C, 0% RH; 6, K-saturated, 300°C, 0% RH; 7, K-saturated, 550°C, 0% RH. d-spacing in Angstroms.

Figure 2

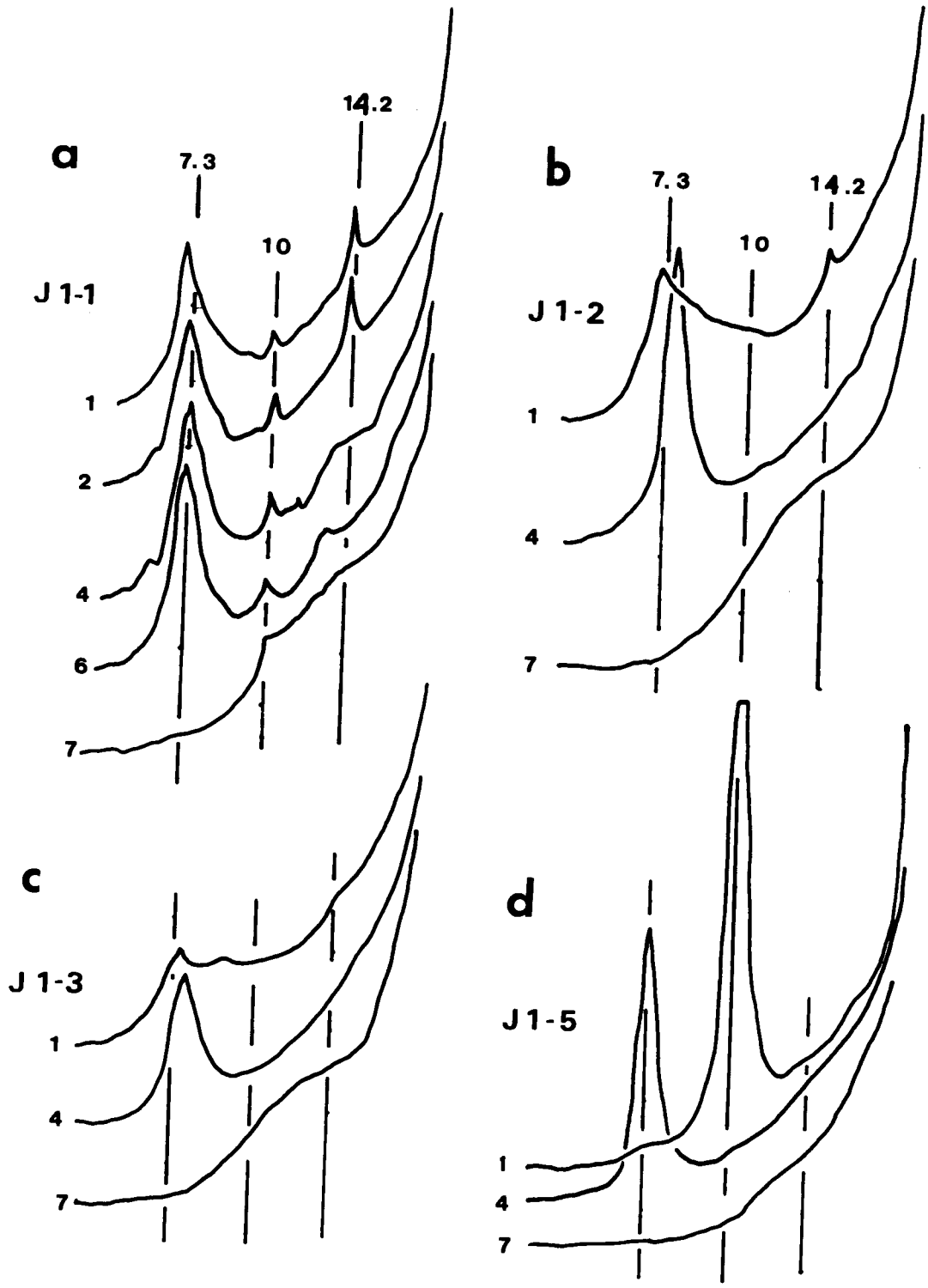

Plate 1. (a) TEM micrograph of <2-μm fraction of J1-2 showing hexagonal kaolinite plates and iron oxide particles. Weak suggestion of small tubular forms, possibly representing minor amounts of halloysite. (b) TEM micrograph of J1-5 clay fraction, showing the presence of spheroidal and tubular halloysite with minor amounts of iron oxide. (c) SEM micrograph of undisturbed soil from J1-5 showing soil matrix consists of dense aggregates of tubular halloysite and globular forms (spheroidal halloysite ?). (d) Area of J1-5 dominated by globular clay forms.

Plate 1

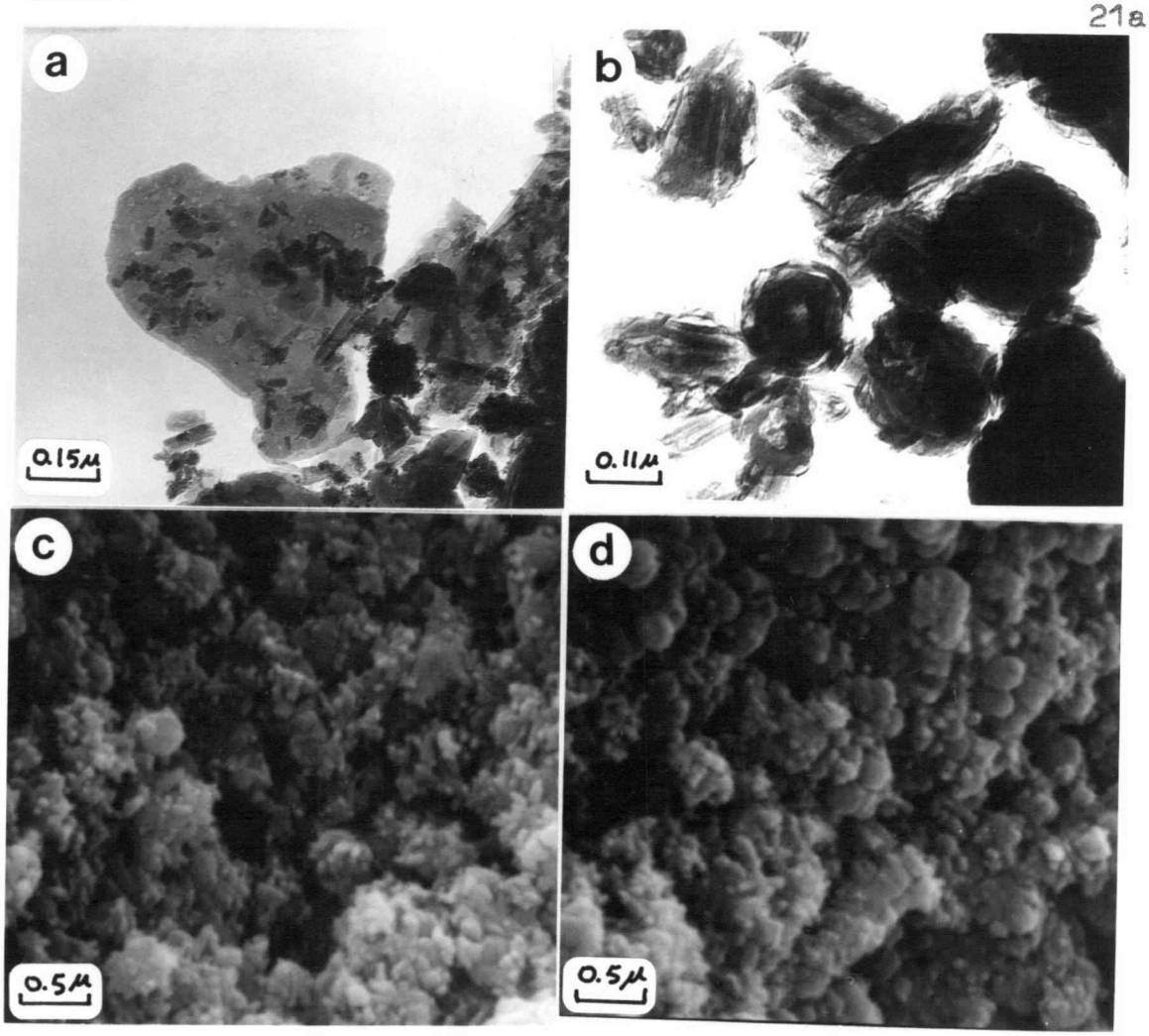

(Figs. 2c and d, respectively). In Fig. 2c, hydrated halloysite is suggested by the broad, low diffraction peak below 10 Å on moist, K-saturated, 105°C heat treated samples with accompanying intensifications of the 7.3 Å peak. This response is characteristic of soil clays which consist of a mixture of hydrated and dehydrated halloysite (see Table 1, Glasmann and Simonson, 1982a). 2C horizon clay (Fig. 2d) consists almost entirely of hydrated halloysite, characterized by an intense 10 Å diffraction peak for moist samples which collapses irreversibly to 7.3 Å upon drying. TEM analyses of 2C horizon colloids indicate the presence of tubular and spheroidal halloysite, as well as iron oxides (Plate 1b). Halloysite is also evident in SEM micrographs of the 2C horizon (Plates 1c, d).

Additional XRD analyses of bulk soil (sand, silt, and clay) from major horizons at site 1 indicate that the soil below approximately 40-50 cm is devoid of weatherable minerals (Figs. 3a, b, c), containing only kaolinite, iron oxides, minor amounts of quartz, and gibbsite. Iron oxides include goethite, hematite, and maghemite (Fig. 3b, c). The latter two minerals generally do not form in soils of humid temperate zones, but are characteristic of soils developed in warmer climates (Schwertman and Taylor, 1977). A horizon soil material contains feldspar, quartz, mica, and 2;1 clays (Fig. 3a).

Micromorphology

Petrographic analyses of thin sections representing major soil horizons of the Jory profile at site 1 provide a basis for the genetic interpretation of the soil clay mineralogy presented in the previous section. Silt-sized angular feldspar and quartz constitute approximately 35% of the A horizon soil matrix (Plate 2a). These grains are set in a

Figure 3. XRD patterns of bulk soil from deep, red, Jory profile at site 1, Mg-saturated, 54% RH. (a) Sample J1-1, A horizon. (b) Sample J1-2, AB horizon. (c) Sample J1-4, 2BC horizon. Mineralogical designations: f=feldspar, g=goethite, gi=gibbsite, h=hematite, hh=hydrated halloysite, k=kaolinite, mh maghemite, q=quartz.

Figure 3.

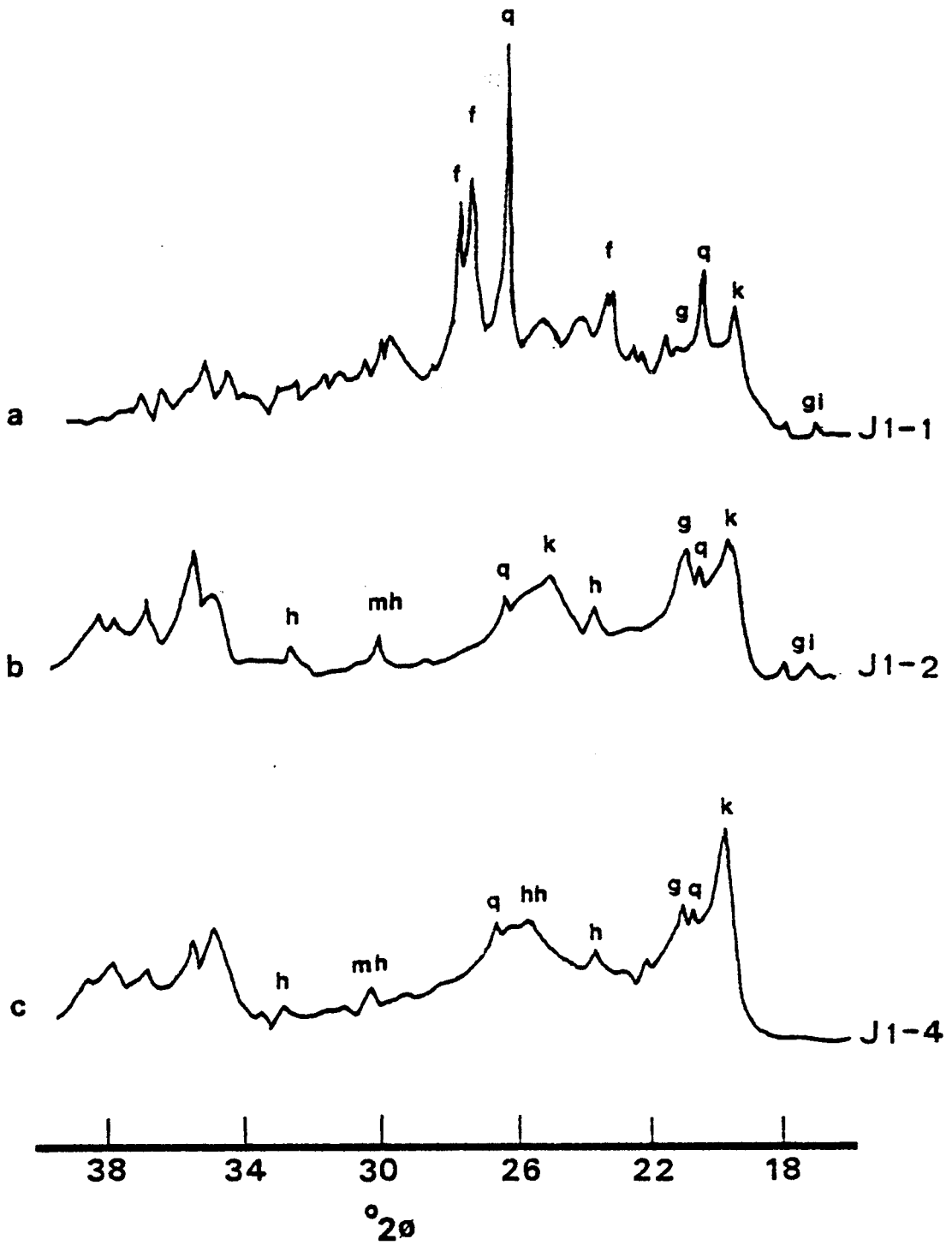
a
q
f
f
f
q
g
k
gi
J1-1
b
h
mh
q
k
h
g
q
k
gi
J1-2
c
h
mh
q
hh
h
g
q
k
J1-4
38
34
30
26
22
18
°2ø

Plate 2. Photomicrographs of profile J1, site 1. (a) A horizon, illustrating gibbsite nodules (lower center), runiquartz (large grain above gibbsite nodule), angular silt-sized components and clayey matrix. (b) Pyroclastic feldspar in A horizon characterized by adhering bubble wall glass. (c) Pyroclastic feldspar showing complex dotted alteration evidenced by development of isotropic zones under cross polarizers. Plasmic fabric is argillasepic to isotic. (d) High magnification view of gibbsite nodule in 2a, illustrating complex internal structure. (e) Bt horizon, illustrating kaolinitic s-matrix, corroded runiquartz, iron oxide concretions, papules (upper right). (f) Cross polar view of 2e, showing isotic plasmic fabric, isotropic character of papule, lesser amount of silt-sized grains than A horizon (Plate 2c). (g) Basaltic litho-relict and poorly developed argillans in B2t horizon. Litho-relic consists of opaque iron oxides with rectangular voids left after feldspar dissolution.

Plate 2

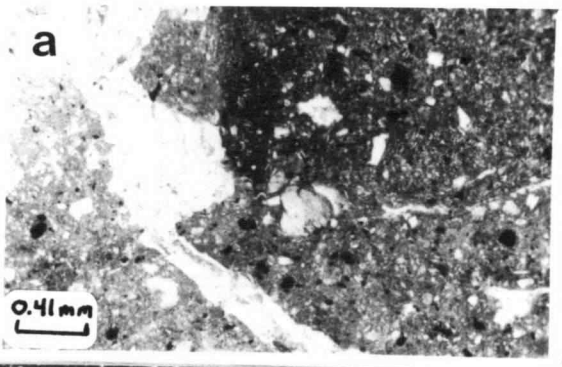

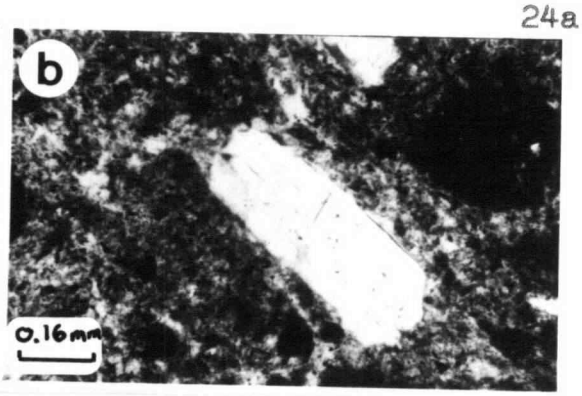

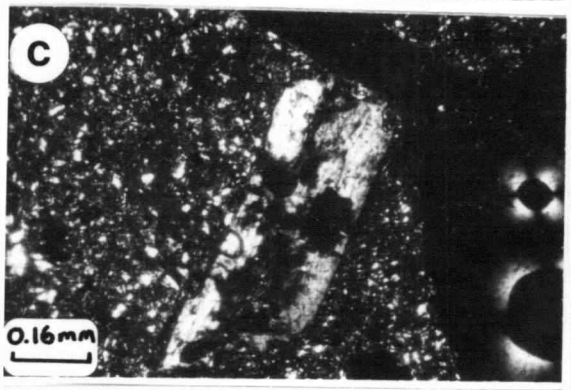

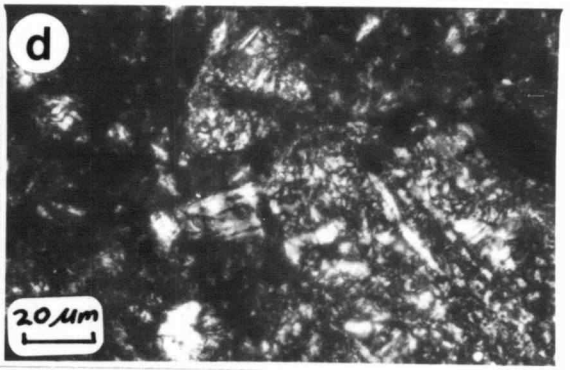

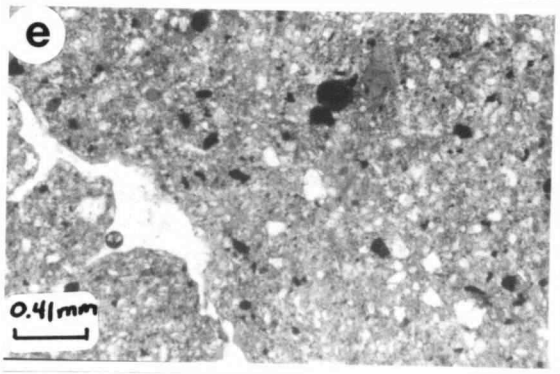

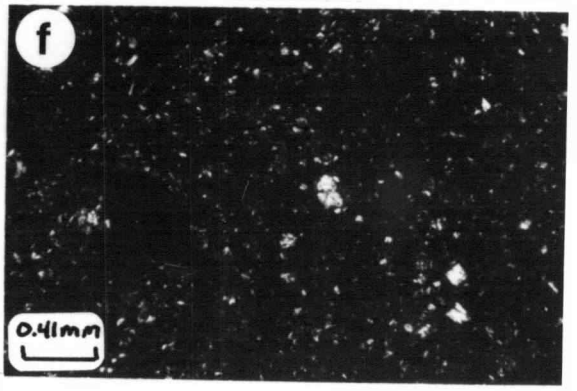

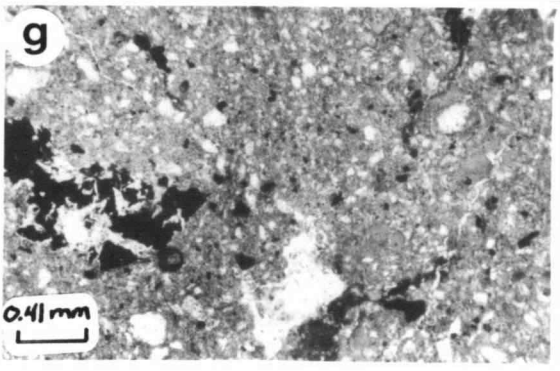

dark reddish brown, clayey matrix that has argillasepic to isotic plasmic fabric (terminology of Brewer, 1976). Mica, including both muscovite and biotite, constitutes <2% of the soil, based on point counts of three A horizon thin sections. Trace amounts of sand-sized, glass-shrouded, zoned plagioclase crystals also occur in the A horizon (Plates 2b, c). The morphology and zoned nature of these plagioclase grains indicate that they are of pyroclastic origin, and probably represent material added to the soil surface during periods of volcanic ash fall.

Remaining A horizon sand-sized material consists of gibbsite nodules (Plates 2a, d), runiquartz (Plate 2a, Eswaran et al., 1977), iron oxide concentrations, and scattered intensely altered basaltic lithorelicts (Plate 2e). Such sands indicate intense weathering and are common throughout the solum, whereas weatherable minerals, such as feldspar and pyroxene, occur only in the A horizon. The rounded, fractured appearance of the gibbsite nodules (Plates 2a, d) and the fractured, intensely altered lithorelicts suggest that these materials have been subjected to transport. Evidence of soil transport is also provided by the presence of fragmented argillans as papules embedded in the soil matrix (Plate 2f). The papules are usually reddish brown to light reddish brown in color and are weakly birefringent to isotropic, possibly due to masking of birefringence by amorphous iron coatings. Traces of papules showing strong, continuous orientation were also observed.

The abundance of fresh, angular silt-sized feldspar and quartz, along with fine sand and silt-sized mica, suggests contamination of the surface soil by loess. The loessal materials were depcsited onto the surface of a soil developed in intensely weathered basaltic colluvium and mixed into the upper 40-50 cm, probably by faunal activity. The intensely weathered

character of the colluvium is also expressed in the degraded appearance of clay skins in the Bt horizon. Identification of clay skins was tenuous in the field and the few argillans seen in thin section (Plates 2e, f) are thin, weakly birefringent to isotropic, and appear granulated. In Plate 2e, a joint plane ferri-argillan occurs in the lower right corner of the micrograph. This argillan is optically similar to the light reddish brown, nearly isotropic papules described earlier. A very thin, isotropic channel ferri-argillan is pictured lining the irregular channel in the lower left corner of Plate 2f. Argillans account for <2% of the soil based on point counts of the Bt horizon. The characteristics of argillans in this profile at site 1 differ greatly from the thick, continuous, well oriented argillans typical of other Jory profiles.[3]

The micromorphological properties of the soil at site 1 suggest that the mixed clay mineralogy of the A horizon has resulted from contamination of intensely weathered, kaolinitic colluvium by relatively unweathered loessal and pyroclastic material. Clay illuviation has not been an important process during the current cycle of pedogenesis and is probably hindered by the dominance of low activity clays in the soil matrix (Eswaran and Sys, 1979), and by stabilization of the soil matrix by amorphous and crystalline iron oxides. The dominance of low activity clay and iron oxides in the soil matrix also affects the soil plasmic fabric, which is isotic to argillasepic throughout the solum. The cation exchange capacity (CEC) of the Bt horizon is below 16 meq/100g

---

[3]Norgren, J. A. 1962. Thin Section Morphology of Eight Oregon Soils. Unpublished M.S. Thesis. Oregon State University, Corvallis, OR 97331.

soil and base saturation is extremely low for all horizons. Although KCl extractable Al was not determined, the pronounced lowering of soil pH measured in 2:1 KCl:soil mixtures suggests that Al is an important exchangeable component of colloid surfaces. Although Oxisols are not recognized in soil survey reports or soil classification work from western Oregon, the results of this study indicate that Oxisol-like profiles occur on scattered remnants of old erosion surfaces in the Willamette Valley, and can be anticipated on similar remnant surfaces in southwest Oregon.

Solution Chemistry/Mineral Relations

Based on the mineralogy of the soils at site 1, the low values of pH_4SiO_4 and other dissolved species probably reflect the intensely altered oxic character of the soil. Evidence of kaolinite formation is limited to alteration of pyroclastic feldspar in the A horizon and the conversion of hydrated halloysite to kaolinite with decreasing depth in the soil profile. Halloysite, which is metastable with respect to kaolinite at earth surface conditions (Kittrick, 1969), apparently alters to kaolinite via the pathway: hydrated halloysite → dehydrated halloysite → kaolinite in the oxic soils at site 1. In view of the metastability of halloysite with respect to kaolinite, it is unclear why the deep, very old basaltic residuum underlying the oxic profile at site 1 has not converted to kaolinite.

Site 2

Soil Solution Chemistry

Temporary perched water tables were also observed in soils of site 2 during the winter rainy season. Results of solution analyses are listed in Table 1 and values of pH-pK, pH-pNa, and 2pH-pCa as functions

of pH_4SiO_4 are plotted in Fig. 1. Soil solution data points from site 2 plot in the kaolinite stability field in the region below quartz solubility, but slightly more siliceous than soil solutions from site 1. The composition of surface water samples from an ephemeral stream which drains the study area also plots in the kaolinite stability field, but is considerably richer in dissolved solids than site 2 soil solutions and plots close to the kaolinite-montmorillonite boundary. The sharp difference in water chemistry between saturated soils and their associated natural drainage was an unexpected result, especially since stream flow at the time of sampling was completely due to soil subsurface flow. Water samples from a shallow well dug into the stream channel during periods of zero surface discharge are chemically similar to surface waters (compare samples HSC and H7-1), yet quite different from soil solution extracted from a nearby piezometer (sample H6-3). This piezometer was located parallel to the stream channel in the 2Cr horizon of a soil 5 m upslope from the stream channel well.

Silica concentrations measured by solution equilibration experiments (Table 3) using soil material from piezometer sites of the study area are higher than concentrations measured in corresponding piezometer samples. This relationship suggests that the waters obtained by field sampling may not be in equilibrium with neighboring mineral phases. Similar results have been reported in clay genesis studies which compared field and laboratory equilibrated soil solutions (Coen and Arnold, 1972); however, Weaver et al. (1971) reported higher silica concentrations in field soil solutions than in equilibrated soil samples. They suggest that the higher silica concentrations in natural soils may be due to

Table 2. pH_4SiO_4 and pH of equilibrated soil solutions from sites 2 and 3.

Pedon	Horizon	Depth	pH_4SiO_4	pH
		--cm--		
H1	A	21-30	4.04	5.58
	Bt	80-90	3.69	5.31
	2Cr	140-150	3.60	5.28
H5-1	A	15-25	3.96	5.55
	Bt	75-85	4.11	5.32
H6	A	15-25	4.02	5.65
	Bt	65-75	3.91	5.43
H7	A	15-25	3.62	5.63
E4T1	Ap	0-25	3.89	5.32
	A2	25-57	3.78	5.63
	A/B	57-70	3.68	5.60
	2Bt1	70-81	3.64	5.66
	2Bt2	81-92	3.58	5.43
	2Bt3	92-102	3.40	5.28
	3BCt	102-108	3.14	5.30
	3Cr	108-150	2.90	5.00

displacement of silica adsorbed on mineral surfaces or increased dissolution of silica by the lower pH of field soil waters.

Solutions obtained by field sampling at site 2 were in contact with the soil during brief periods of soil saturation, which usually lasted no more than 24 hours following major winter storms. Rapid lateral movement of soil water through macropores may hinder the development of equilibrium conditions in pore fluids in these Coast Range soils.

Stream discharge at site 2 during sampling periods was entirely due to subsurface soil flow. Stream solutions (samples HSC, H7-1) are more concentrated than soil solutions from within the drainage basin (Table 1 and 3). This difference in chemistry suggests that surface waters are not simply products of rapid subsurface moisture flow through the highly weathered soil mantle. The high concentration of dissolved solids in stream water samples at site 2 suggests that these waters have a provenance other than the weathered soil mantle. Lateral moisture flow along the soil-rock weathering interface is probably an important factor in generating the high concentrations of dissolved solids measured in surface waters. The probable mechanisms affecting the chemistry of these waters are discussed in a subsequent section.

Clay Mineralogy

Portions of the results of XRD analyses of the <2 μm fraction of soils from different geomorphic positions at site 2 are presented in Fig. 4. Patterns representing the Mg-saturated, ethylene glycol solvated and K-saturated, 300°C, 0% RH treatments are shown (treatments 2 and 6, respectively). Figure 4 illustrates the clay mineralogy of 3 horizons of a ridgetop soil (H1-1, A horizon, 20 cm; H1-2, Bt horizon, 70 cm; H1-5, 2Cr horizon, 175 cm). A horizon clays are characterized by chloritic

Figure 4. XRD patterns of <2-μm material from soils representing different geomorphic positions at site 2. (a) Ridgetop soil. Sample H1-1 represents A horizon, H1-2 represents Bt horizon, and H1-5 represents 2Cr horizon. (b) Sideslope soil. H5-1 represents A horizon, H5-3 represents Bt horizon, and H5-4 represents 2Cr horizon. (c) Footslope soil. H6-1 represents A horizon, H6-2 represents Bt horizon, H6-3 represents 2Cr horizon. (d) Toeslope (swale) soil. H7-1 represents A Horizon. d-spacing in Angstoms.

Figure 4

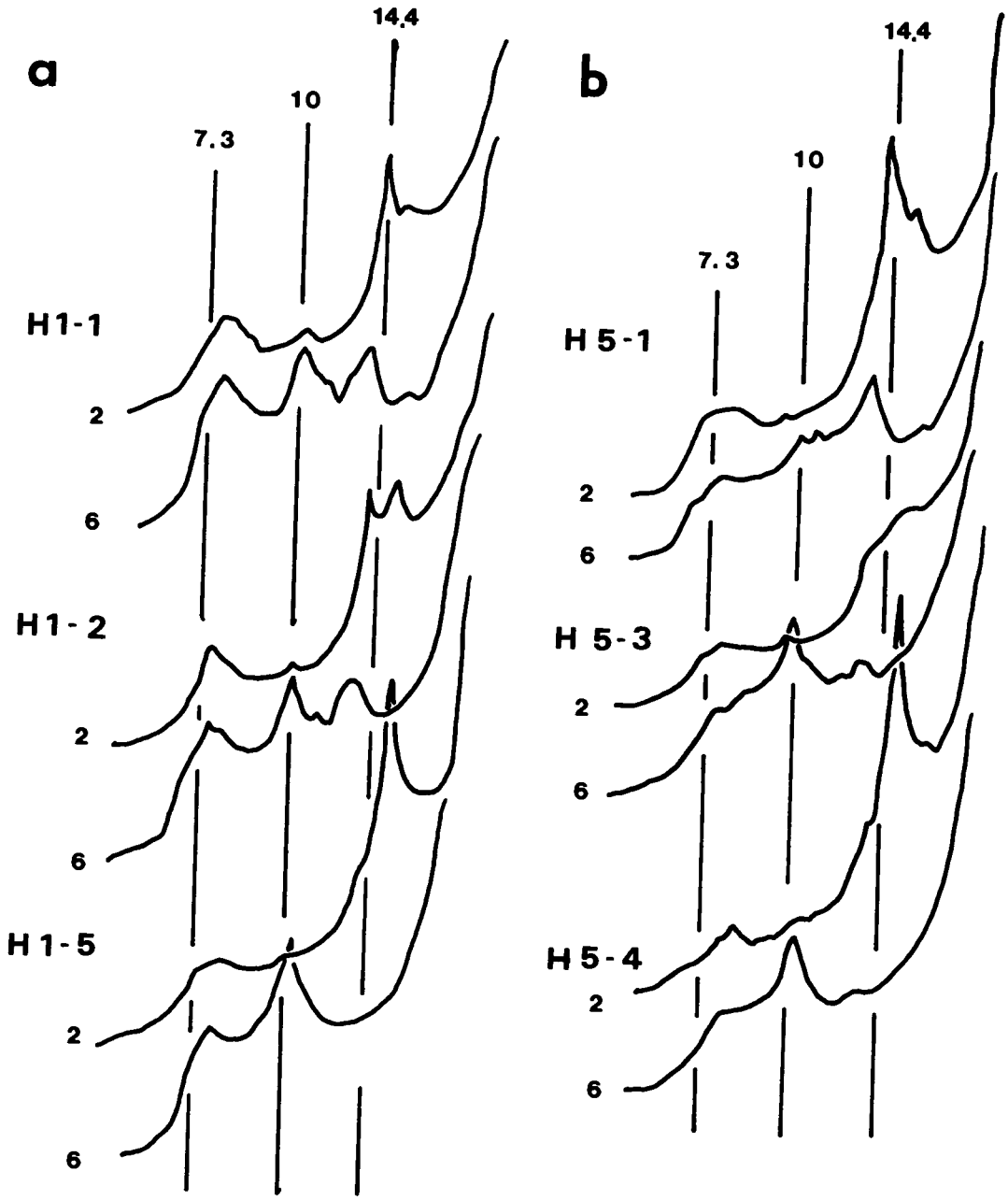

Figure 4 (cont.)

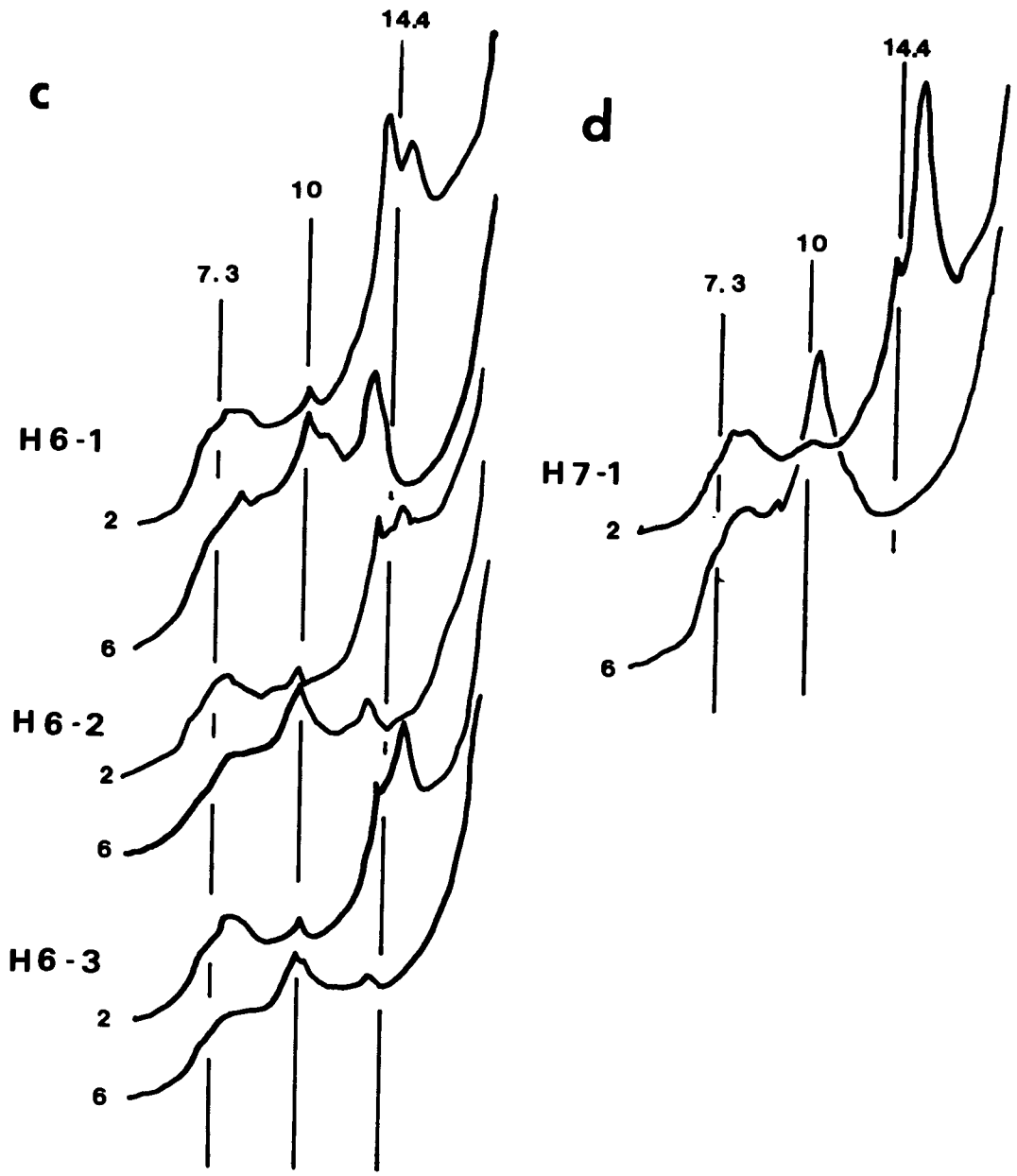

intergrade (hydroxy interlayered smectite), with lesser amounts of mica and poorly crystalline kaolinite (possibly dehydrated halloysite). The possibility that some vermiculite may also be present can not be excluded in the presence of chloritic intergrade since diffraction peaks of the two minerals overlap. The chloritic intergrade shows strong resistance to expansion with solvation and strong resistance to collapse with K-saturation and heating, suggesting the presence of well formed, stable interlayer hydroxy sheets. Chloritic intergrades showing this type of response to characterization treatments are approaching the characteristics of true chlorites.

When interlayering of the smectite lattice is incompletely developed, expansion of the smectite component is possible with solvation, but collapse upon K-saturation and heating is usually incomplete (Carstea et al., 1970). The Bt horizon clay illustrated in Fig. 3a shows response to characterization treatments typical of such moderately stable chloritic intergrades. Expansion of the smectite lattice is evident in the presence of a 17 Å peak with treatment 2. Lesser amounts of mica and dehydrated halloysite are also indicated. 2C horizon clays are devoid of chloritic intergrade and consist largely of a smectite mineral, probably beidellite, since lattice expansion failed to occur with glyceral solvation. The presence of vermiculite is indicated by the weak shoulder at 14 Å in treatment 2 which collapses irreversibly to 10 Å with K-saturation. Dehydrated halloysite is suggested by the broad 7.3-7.5 Å peak. The weak 10 Å peak in treatment 2 of the 2C horizon sample probably indicates mica, but may also indicate hydrated halloysite. TEM micrographs of this material showed the presence of tubular halloysite in minor amounts and may represent hydrated halloysite (Plate 4a).

Plate 3. (a) TEM micrograph of profile H1 2Cr horizon clay fraction showing presence of tubular morphologies, irregular platy material and electorn dense iron oxides. (b) Photomicrograph of gibbsite nodule in AB horizon, pedon H1. (c) Well-oriented papule in the Bt horizon of pedon H5, also stress oriented neostirans on ped and lithorelict surfaces. (d) Photomicrograph of Bt horizon, pedon H1, illustrating vomasepic plasmic fabric. (e) Well-oriented argillan on surface of altered lithorelict in 2BC horizon, pedon H5. (f) Fecal pellets clustered in tubular channel, A1 horizon, pedon H5.

Plate 3

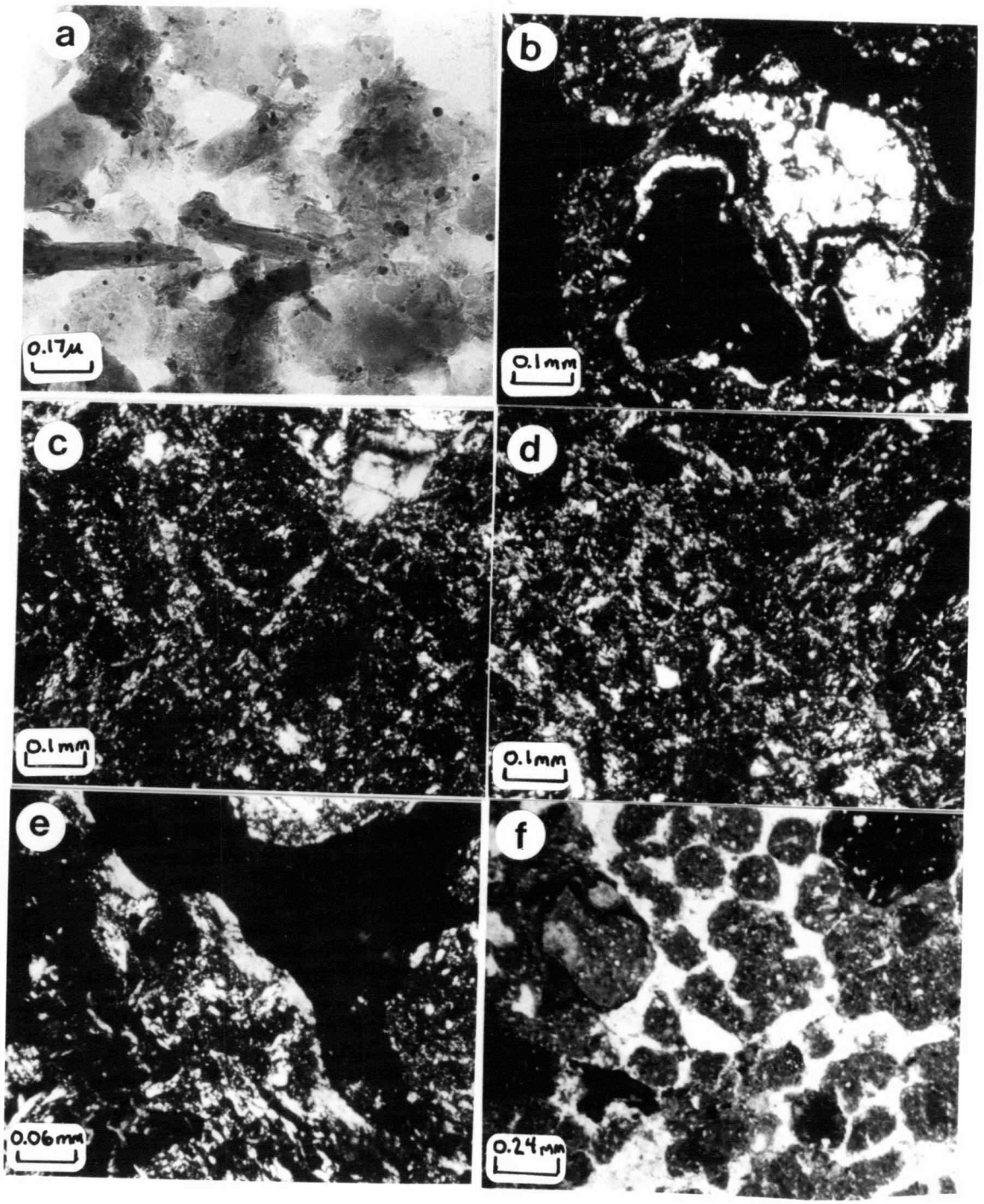

The pattern of clay mineral distribution observed in the ridgetop soil (pedon H1) is repeated in sideslope soils (pedon H5, Fig. 4b) and footslope soils (pedon H6, Fig. 4). Toeslope soils and stream channel alluvium (sample H7-1, 20 cm, Fig. 4d), however, do not show the presence of chloritic intergrade in the upper solum, but are instead characterized by beidellite, with lesser amounts of vermiculite, mica, and dehydrated halloysite. These low lying soils are saturated during most of the rainy season and remain moist during dry summer periods. Topographically higher soils are characterized by brief periods of saturation during winter months and frequent wetting and drying cycles.

The conditions favoring formation of chloritic intergrades have been summarized by Rich (1968). Of the conditions mentioned by Rich, wetting and drying cycles apparently are most important in the genesis and stability of chloritic intergrades (Huang and Lee, 1969). The surface horizons of ridgetop, sideslope, and footslope soils at site 2 are characterized by frequent wetting and drying cycles, whereas soil conditions in the lower solum and toeslope soils are more uniformly moist. These differing soil conditions favor the formation of chloritic intergrade in surface horizons of well drained soils and the stability of smectite in the moister environments.

Micromorphology

Thin sections from 2 pedons were studied, representing a ridgetop and a sideslope soil. Sand-sized gibbsite nodules occur in both profiles (Plate 3b), generally restricted to the upper part of the solum and their rounded and fractured appearance suggests that they have been subjected to transport. Abraided, well-oriented papules also occur in the upper part of the solum (Plate 3c). Rounded, fractured, highly

altered sedimentary and basaltic lithorelicts constitute 5-20% of the solum. These lithorelicts are enveloped by thick neostrians in the argillic horizon (Plate 3c). Bt horizon plasmic fabric is commonly skel-masepic (Plate 3d) grading to vo-masepic in horizons with fewer coarse fragments. The weathered sedimentary lithorelicts are unusual in that they break down easily with slight physical pressure when moist, yet do not readily disperse during laboratory particle size determination once the material has been thoroughly dried.

Sand-sized pyroclastic feldspar, silt-sized feldspar, quartz, and volcanic glass are present in the A horizon of both pedons studied, similar to the material described at site 1. However, relatively unaltered feldspar occurs in the lower solum of the soils at site 2, constituting about 10% of the sand fraction.

The character of the gibbsite nodules, fragmented papules, lithorelicts, and weakly altered to fresh pyroclastic material suggests that the upper solum of each of the pedons studied at site 2 formed in highly weathered colluvium, contaminated by more recent additions of volcanic ash and loess. Active soil bioturbation in these forested soils, evidenced by large amounts of fecal pellets (Plate 3e) and field evidence of tree throw, has mixed surface contaminants well into the B horizon. The presence of expansible 2:1 layer silicates in these soils has contributed to the development of more complex plasmic fabric at site 2 than in the kaolinitic soils at site 1.

Solution Chemistry/Mineralogy Relations

Low concentrations of dissolved silica and cations in soil solutions from site 2 are probably related to the occurrence of strongly developed chloritic intergrade in the soil. Hydroxy alumina (or hydroxy Fe, Mg)

on chloritic intergrade surfaces provide sites for $Si(OH)_4$ sorption (Beckwith and Reeve, 1963) and may raise the pH_4SiO_4 of soil solutions at site 2. Higher silica concentrations in swale soils (H7-1) appear at first to be related to the presence of beidellite, but if this were so, then solution samples from 2Cr horizon piezometers at each sampling station should have pH_4SiO_4 values similar to the swale water samples (Table 1), since the mineralogy of 2Cr horizons at each of these sites is dominantly beidellitic. This is not the case in either field solution samples or in artifical solution samples obtained by solution equilibration experiments (Table 2). The concentrated solutions characterizing stream channel surface and subsurface flow must originate by solution processes other than those occurring in the solum.

Bedrock Mineralogy, Site 2

In attempting to solve the dichotomous distribution of solution chemistry at site 2, deep weathering of underlying sedimentary and igneous bedrock was studied. Sedimentary rocks of the Kings Valley Siltstone Member of the Siletz River Volcanics crop out along the ephemeral drainage at site 2 and sedimentary rock fragments in various stages of alteration constitute up to 40% of alluvial soils in the swale position based on particle size (Table 2) and petrographic analyses of particle size separates. Figure 5a illustrates an XRD analysis of relatively unweathered Kings Valley Siltstone obtained from an outcrop in the ephemeral drainage. Strong diffraction peaks for chlorite and mica are evident, and while kaolinite is a possibility, its presence can not be verified by XRD in the presence of chlorite by the analytical methodology used in this study. Thin sections of the unweathered siltstone show it consists of silt and fine sand-sized plagioclase (Ab35-Ab55), sand-sized

Table 3. Some physical and chemical properties of soils representing different geomorphic surfaces in western Oregon.

Horizon	Depth	Moist Color	Texture (s,si,c)	Structure	pH	NH_4OAC C.E.C.	Exch. Cat. Ca	Mg	K	NH_4OAC B.S.
	--cm--				(H_2O/KCl)	-------meq/100 g----				%
				Profile J1, Site 1						
A1	0-38	5YR 3/3	sic	2mgr→2vfsbk	5.50/4.20	17.9	0.7	1.2	0.3	15.1
A2	38-63	5YR 3/3	sic	2fsbk→2vfsbk						
AB	63-94	2.5YR 4/6	c (8, 34, 58)	2msbk→2vfsbk	5.32/3.97	12.7	1.5	1.3	0.1	22.8
B1	94-127	2.5YR 4/6	c	2msbk→2vfsbk						
2Bt2	127-190	2.5YR 4/8	c (14, 40, 52)	2msbk→2vfsbk	5.15/3.92	16.8	1.1	0.7	0.1	11.3
2BC	190-254	2.5YR 4/8	sic (+)	1msbk+m						
2C	254-	10YR 8/2 in veins, bounded by 10YR 3/1 zones; 7.5YR 7/6	sic	m	4/40/3.90	20.3	0.5	0.6	0.1	5.9
				Profile H5, Site 2						
A1	5-15	5YR 3/3	sicl	3fgr	5.85/4.30	34.2	5.4	5.6	0.3	33.0
AB	50-70	2.5YR 3/6	c (25, 29, 46)	2f, vfsbk	5.55/4.05	33.4	6.5	5.2	0.4	36.2
Bt	90-105	2.5YR 3/6	c (28, 18, 54)	2f + msbk	5/65/3.95	33.0	4.6	6.9	0.4	36.0
2BCt	130-150	2.5YR 3/6	cl (38, 30, 32) 16% c.f.	1msbk	5.40/3.70	41.6	4.5	10.0	0.2	35.3

Table 2 (continued).

Horizon	Depth	Moist Color	Texture (s,si,c)	Structure	pH	NH_4OAl C.E.C.	Exch. Cat. Ca	Mg	K	NH_4OAC B.S.
	--cm---				(H_2O/KCl)	------meq/100 g-----				%
				Profile H6, Site 2						
A	10-25	5YR 3/3	c (26, 31, 43)	2mgr→2vrsbk	5.85/4.30	35.4	6.4	5.6	0.3	34.7
Bt	50-70	2.5YR 3/6	c (29, 17, 54)	2msbk→2fsbk	5.42/3.85	34.2	5.4	5.9	0.3	33.9
2BCt	90-110	2.5YR 3/6	cl (37, 25, 38) 15% c.f.	1msbk→1am.si.s.	5.32/3.70	39.5	3.6	7.6	0.2	28.9
				Profile H7, Site 2						
A	10-25	5YR 3/4	1 (35, 38, 27) 15% c.f.	2fgr	6.10/4.80	32.2	5.3	5.1	0.4	33.5
				Profile E4T1, Site 3						
Ap	0-25	10YR 3/2	sil (21, 55, 24)	2f+vfsbk	5.3/	21.9	5.8	1.5	0.4	35.4
A2	25-34	10YR 3/2	sicl (20, 50, 30)	2msbk	5.8/	20.3	7.2	2.5	0.3	49.7
AB	34-70	10YR 3/3 and 10YR 4/4	cl (22, 49, 29)	2m+fsbk	5.7/	18.8	6.1	3.5	0.1	
2ABb	70-81	10YR 5/6	cl (22, 47, 31)	2msbk	5.6/	18.4	5.8	5.0	0.1	60.8
2Btb1	81-92	10YR 5/6	c (23, 32, 45)	2msbk	5.7/	26.7	8.3	7.2	0.1	58.9
2Btb2	92-102	10YR 5/6	c (27, 30, 43)	2msbk	5.7/	26.6	8.1	7.3	0.1	59.0
3BCtb	102-108	2.5YR 4/4 and 10YR 5/6	c (15, 23, 62)	m	5.3	32.3	12.5	12.0	0.3	78.0
3Cr	108-151	2.5YR 5/2	c (5, 15, 70)	m	5.4	40.1	15.3	13.0	0.4	72.3

Figure 5. XRD patterns of <10-μm material from unweathered and weathered Kings Valley Siltstone, site 2. (a) Unweathered siltstone. (b) Weathered siltstone lithorelict from 2BC horizon of profile H6. Both patterns represent Mg-saturated, ethylene glycol solvated material. c = chlorite, f = feldspar, m = mica, q = quartz, s = smectite.

Figure 5.

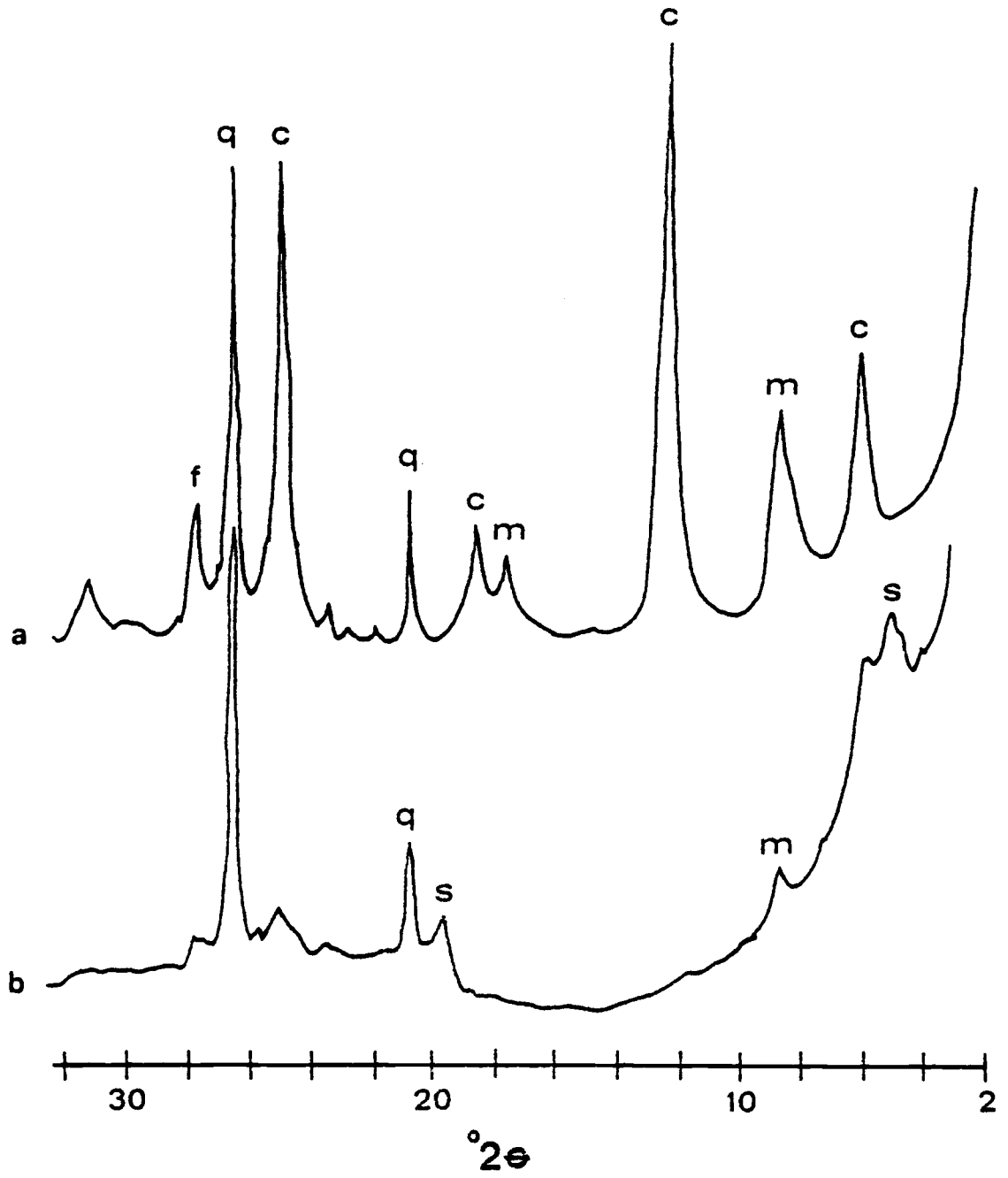

basaltic rock fragments, fragmented pyroclastic grains, and fine sand-sized mica, set in a dense, carbonaceous chloritic matrix. Plagioclase is often replaced by calcite, probably as a result of burial diagenesis. Tuffaceous pyroclastic fragments are characterized by devitrification of glassy constituents, which has led to an apparent increase in the amount of chloritic matrix of the siltstone.

XRD analyses of highly weathered sedimentary lithorelicts (Fig. 5b) show the presence of beidellite (possibility that beidellite-like characteristics are due to weakly developed chloritic intergrade), mica, and poorly crystalline halloysite. The formation of beidellite during weathering may be related to alteration of basaltic clasts or plagioclase (Glasmann and Simonson, 1982a) in the siltstone, and/or alteration of chlorite. True chlorites are commonly regarded as indicators of metamorphic provenance in sediments (Keller, 1970), but recent studies in sediment diagenesis (Hoffman and Hower, 1979) have shown that smectite often alters rapidly to chlorite under conditions of moderate burial. Provenance determination based on the lithology of detrital clasts in the Kings Valley Siltstone suggests local derivation from epiclastic and pyroclastic material of the Siletz River Volcanics, with no indication of metamorphic inputs. Thus, the chlorite present in unweathered samples of Kings Valley Siltstone probably represents advanced diagenetic alteration of volcanic materials.

The formation of beidellite during alteration of this diagenetic chlorite may result from stripping of interlayer brucite sheets, leading to an intermediate phase characterized by chloritic intergrade. This process would explain the extremely high values of exchangeable Mg (Table 3) characteristic of colloids from the lower solum and Cr horizons.

Figure 6. Stability relations of clay phases in the system $MgO-Al_2O_3-SiO_2-H_2O$ at 25°C and 1 atm as the matrix solution activity functions, ph - $1/2pMg^{2+}$ and pH_4SiO_4 (after Weaver, et al., 1971). Solid stars represent solutions from site 2. Open squares represent solutions from site 3. Heavy dotted lines reflect the uncertainty in kaolinite-montmorillonite join position based on uncertainties in the ΔG_f° values of kaolinite and montmorillonite.

Figure 6.

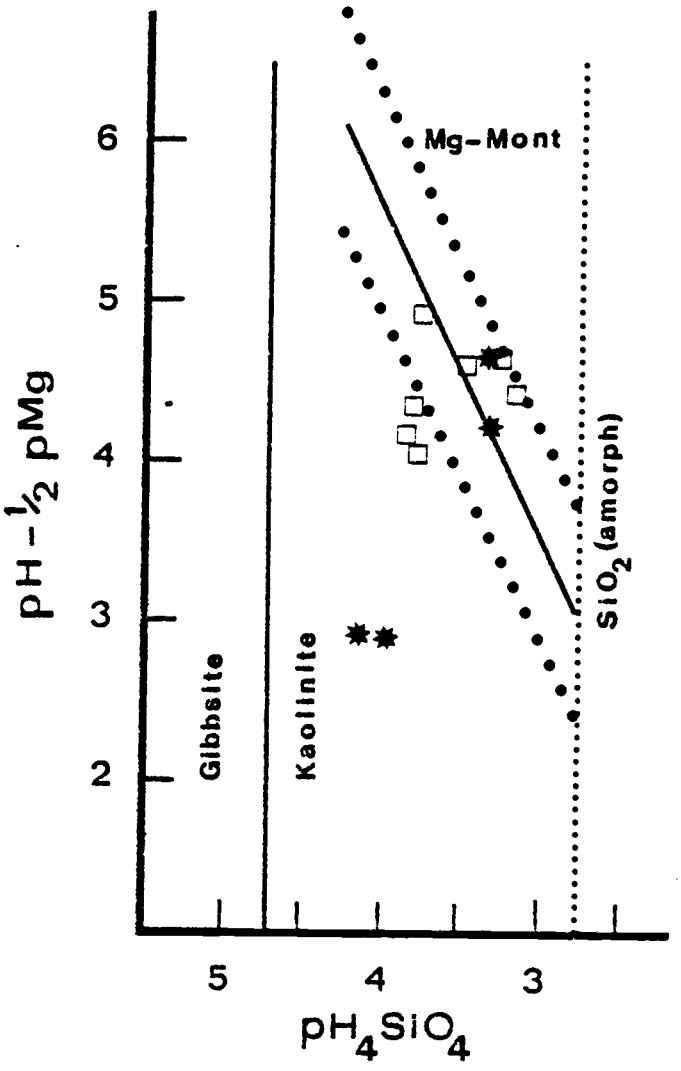
Mg-Mont
SiO_2 (amorph)
Gibbsite
Kaolinite
$pH - \frac{1}{2}\ pMg$
6
5
4
3
2
5
4
3
pH_4SiO_4

Final verification of this hypothesis would require determination of the composition of interlayer hydroxy sheets in the unaltered chlorite.

When water chemistry is plotted on predominance diagrams using solute activity functions $pH-\frac{1}{2}pMg$ and pH_4SiO_4 (after Weaver et al., 1971), stream solutions from site 2 plot in the Mg-montmorillonite stability field (Fig. 6). Soil solutions from this site plot in the kaolinite stability field. This suggests that Mg-saturated smectite is stable in solutions which have been contact with the zone of active bedrock weathering. These solutions surface as stream runoff during periods of temporary soil saturation and account for the concentrated silicate chemistry of stream waters.

Dissolution of diagenetic carbonate and labradorite during bedrock weathering probably produces the high pCa of stream waters. Weathering of tuffaceous pyroclastic and epiclastic material is probably the source of the high pH_4SiO_4 in stream discharge, and the near neutral pH of these waters is probably a result of hydrolysis reactions or carbonate dissolution. Soil solutions, which are more acid, less silicous, and of low ionic strength, probably spill over into the stream during temporary periods of soil saturation, resulting in dilution of stream water chemistry immediately following major precipitation events (Table 4).

Other mineralogical evidence from weathering rind studies (Glasmann and Simonson, 1982a) on basaltic lithorelicts in the soils at site 2 suggest that kaolinite is the stable phase in the upper solum. Smectite forms in poorly drained microenvironments characterized by the microporous weathering crust, but is unstable with respect to halloysite along cracks and channels in the saprolite. The conversion of smectite to halloysite is apparently a slow enough process that much of the 2:1 clay

Table 4. Stream water pH_4SiO_4 and pH related to stream flow.

	15/Jan/80	23/Feb/80	6/Mar/80	11/Dec/80	26/Feb/80†
pH_4SiO_4	3.38	3.33	3.36	3.36	3.31
pH	6.5	6.7	6.6	6.7	6.3
Discharge‡ (dm^3s^{-1})	75	20	30	20	0

†Sample from shallow well in stream channel.

‡Estimated from measured section and stream velocity.

is instead converted to chloritic intergrade during plasmification of saprolitic material in the solum.

Site 3

Soil Solution Chemistry

Results of solution analyses of soil water from Elkins Road Watershed (site 3) are listed in Table 1 and plotted on predominance diagrams in Fig. 1. Data points are centered in the kaolinite stability field. All data points are characterized by pH_4SiO_4 values above quartz solubility and several points plot close to the kaolinite-montmorillonite boundary, especially when Mg-montmorillonite is considered (Fig. 6). Silica concentrations measured by soil equilibration experiments using soil from major horizons from profile E4T1 (see profile description, Table 2) are listed in Table 3. Piezometer water samples from this soil profile (samples E7-3, E7-4, E3-3, and E3-4, Table 1) are characterized by higher pH_4SiO_4 than the equilibrated samples, suggesting that the field solutions may not be in equilibrium with the mineral soil. Solution compositions show considerable variability from horizon to horizon in a particular pedon, as well as between different pedons, contrasting with the fairly uniform solution chemistry of the highly weathered soils at sites 1 and 2. These differences are probably due to the greater geologic variability and age of soil parent materials at site 3 compared to the predominantly basaltic parent materials characteristic of the other sites.

The soils at site 3 are characterized by the presence of a thin surface mantle of lacustrine silts (Glasmann and Kling, 1980) below 122 m elevation. A tile drain system was placed in a subwatershed at site 3 (Lowrey et al., 1981), with the tile lines located approximately

90 cm below ground surface. This location corresponds to the base of the lacustrine silts over much of the subwatershed (Glasmann et al., 1980). Tile discharge was monitored continuously via a V-notch weir which enabled correlation of tile solution chemistry with tile discharge. Recording raingages on the subwatershed permitted comparison of time of peak rainfall with time of peak tile discharge. This experimental design facilitated the collection of water samples characterizing a homogeneous slice of the subwatershed soils and analyzing solution chemistry as a function of relative residence time in the upper 90 cm of the soil. Relative residence time is interpreted from tile discharge. Water samples obtained during periods of high tile discharge, especially on steep portions of the tile line hydrograph, are interpreted as having relatively brief residence time in the soil. Base flow discharge is interpreted as having a longer residence time.

Table 5 presents tile line solution chemistry as a function of tile discharge on several dates. On December 2, 1979, a major storm occurred which produced peak tile instantaneous discharge of 3.75 $dm^3 s^{-1}$ (0.13 c.f.s). When samples were taken the following day, tile discharge had dropped to 0.71 $dm^3 s^{-1}$ and had been at this rate for several hours. Tile water chemistry on this date is similar to other samples obtained during periods of low tile discharge when positive pore water pressure in the silt mantle was low (Lowrey et al., 1981). Cationic species show a general decline in concentration on successive sampling dates, but silica in solution remains constant from sample to sample at comparative tile discharges. Because of the addition of agricultural fertilizers to the soils drained by the tile system, the decreasing concentration of cationic species may be related to leaching of fertilizer salts. Other

Table 5. Solution chemistry as a function of tile line discharge at tile outlet, E4V1, Elkins Road Watershed.

	Date			
	12/3/79	12/19/79	1/2/80	1/14/80
Discharge† $dm^3 s^{-1}$	0.71-	0.99-	0.47+	2.60---
pH	5.6	5.7	5.9	6.1
pH_4SiO_4	3.62	3.63	3.63	3.71
pCa	3.15	3.22	3.26	3.36
pMg	3.23	3.32	3.34	3.46
pK	4.95	4.99	4.99	4.78
pNa	3.60	3.68	3.72	3.87

†+, rising limb of hydrograph
-, falling limb
---, rapidly falling.

research on the watershed has documented the rapid loss of N and herbicides applied to the soil by subsurface soil flow (Hickman et al., 1980; Simmons, 1980). The constant pH_4SiO_4 values over time suggest that silica levels are characteristic of soil mineralogy and not soil amendments. This indicates that the strong dilution of silica in tile water samples obtained during periods of high discharge (data for 1-14-80, Table 5) reflects the kinetics of mineral dissolution, since such samples have relatively short residence time in the soil.

The tile water chemical data also indicate that soil solution is not in equilibrium with soil solid phases. The soil solution chemistry of piezometer samples is probably affected by the rate of lateral subsurface moisture flow in the soil profile, in addition to mineralogical differences between different soil horizons or pedons. Since subsurface moisture flow rates are not the same in different soil horizons (Lowrey et al., 1981), the relative contribution of residence time versus mineralogy to soil solution chemistry is difficult to assess.

Clay Mineralogy

Soil clay mineralogy has been intensively studied at Elkins Road Watershed as a means of separating different soil parent materials (Glasmann and Kling, 1980), clay genesis (Glasmann and Simonson, 1982b), and tracing sediment characteristics during runoff events (Laird and Harward, 1982). These studies have shown that chloritic intergrade and kaolinite are most abundant in the clay fraction of the upper solum, with lesser amounts of mica and vermiculite. The chloritic intergrade is not as stable as the chloritic intergrade characteristic of Coast Range soils (site 2), as evidenced by the reduction in 14 Å peak intensity

Figure 7. XRD patterns of <2-μm material from profile E4T1, site 3. (a) A horizon, 15-25 cm. (b) 2Bt2 horizon. (c) 3Cr horizon. Treatments: 2 = Mg-saturated, ethylene glycol solvated, 4 = K-saturated, 110°C, 0% RH, 6 = K-saturated, 300°C, 0% RH. d-spacings indicated in Angstroms.

Figure 7.

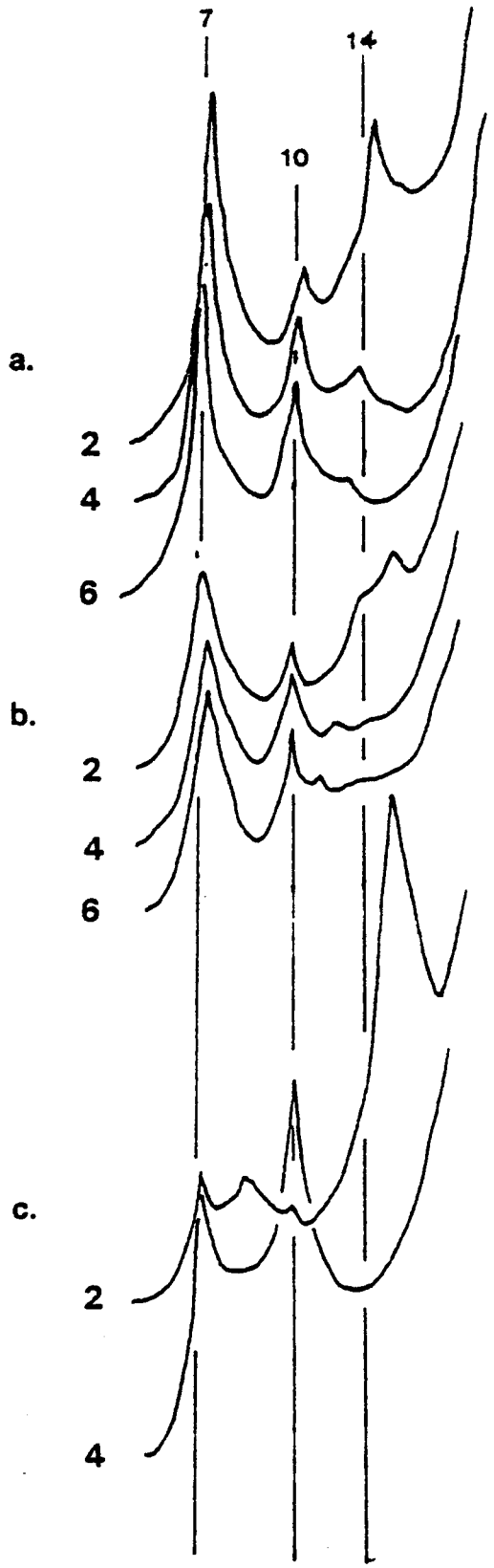

with K-saturation and heating to 300°C (compare Fig. 7a with Fig. 4a, A horizon sample).

Paleosol clay mineralogy shows considerable variation from pedon to pedon at site 3 due to the influence of variable geologic materials from which the paleosols developed (Glasmann and Kling, 1980). At piezometer site E4Z3-3, paleosol clay mineralogy in the 2Bt2 horizon (95 cm) is characterized by chloritic intergrade and kaolinite, with lesser amounts of mica (Fig. 7b). The chloritic intergrade is weakly developed and shows smectite-like characteristics. Piezometer E4Z3-4 is located in the 3Cr horizon of the same profile, and the clay mineralogy of this horizon is dominated by smectite (Fig. 7c). Solution analyses corresponding to these piezometer locations (Table 1, samples E7-4 and E3-4) indicate that the 3Cr horizon solutions plot close to the kaolinite-montmorillonite boundary (Fig. 1). The 2Bt2 solution chemistry plots in the center of the kaolinite stability region, even though the mineralogy of the 2Bt2 and 3Cr horizons are closely akin to each other. The 3Cr horizon consists of weathered tuffaceous sedimentary rock (see profile description, Table 2, profile E4T1). This horizon is characterized by clayey texture and the presence of altered glassy volcanic sands. The glassy materials have probably altered to smectite, and the presence of amorphous silica in the geologic parent materials is indicated by high levels of soluble silica from piezometer and equilibration solution samples. Pedogenic alteration of the easily weatherable tuffaceous materials during paleosol development apparently resulted in the leaching of most readily soluble silica from the profile and transformation of smectite to chloritic intergrade and kaolinite. As silica in the soil solution decreased, kaolinite became the stable phase in the 2Bt2

horizon. Rapid lateral movement of soil water also occurs at the paleosol/3Cr horizon and silt mantle/paleosol interfaces (Lowrey et al., 1981) and probably results in further leaching of soluble components from these regions of the soil. Soil morphologic evidence of strong leaching conditions often occurs at the contact between the silt mantle and the underlying restrictive layers of the paleosol in the form of thin E' horizons (Glasmann[4]).

Micromorphology

Soil micromorphological evidence of mineral authigenesis at site 3 has been reported (Glasmann and Simonson, 1982b). Smectite is partially diagenetic and partially a product of subaerial weathering of volcanic detrital clasts. Kaolinite also formed during diagenetic alteration of paleosol parent materials, but is predominantly formed in the soil by alteration of feldspar. The mutual formation of smectite and kaolinite in the same weathering horizon seems to result from local microchemical differences due to the different compositions of weathering species. Basaltic and vitric tuffaceous clasts of basic to intermediate composition apparently maintain low pH_4SiO_4 in the weathering micro-system, which results in montmorillonite stability, even though kaolinite is the stable phase based on soil solution chemistry. The tortuous microporosity developed during alteration of volcanic clasts (Glasmann, 1982) probably limits outward diffusion of dissolved species into the bulk soil solution. This limiting effect results in stagnant conditions within individual

---

[4]Glasmann, J. R. 1979. The geomorphology and stratigraphy of Elkins Road Watershed. Unpub. M. S. Thesis. Oregon State University, Corvallis, OR.

weathering clasts favoring smectite genesis. Alteration of monomineralic grains also proceeds along tortuous etch porosity which develops along cleavage traces and dislocations on grain surfaces (Berner and Holdren, 1977; Rodgers and Holland, 1979), but these pores are not "buried" within additional microporosity which characterizes altering rock fragments. Thus, diffusion of dissolved components away from altering monomineralic grains into the bulk soil solution is probably more rapid than in altering lithic clasts, and kaolinite forms instead of smectite.

CONCLUSIONS

A number of factors affect soil solution chemistry, including solid phase composition, dissolution kinetics, apparent rate of diffusion of dissolved species through micropores in weathering materials, and relative residence time of solutions in the soil. These factors probably vary in importance under different macroclimatic conditions. This is suggested by the predominance of kaolinitic weathering products from basalt in soils on old landscapes influenced by tropical weathering climates, as compared to the predominantly smectitic weathering products developed from basaltic materials on younger geomorphic surfaces under cooler and drier climatic conditions. It is difficult to interpret the weathering reactions controlling solution chemistry from the chemistry of piezometer solution samples because of the lack of equilibrium between such waters and corresponding soil solid phases; however, with additional data from soil-equilibration and parallel soil micromorphological studies, solution factors affecting clay mineral genesis can be evaluated and interpreted on a microenvironmental basis. Micromorphological examination of solid phase alteration can often help in interpreting the relationship of bulk

solution chemistry to clay genesis by revealing the characteristics of *in situ* weathering products in relation to position in the weathering profile.

CHAPTER II

ALTERATION OF BASALT IN SOILS OF WESTERN OREGON

J. R. Glasmann and G. H. Simonson

Department of Soil Science

Oregon State Universtiy

ALTERATION OF BASALT IN SOILS OF WESTERN OREGON[1]

J. R. Glasmann and G. H. Simonson[2]

ABSTRACT

Basalt alteration from different pedo-microenvironments in western Oregon was studied using petrographic, electron microscope, X-ray diffraction, and differential thermal techniques. Initial alteration was similar in each environment and consisted primarily of mineral dissolution associated with the formation of etch pits and hairline cracks and the development of isotropic domains within feldspar phenocrysts. The stage of alteration characterized by secondary mineral formation was distinctly microenvironment dependent. Smectite formed as the initial crystalline weathering product of basalts in the Oregon Coast Range, but was metastable with respect to hydrated halloysite along fracture zones in the weathering crust where more leaching microenvironments occurred. Smectite altered to chloritic intergrade and halloysite in cyclic wet and dry pedo-environments. The occurrence of gibbsite was related to the alteration of glassy basalt lithologies under acid leaching conditions. Goethite formed from the alteration of an initial non-crystalline iron oxide phase.

---

[1]Oregon Agricultural Experiment Station Technical Paper no. _____.
Contribution of the Dept. of Soil Science. Received _____.

[2]Graduate research assistant and professor of soil science, respectively, Oregon State University, Corvallis, OR 97331.

Additional index words: Weathering, basalt alteration, smectite, beidellite, chloritic intergrade, hydrated halloysite, gibbsite, goethite, microenvironment, scanning electron microscope.

INTRODUCTION

Tertiary basalts underlie large areas of western Oregon. In the central part of the Oregon Coast Range the oldest rocks exposed are Eocene tholeiitic and alkalic basalts and associated porphyritic rocks of the Siletz River Volcanics (Snavely et al., 1968). Prominent headlands along the central and northern Oregon coast are underlain by late Eocene and Miocene basalts (MacLeod and Snavely, 1973). Miocene-age Columbia River Group basalts are exposed in the central Willamette Valley, and Plio-Pleistocene basalts are exposed in the Cascades (Baldwin, 1976). The exposure of rocks of similar texture and composition over a wide geographic area presents an excellent opportunity to study rock weathering under varying climatic and geomorphic conditions. Soil parent materials developed from basaltic rocks in western Oregon include saprolite, colluvium, and alluvium. Weathering products in these materials influence the physical and chemical properties of the soils and affect soil management and land use decisions in western Oregon (Taskey et al., 1978; Istok[3]). Therefore, better understanding of the processes of alteration of basaltic materials and the nature of secondary minerals formed can lead to improvements in soil management and land use decisions.

Most studies of basalt alteration have been concerned with weathering in tropical environments (Eswaran, 1979; Wada et al., 1972; Eswaran and DeConinck, 1971; Parham, 1969; Siefferman and Milliot, 1969; Cady, 1960), although a few weathering studies from temperate climates have

---

[3]Istok, J. 1981. Clay mineralogy in relation to landscape instability in the Coast Range of Oregon. Unpub. M.S. Thesis. Oregon State University, Corvallis, OR 97331.

been reported (Curtin and Smillie, 1981; McAleese and Mitchell, 1958; Smith, 1957). Alteration products of basalt in well drained, high rainfall environments include allophane, imogolite, halloysite, kaolinite, and gibbsite, as well as goethite, hematite, and maghemite. Smectites are typical alteration products under conditions of poor drainage, and they have been found in lower profiles of well drained soils as well, where they are thought to be unstable with respect to kaolinite (Eswaran and DeConinck, 1971). Mineral transformations during rock weathering are governed by the chemistry of pedologic and geologic microenvironments, which may vary considerably over short distances (Glasmann, 1982; Eswaran, 1979). Microenvironmental conditions may also vary with time, both periodically, such as during wetting and drying cycles, and geologically, in response to major climatic fluctuations. The degree to which long term climatic fluctuations leave an imprint on mineral transformations in the soil is related to the age and stability of geomorphic surfaces on which the soils occur.

The objectives of this research were to study basalt alteration under diverse weathering environments, to characterize weathering products, and to relate the genesis of secondary phases to conditions of the weathering microenvironment. Diverse weathering environments in western Oregon are provided by geomorphic surfaces of different age and stability under a variety of climatic conditions. In the Willamette Valley, remnants of extremely old erosion surfaces are underlain by basalt. Deep red bauxitic soils occur on these surfaces and are considered relicts of intense weathering under warm humid climatic conditions which existed during Miocene time (Corcoran and Libbey, 1956). The present climate, however, is cool and seasonally dry. Remnants of old erosion

surfaces also occur in the Coast Range, but many have been truncated, and materials that once lay deep within a weathering profile are now exposed to the surface environment or have been mixed with other materials in thick colluvial deposits (Balster and Parsons, 1968). The climate where these soils occur is cool and uniformly moist. Younger geomorphic surfaces in western Oregon include Pleistocene and Holocene alluvial and marine terraces. Basaltic sands and gravels are important components of soils developed in these positions. The soils characteristic of younger surfaces have developed under more uniform macroclimatic conditions than the soils of older geomorphic surfaces, although deposits underlying younger surfaces may have been influenced by prior weathering cycles. The weathering microenvironment of each geomorphic surface is a function of site-specific properties, such as parent material composition, soil drainage, landscape position, soil depth and horizonation, and biotic influences. These factors act to modify macroclimatic conditions which are characteristic of broad geographic areas and define the chemical conditions under which clay minerals form.

MATERIALS AND METHODS

Description of Study Area

Altered basalts were studied at four locations in western Oregon. Site OR, located about 1 km south of the town of Otter Rock on the central Oregon Coast (SW 1/4, SE 1/4, Sec. 32, T9S, R11W), lies on an elevated Pleistocene marine terrace about 31 m above sea level. The area receives about 1800-1900 mm precipitation annually and has an average annual temperature of 10.2°C (51°F). Soils have udic moisture regimes and isomesic temperature regimes. The terrace was cut into

Miocene-age sandstone and siltstone of the Astoria Fm. and is mantled by Pleistocene beach and fluvial deposits. Soils on this terrace are predominantly Haplorthods developed from stratified marine and fluvial sands which contain rounded and subangular basaltic clasts. The source of the clasts was probably the Columbia River Group Cape Foulweather Basalts which are exposed in the prominent headlands just north of Otter Rock. These rocks consist of palagonitized tuff breccia, subaerial basalt flows, subaqueous water-laid fragmental debris, and related feeder dikes and sills (Snavely et al., 1969). The basalt is characterized by sparse, large, labradorite phenocrysts in an aphanitic (microcrystalline) ground mass, and shows vitrophyric, hyalo-ophitic, intersertal, intergranular, and amygdaloidal textures.

Sites H13 and H14 are located in dissected mountainous topography of the central Oregon Coast Range in the Corvallis Watershed (H13: SW 1/4, SE 1/4, Sec. 12, T12S, R7W; H14: SW 1/4, NW 1/4, Sec. 12, T12S, R7W). Both sites are situated along Old Peak Road in an area characterized by an upland of moderately undulating topography intersected by steep walled valleys. Precipitation in the area averages 1600-1700 mm annually, most of which falls during the winter as rain. The soil moisture regime, however, is udic. The average annual temperature is 10.1°C (50.5°F), and the soil temperature regime is mesic. The soils are predominantly deep red Ultisols (Typic Haplohumults) formed from basalts and basaltic colluvium from the Eocene Siletz River Volcanics. The Siletz River Volcanics consist of pillow basalts, breccias, flows, tuffs, and related sediments (Snavely et al., 1968). Rocks in the study area are characterized by amygdaloidal, aphanitic to fine-grained tholeiitic pillow basalts, but massive to rudely columnar jointed basalt sills and

flows also occur. Zeolites and calcite are common in brecciated deposits and occur as amygdules in the basalt. Holocrystalline to hypocrystalline, commonly intersertal or vitrophyric textures dominate, with less common subophitic and intergranular textures.

Site BP is located on the western margin of the Willamette Valley in low foothills underlain by Eocene sedimentary rocks (NW 1/4, SE 1/4, Sec. 35, T12S, R6W). These rocks have been intruded by a basaltic sill (Oligocene?) which is exposed in the summit area and has contributed to the colluvium from which the soils of the area developed. The area receives about 1100-1200 mm precipitation annually and has an average annual temperature of 10.5°C (52°F). The soils are Haplohumults that have a xeric moisture regime and a mesic temperature regime.

Field and Laboratory Procedures

Samples at Site OR were taken from the major horizons of a Yaquina soil (Aquic Troporthod). Samples at site H13 were taken from spheroidally weathered, columnar jointed basalt exposed in an abandoned quarry. One set of samples was taken from the fresh rock-weathering rind interface. Another was taken from red, platy portions of the weathering rind 3-5 cm thick. A third was taken from irregular light reddish brown zones separating the weathering rinds along vertical and horizontal joint planes. Samples at site H14 were comprised of weathered basaltic cobbles from a depth of 1 m in the argillic horizon of a Honeygrove soil (Typic Haplohumult) exposed in a road cut. Major soil horizons of this profile were also sampled. Samples at site BP consisted of weathered basaltic cobbles taken from the B horizon of a Bellpine soil (Xeric Haplohumult).

All samples were sealed in plastic containers while in the field to retain their field moist status. Undisturbed, oriented samples at site OR were taken in modified Kubiena boxes for later thin section analyses. Bulk soil samples were taken at Site OR for clay mineral analyses, pH measurement (2:1 H_2O and KCl), and particle size determinations using a hydrometer method. Weathering rinds at sites H13, H14, and BP were subsampled for clay mineral analysis while in field moist condition after carefully removing adhering soil material. Thick rinds showing concentric parting were further subsampled to separate natural breakage units. Thin, apparently monomineralic zones were subsampled from the weathering rinds using a binocular microscope and a microscalpel to scrape off sufficient material for analysis. All subsamples were prepared for clay mineral analyses by dispersing them in dilute Na_2CO_3 and separating the samples into silt and clay fractions by centrifugation. The separates were Mg-saturated by washing three times with 1 N $MgCl_2$ followed by three washings with distilled water. Subsamples of the Mg-saturated clay were used for transmission electron microscope (TEM) and differential thermal analysis (DTA). Portions of the Mg-saturated separates were used to prepare oriented clay films for X-ray diffraction (XRD) analysis using a paste method (Theisen and Harward, 1962). The remaining material was K-saturated using 1 N KCl and distilled water washing, after which slides for XRD analysis were again prepared. The criteria upon which mineral identification were based are presented in Table 6. Analyses were made with a Norelco Diffractometer equipped with a focusing monochromator using Cu K alpha radiation.

Characterization of the clay fraction by TEM analysis was performed using a Phillips EM 300 operated at 80-100 kV and 7 μa and equipped with

Table 6. Criteria for clay mineral identification based on $d_{(001)}$ spacings (in Å) under various treatments.

	Kaolinite	Halloy-site	Mica	Vermi-culite	Montmor-illonite	Beidel-lite	Chlorite	Chloritic Intergrade
Mg-saturated								
54% RH:	7.15	7.3-10	10-10.5	14-14.5	15	14.5-15	14.2	14-15
ethylene glycol:	7.15	7.3-10	10-10.5	14-14.5	16.5-17	16.5-17	14.2	14-17
glycerol:	7.15	7.3-10	10-10.5	14-14.5	17.5	14.5	14.2	14-17
K-saturated								
105°C:	7.15	7.3-7.5	10	10-10.5	10-10.5	10-10.5	14	11-14
54% RH:	7.15	7.3-7.5	10	10-10.2	12	11.5-12	14	14
300°C:	7.15	7.3-7.5	10	10-10.2	9.9-10.4	10-10.5	14	11-14
500°C:	--	--	10	10	9.8-10.2	10	14	10-13

Note: Hydroxy interlayered smectities and chloritic intergrades may respond to solvation treatments in a manner similar to beidellite. Also, kaolinite may not be recognized in the presence of chlorite (esp. Fe-rich chlorites), due to overlap of chlorite $d_{(002)}$ and kaolinite $d_{(001)}$ diffraction lines.

a liquid nitrogen decontamination system. Specimens were prepared by dropping a dilute clay suspension onto holey, Formar coated copper grids. Micrographs were obtained on a "shoot first, ask questions later" basis to avoid the adverse effects of prolonged specimen-electron beam interaction (Jones and Uehara, 1973). A DuPont Model 900 Differential Thermal Analyzer was used for DTA characterization of Mg-saturated samples.

Thin sections of basalt cobbles, weathering rinds, and undisturbed soil samples were prepared after impregnating oven dry samples with a 70/30 resin/methyl methacrylate mixture under vacuum. The mixture was allowed to harden over a period of two weeks to avoid formation of stress cracks due to too rapid curing of the plastic. Point counts were made to determine species composition of marine and fluvial sands at site OR. Photomicrographs of all samples were taken to facilitate comparison of weathering trends between the different sites.

Fracture surfaces from different zones of the weathering crusts of samples from sites H13, H14, and BP were prepared and examined with a binocular microscope to map distinguishing features. Fractured clods from major soil horizons at site OR were prepared in a similar manner. The specimens were then mounted on brass stubs using Duco cement and sputter coated with gold in a vacuum evaporator for scanning electron microscope analysis (SEM) using an AMR 1000 SEM. Specimen surfaces other than those to be observed were painted with a colloidal graphite compound to help minimize charging problems caused by specimen/electron beam interaction. The morphologic information obtained by SEM analysis has proven extremely helpful in evaluating the progress of mineral alteration when combined with parallel petrographic and clay mineral characterization studies (Glasmann, 1982; Eswaran, 1979).

RESULTS AND DISCUSSION

Thin sections of Siletz River Basalt from the Oregon Coast Range (sites H13, H14) show intergranular to subophitic textures, with augite occurring as aggregates of grains in the intersticies of a network of randomly oriented labradorite laths. A few large augite euhedra occur, along with accessory magnetite and altered basaltic glass. The glass represents the mesostasis of the basalt and has devitrified to a green, fibrous, weakly anisotropic clay mineral (chlorophaeite). This clay occurs in up to 10 percent of the samples studied and is not considered to be a product of subaerial weathering since its occurrence is widespread throughout much of the Siletz River Volcanics (Snavely et al., 1968).

Unweathered portions of cobbles from the foothills intrusion (site BP) show subophitic to diabasic texture, containing laths of normally zoned plagioclase (average composition An_{60}) and pyroxene, with lesser amounts of magnetite, ilmenite, and minor quartz. Some cobbles contain abundant glass and probably represent material from the chilled margin of the intrusion. The presence of quartz and the more sodic nature of the plagioclase suggests that the sill from which the cobbles originated was approaching diorite in composition.

Detrital basaltic clasts from the marine terrace (site OR, Plates 4a, 4b) are dominated by glassy (vitrophyric) (Plate 4b) and microcrystalline (aphanitic) (Plate 4a) types with labradorite being the only phenocrystic phase. Significant differences in soil morphology and basalt abundance and lithology occur across the lithologic discontinuity between the 2C horizon and the 3Bsb and 3Eb horizons (Table 7). The buried soil which formed in well sorted, somewhat negatively skewed, rounded, fine grained beach sands. Below the discontinuity basaltic clasts in the

Plate 4. (a, b, c, d) Photomicrographs of basalt alteration. (a) Sands from 3Bsb horizon at Site OR showing weakly altered basaltic clast and weak pellicular dissolution of adjacent augite grains. (b) Altered vitrophyric amygdaloidal basalt clasts from 2C horizon at Site OR. (c) Zone 1 alteration of Siletz River Basalt, Site H14, illustrating etching of plagioclase, development of isotropic domains, and alteration haloes surrounding chlorophaeite. (d) Initial alteration of intrusive rock, Site BP. (e, f, g, h) Scanning electron micrograph of zone 1 basalt alteration. (e) Zone 1 alteration consisting of minor dissolution and the development of hairline cracks. (f) Non-crystalline material lining dissolution void in plagioclase. (g) Altered plagioclase with granular, apparently amorphous, alteration product. (g) Etched augite.

Plate 4

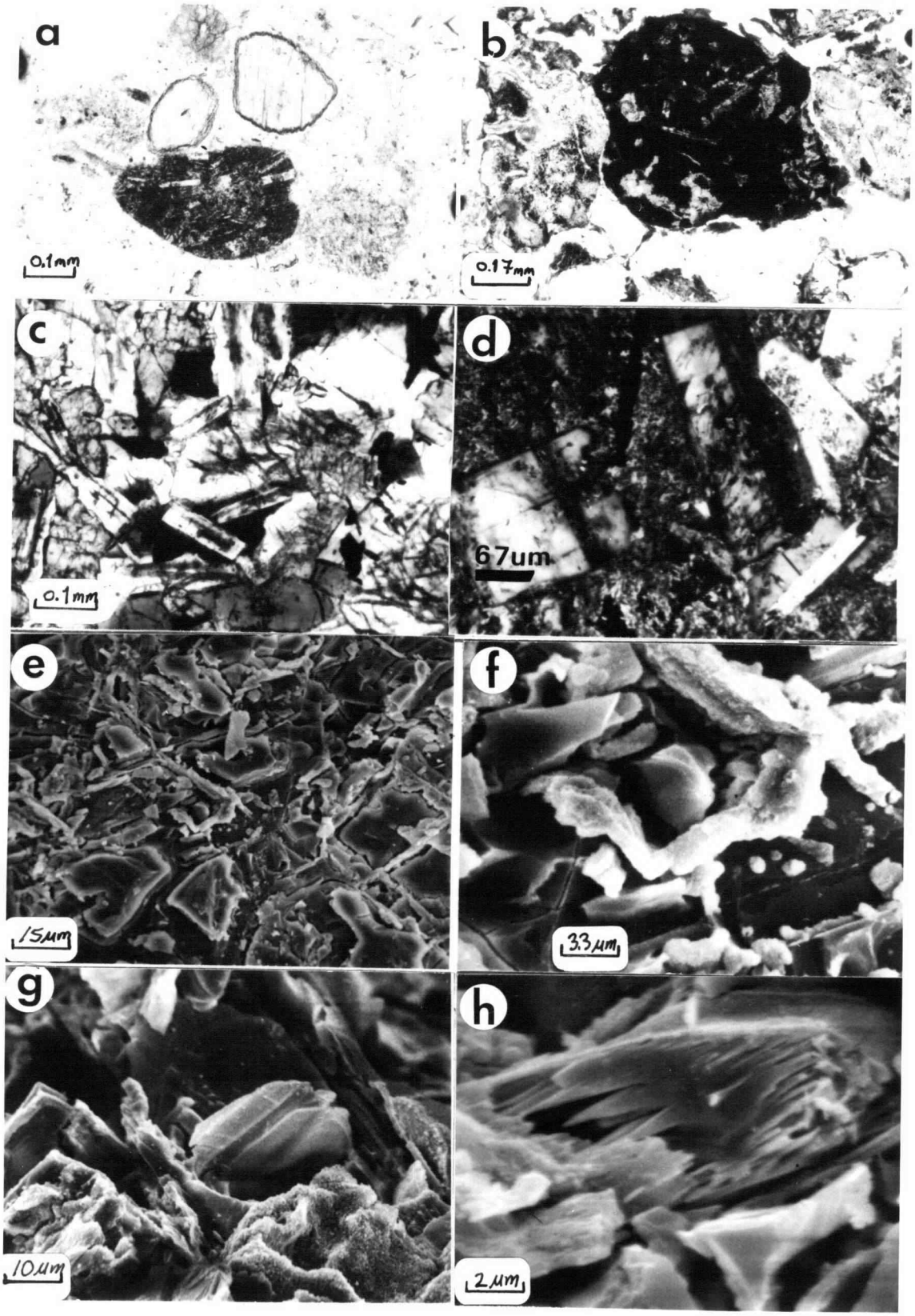

Table 7. Some properties of the Yaquina soil at site OR.

Horizon	Depth (cm)	Color (Munsell)	Texture (s, si, c)	pH KCL/H_2O	Fabric/Mineralogy*
Bs	45-100	10YR4/4	cl (37.1, 30.2, 32.7)	4.1/5.2	Argillasepic plasmic fabric. Q = 80% of sand fraction. Strong dissolution of F, A, H.
2C	100-195	2.5YR4/8	sl (71.4, 20.4, 8.2)	4.3/4.8	Laminated very fine-coarse sand, free grain organo-sesquans, gibbsans. 90% Ba in coarse laminae; <30% Ba in fine laminae. All Ba highly altered.
3Eb	195-215	5YR8/1	sl (73.3, 18.7, 8.0)	4.7/4.9	Silasepic plasmic fabric, common carbonized wood fragments. 40% Q, 45% F (most altered), ≤5% A + M, 3-5% altered Ba.
3Bsb	215	7.5YR5/6	s (92.6, 3.7, 3.7)	4.9/5.4	Rounded, well-sorted, fine sand, few simple vugh organo-sesquans. 45% Q, 40-45% F (unaltered), ≤5% A + H + M, 3-5% weakly altered Ba.

*Q = quartz, F = feldspar, A = augite, H = hornblende, M = magnetite, Ba = basaltic clasts.

3Bsb horizon make up about five percent of the sand and are largely aphanitic varieties containing sparse phenocrysts of labradorite (Plate 4a). Minor intersertal, subophitic, amygdaloidal, and palagonitic varieties were also observed. Above the discontinuity, basaltic sands of the 2C horizon are much more abundant, and they are trough cross-bedded, poorly sorted, angular to subangular, and contain gravels up to 3 cm in diameter. The coarse fragments consist dominantly of palagonitized tuff breccia and vitrophyric amygdaloidal basalt (Plate 4b). The sorting, angularity, composition, and sedimentary structures observed in this sand indicate that it is of fluvial origin. The difference in basalt lithology between the 2C horizon and the underlying material is probably due to destruction of the softer, more porous and weakly cemented breccias and glassy particles in the high energy beach environment, thus concentrating the more resistant aphanitic basalts in the beach sands. Basaltic clasts were not identifiable in the A or B horizons of the soil at site OR. However, rounded, well sorted quartz grains in the sand fraction of these horizons are like the sands in the 3Eb and suggest that the parent materials of the A and B horizons formed by deposition in a beach environment. Therefore, the finer texture of the B horizon is a result of weathering and does not reflect depositional environment.

The progressive alteration of basalt from fresh rock to essentially soil matrix was observable at each sample site. Similar trends in primary mineral alteration were noted between sites, although the materials studied occur on geomorphic surfaces of different age and climate, and the characteristics of secondary minerals formed differ from site to site. For the purpose of discussion, descriptions of unrelated samples which show similar stages of alteration are grouped into zones. The

initial alteration of fresh rock or basaltic sediment is included in zone 1. Mineralogical changes characteristic of this zone were observed at the fresh rock-weathering rind interface in hard rock samples from sites H13, H14, and BP, and in 3Bsb sands at site OR. Mineralogical changes which are intermediate between fresh rock and saprolite are discussed under zone 2. Advanced alteration leading to the formation of saprolitic material is discussed under zone 3. Alteration resulting in destruction of saprolitic texture is covered under zone 4. These zones are not rigidly defined in nature. For example, alteration characteristic of zone 4 may extend along cracks and channels into weathering rinds dominated by zone 3 alteration, and biotic factors may modify the distribution of weathering zones.

Zone 1

The initial phase of basalt alteration is characterized by the development of etch porosity on the surfaces of feldspars and pyroxenes (Plate 4c, d). The glassy or chlorophaeitic material is greenish brown in fresh rock and changes color to red or reddish brown during initial alteration, probably indicating the oxidation of iron in these materials. Plagioclase usually shows a dotted alteration pattern (Stoops et al., 1979) which is probably due to the dissolution of material along cleavage traces or dislocations in the crystal structure (Berner and Holdren, 1977). Augite shows weak pellicular congruent dissolution. Weak mineral etching extends for several millimeters into the fresh basalt beyond the sharp, well defined boundary of the weathering crust. This abrupt boundary is defined by the strong reddish color of the mesostasic material and by the presence of alteration haloes from oxidation of iron in the devitrified glass which stain adjacent crystalline grains. Dissolution

voids in plagioclase begin to show lining by weakly birefringent hyaline material in this initial zone of alteration.

Scanning electron micrographs of the initial phase of alteration show the presence of hairline cracks and etch pits of various morphologies, some partially rimmed by amorphous material (Plate 4e). Some of the cracks may have developed during the preparation of fresh fracture surfaces for SEM observation, but others, especially those lined by amorphous material, clearly owe their presence to weathering (Plate 4f). Characteristic almond and rectangular shaped etch pits occur on plagioclase and are helpful in identifying feldspars whose lath morphology is not readily apparent on specimen fracture surfaces which show zone 1 alteration (Plate 4e). The lath morphology becomes increasingly noticeable as alteration increases and specimen fracturing reflects weaknesses developed during weathering, rather than tensile failure across mineral grains (Plate 4g). Pyroxenes from the initial zone of weathering often show distinctive saw-toothed etching (Plate 4h), similar to that reported previously (Glasmann, 1982). The initial products of basalt alteration in western Oregon soils show strong morphological similarities to first phase alteration products for tropically weathered basalts (Eswaran, 1979; Plates 6a, b) and altered western Oregon andesites (Glasmann, 1982).

Basaltic clasts from the 3Bsb horizon of the soil at site OR show labradorite alteration similar to that described for Zone 1. Palagonitic clasts show strong reddish brown staining and the development of minute birefringent domains. Most of the grains in this horizon are coated with pale reddish brown, isotropic free-grain organo-sesquans (Brewer, 1976). It is possible that some of the staining which occurs along

dissolution pores in plagioclase laths is due to infiltration of illuvial amorphous material into the etched basaltic clasts.

The results of X-ray diffraction analyses of pulverized material from the initial zone of alteration are summarized in Table 8. Strong peaks for plagioclase, augite, and other primary minerals identified in section were present. Poorly crystalline smectite occurs in samples of Siletz River Basalt and probably represents clay formed during initial alteration of basaltic glass or chlorophaeite, which is loosely defined as a smectite or chlorite-like mineraloid. Poorly crystalline smectite also occurs as the initial alteration product of palagonitic grains in the Cape Foulweather Basalt (Fig. 8a).

Zone 2

Zone 2 alteration is characterized by increased solution etching and the pronounced development of isotropic domains within plagioclase (Plate 5a, b). These domains enlarge until plagioclase laths become completely isotropic, except for the presence of reddish yellow, weakly birefringent hyaline material which often occurs in the reticulate network of dissolution porosity. Altered basaltic cobbles in the colluvium at site BP show the presence of opaque material within the feldspar microcracks (Plate 5a). The transition from weakly etched plagioclase to completely isotropic laths occurs over a narrow front, often no wider than the length of a single feldspar lath. Augite undergoes a similar drastic change over this short distance, showing near complete dissolution leading to the formation of rounded voids which are often bounded by dark reddish brown isotropic material. The rounded voids are subsequently filled with fibrous clay. The alteration of basalt along sharp fronts has also been reported in tropical weathering

Table 8. Mineralogy characteristic of different weathering zones for sites H13 and H14, BP, and OR summarized from XRD analyses. A = augite, B = beidellite, C = chlorite, CI = chloritic intergrade, F = feldspar, Gi = gibbsite, Go = goethite, dH = dehydrated halloysite, hH = hydrated halloysite, Hb = hornblende, M = mica, Ma = magnetite, Q = quartz, S = smectite.

Site	H13, H14	BP	OR
Zone 1[†]	F, A, Ma, S[≠], Q[§]	F, A, Hb, Ma, S[≠], Q	S[≠]
Zone 2	F, B, Go	F, CI, Go	CI, M
Zone 3	B, Go, hH	CI, Go, dH	C, Gi
Zone 4	B, hH, Go	CI, dH, Go	CI, C, Gi

[†]XRD of crushed rock, sites BP, H13, and H14, and clay dispersed from 3Bsb horizon, site OR.

[≠]denotes poorly crystalline smectite.

[§]quartz is a minor component of tholeiitic basalts of the Siletz River Volcanics.

Figure 8. XRD pattern of basalt alteration products. (a) Poorly crystalline smectite from 3Bsb horizon, Site OR. (b) Heat-stable chloritic intergrade, minor mica, and possible kaolinite from 3Eb horizon, Site OR. Mica is of detrital origin. (c) Gibbsite, chloritic intergrade, and possible kaolinite from 2C horizon, Site OR. (d) Chloritic intergrade (less heat-stable than 3Eb clays), and possible kaolnite from B horizon, Site OR. (e) Poorly crystalline smectite and possible halloysite characterizing zone 1 alteration, site BP. (f) Smectite showing development of hydroxy interlayering evidenced by resistance to collapse with K-saturation and heating, zone 2 alteration, Site BP. (g) Beidellite and poorly crystalline halloysite characterizing zone 2 alteration, site H13. (h) Hydrated halloysite and beidellite from zone 4, site H13. d-spacing in Angstroms.

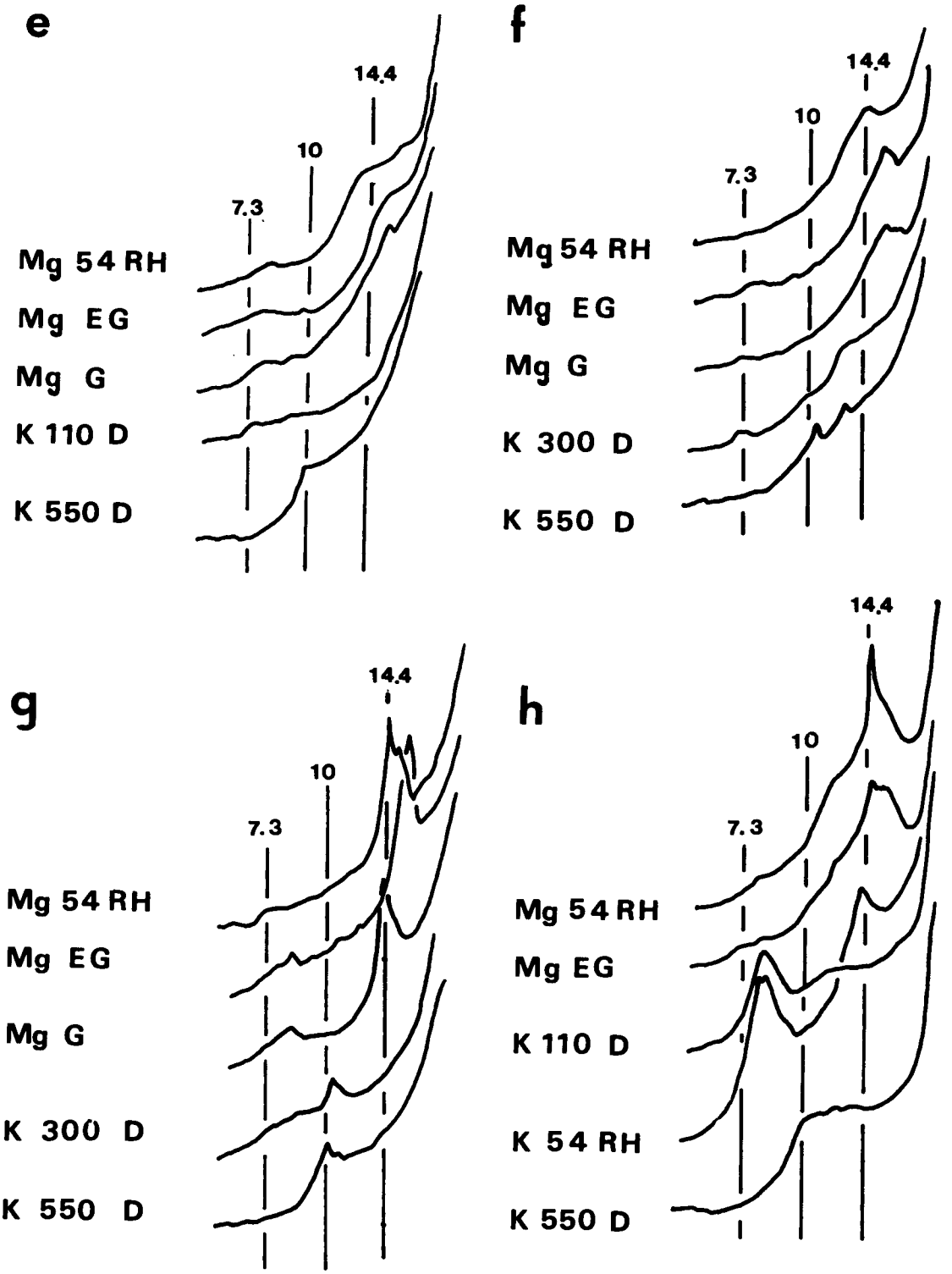
e
14.4
10
7.3
Mg 54 RH
Mg EG
Mg G
K 110 D
K 550 D
f
14.4
10
7.3
Mg 54 RH
Mg EG
Mg G
K 300 D
K 550 D
g
14.4
10
7.3
Mg 54 RH
Mg EG
Mg G
K 300 D
K 550 D
h
14.4
10
7.3
Mg 54 RH
Mg EG
K 110 D
K 54 RH
K 550 D

Plate 5. (a, b) Photomicrographs of basalt alteration characterizing zone 2. (a) Corroded plagioclase laths embedded in birefringent clayey matric, site BP. (b) Crossed nichol view of Plate 2(a), showing isotropic character of altered plagioclase laths. (c, d, e, f, g, h) Scanning electron micrographs of zone 2 basalt alteration. (c) Etched plagioclase from site H14 with fibrous beidellite in foreground which formed by alteration of chlorophaeite. (d) Sheets of beidellite within altered plagioclase. (e) Dissolution of plagioclase and development of large rectangular void surrounded by altered intergranular augite (H13). (f, g, h) Augite alteration. (f) Dissolution of intergranular augite shown in Plate 2(e), showing formation of smectite in dissolution voids. (g) Large rounded void formed by dissolution of augite with partial clay filling. (h) Complete filling of similar void produced beidellite pseudomorph after augite.

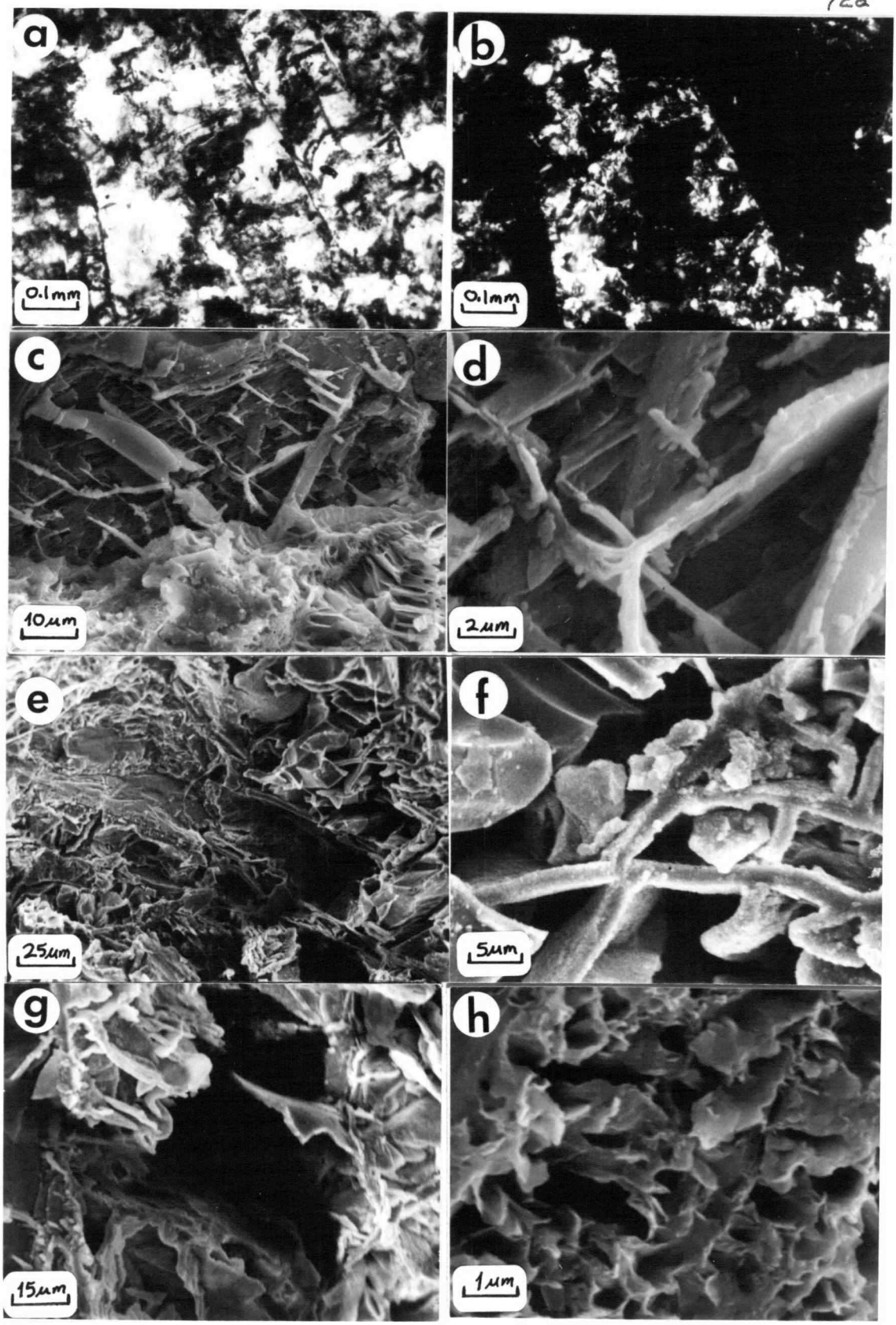
a
0.1mm
b
0.1mm
c
10μm
d
2μm
e
25μm
f
5μm
g
15μm
h
1μm

environments (Cady, 1960; Flach et al., 1968) and seems to be characteristic of alteration of fine grain, mafic igneous rocks.

Plates 5c, d, e, and f illustrate the intermediate type of plagioclase alteration characteristic of zone 2 (Site H14). Plate 5c shows a plagioclase lath with a well developed rectangular etch pattern extending obliquely across the upper part of the micrograph. The outer margins of the crystal are less altered than the core, due to the greater stability of the more sodic zones. The birefringent hyaline material seen in voids in thin section is probably the same as that which forms irregular sheets and fibres seen by SEM (Plate 5c, d). The lath pictured in Plate 5c is surrounded in the lower part of the micrograph by a fibrous alteration product of chlorophaeite. XRD analyses of site H14 subsamples characterized by zone 2 alteration indicate that beidellite is the predominant weathering product (Fig. 8g). Minor amounts of poorly crystalline halloysite are also suggested by Fig. 8g, but this may represent contamination due to difficulty of separating narrow zones of the weathering crust. No halloysite was observed by SEM at site H14 in samples characterized by zone 2 alteration. The altered chlorophaeitic material shown in Plate 5c is optically similar to the birefringent hyaline material which lines dissolution pores in altered plagioclase. This suggests that the irregular sheets and fibers developed within altering plagioclase (Plates 5c, d) may also be beidellite.

Somewhat more advanced zone 2 alteration from sample H13 is shown in Plate 5e. Here the plagioclase lath trends diagonally across the micrograph from upper left to lower right. The lath has been largely hollowed out by dissolution and the formation of irregular sheets of clay is apparent. Intergranular augite above the plagioclase in the

upper right hand corner shows advanced dissolution and the formation of a clayey network within the dissolution voids (Plate 5f). Pyroxene alteration in zone 2 generally results in the complete destruction of the crystals leading to the formation of smectite or goethite pseudomorphs. The sequence of events leading to the formation of these pseudomorphs is illustrated in Plates 5f, g, and h. In Plate 5f, most of the augite has been dissolved and clay has formed in the voids, but a few remnant fragments of apparently fresh pyroxene devoid of surface contaminants occur in the upper left corner. In Plate 5g, complete dissolution of augite has left a rounded void in which clay formation has begun. Continued clay formation finally results in complete filling of such voids by material exhibiting complex honeycomb morphology (Plate 5h). Individual clay crystals are too small to be resolved by SEM, but the honeycomb morphology shown in Plate 5h is common of authigenic smectites (Wilson and Pittman, 1977), and similar to material previously identified as beidellite (Plate 5c). Gibbsite and halloysite pseudomorphs, common in tropically weathered basalts (Eswaran, 1979), were not observed in altered basalts of the Oregon Coast Range, although these minerals occur in altered basalts elsewhere in the Willamette Valley (Corcoran and Libbey, 1956), where they developed during Miocene-age tropical weathering.

Zone 3

Zone 3 alteration is characterized by the complete dissolution of plagioclase, leaving irregular lath-shaped voids in which secondary minerals form (Plates 6a, b). The altered basalt in zone 3 may properly be considered saprolite, since it consists completely of secondary minerals preserving the original rock fabric (Eswaran and Wong Chaw Bin, 1978). This phase of alteration characterizes the outermost zone of

Plate 6. (a, b) Photomicrographs of advanced basalt alteration (zone 3). (a) Irregular, rectangular-shaped void from plagioclase dissolution filled with fibrous smectite (site BP). (b) Crossed nichol view of Plate 3(a), showing birefringent clayey pseudomorph and isotropic, sesquioxide rich matrix. (c, d, e, f, g, h) Scanning electron micrographs of zone 3 alteration. (c) Near complete plagioclase dissolution, site H13. (d) Goethite crystals precipitated on walls of plagioclase dissolution void. (e) Crystal splitting and "walnut" morphology in goethite crystals. Note finely bladed character of background material which may be amorphous iron oxides or much smaller goethite particles. (f) Filling of plagioclase dissolution void by beidellite, site H14. (g) Frond structure of amorphous iron oxides with scattered adhering goethite crystals. (h) Close-up of frond-like structure showing minute bladed particles and goethite.

Plate 6

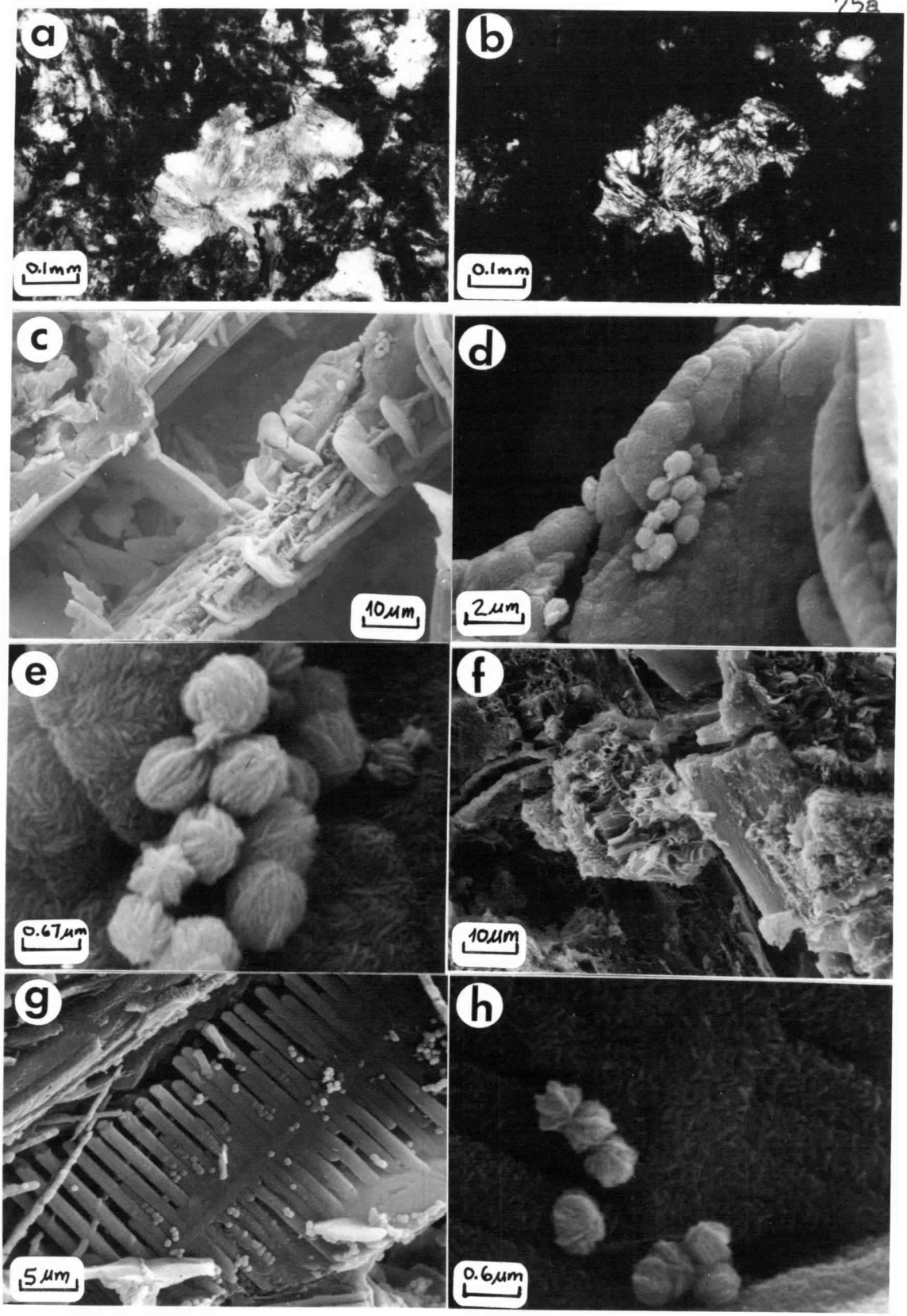

weathering crusts at sites H13, H14, and BP, and 2C horizon basaltic clasts at site OR.

Complete dissolution of plagioclase at site H13 is shown in Plate 6c. Irregularly oriented plates of the host grain remain in the dissolution cavity, and goethite has formed on the surface of the cavity in the upper right corner.

Under higher magnification, the goethite crystals have walnut-like morphology, some crystals showing crystal splitting which has produced six-pointed star-shaped morphologies (Plates 6d, e). Identical crystal splitting in goethite from tropically weathered basalts was reported by Eswaran (1979). The goethite pictured in Plates 6d and e rests on a surface composed of minute bladed material which may be composed of amorphous iron oxides or hydroxides. This material probably corresponds to the opaque rims often seen on plagioclase dissolution voids in thin section. The bladed material may convert to goethite over time. The minute bladed particles also characterize much larger, unusual frond-like structures having tubular arms of various lengths which protrude orthogonally from a central axis (Plates 6g, h). Goethite is again associated with these structures, but the genesis of these "fronds" is obscure. The occurrence of these structures within feldspar dissolution cavities and bordering clayey feldspar pseudomorphs suggests migration of dissolved iron and subsequent precipitation on void walls elsewhere in the weathered basalt. The dissolved iron probably originates during congruent dissolution of augite, which is favored by wet, reducing conditions (Siever and Woodford, 1979). Although reducing conditions are not suggested by profile morphology in the Haplohumults at sites H13, H14, and BP, the soils of these areas do have moments of saturation

during periods of prolonged winter precipitation (Glasmann and Simonson, 1982). The micron-sized pores characterizing most of the weathering crust are probably filled with solution during drier periods of the year. Thus, it may be possible for saturated, reducing conditions to exist on a microscale in weathering lithorelicts in an otherwise well-drained, aerated soil profile.

The formation of a fibrous clayey alteration product in a lath shaped dissolution void characterizing zone 3 altered basalt from sites H13 and H14 is illustrated in Plate 6f. The clay mineralogy of zone 3 weathering products from these sites is summarized in Table 8. Beidellite again shows as the dominant phyllosilicate by XRD and is strongly suggested by DTA analyses of clay from this weathering zone (Fig. 9b). Therefore, the fibrous clayey alteration product seen by SEM in Plate 6f is probably beidellite. Other clay minerals formed during zone 3 alteration include poorly crystalline chloritic intergrade at site BP (Figs. 8e, f, and 9a) and gibbsite at site OR (Fig. 8c and 9e; Plates 7a, b).

Differences in authigenic clay composition between the various sites arise due to differences in specific site weathering microenvironments. At site BP, basaltic cobbles occur in a shallow soil which undergoes frequent wetting and drying cycles. Such conditions have been shown to favor the genesis of chloritic intergrades (Rich, 1968). Basalts from H13 and H14 are from deep within the soil, where annual moisture conditions are more uniformly moist. Present day formation of smectite during basalt alteration in the Coast Range (Sites H13 and 14) is consistent with the chemistry of soil solutions characterizing the active zone of rock weathering (Glasmann and Simonson, 1982). Alteration of western Oregon basalts during Miocene-Pleocene tropical climates

Figure 9. DTA patterns of basalt alteration products. (a) Site BP, zone 1 alteration. DTA pattern suggestive of poorly crystalline smectite. (b) Zone 3 alteration , site H13. Low temperature endotherms suggest smectite and goethite. 507°C endotherm suggests beidellite. Low temperature exotherm may be due to amorphous material. (c) Zone 4 alteration, site H13, showing low temperature endotherms characteristic of smectite and goethite. 550°C endotherm is characteristic of halloysite as is the sharper high temperature exotherm. (d) Sample from light brown material (zone 4) occurring between spheroidally weathered basalts, site H13. Smectite and halloysite. (e) 2C horizon, Site OR, showing strong endotherm characteristic of gibbsite.

Figure 9

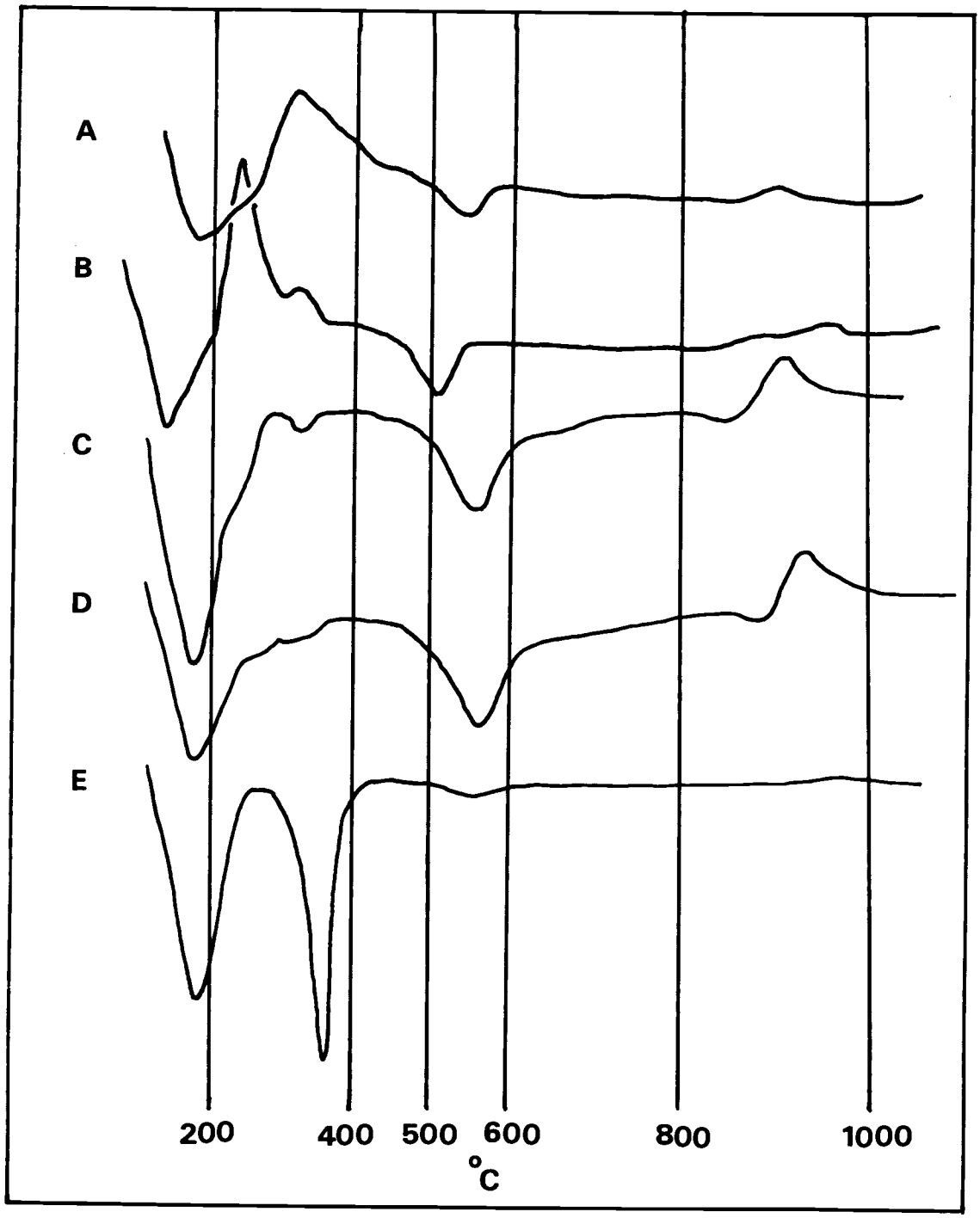

Plate 7. (a, b) Photomicrographs of zone 3 basalt alteration, sample 2C, OR. Amygdaloidal basalt breccia showing alteration to gibbsite. (c) Photomicrograph of zone 4 alteration in weathering rind, sample H13. (d, e) Scanning electron micrographs of zone 4 alteration, sample H13, showing development of granular morphology. (e) Individual granules are composites of tubular halloysite. (f) Fungal mycellia within altered basalt, site H14. (g, h) TEM micrographs of <2-μm fraction. (g) Zone 4, site H13, showing tubular halloysite, iron oxides, smectite. (h) Zone 3, site BP, showing some tubular halloysite, chloritic intergrade, amorphous gel, and iron oxides.

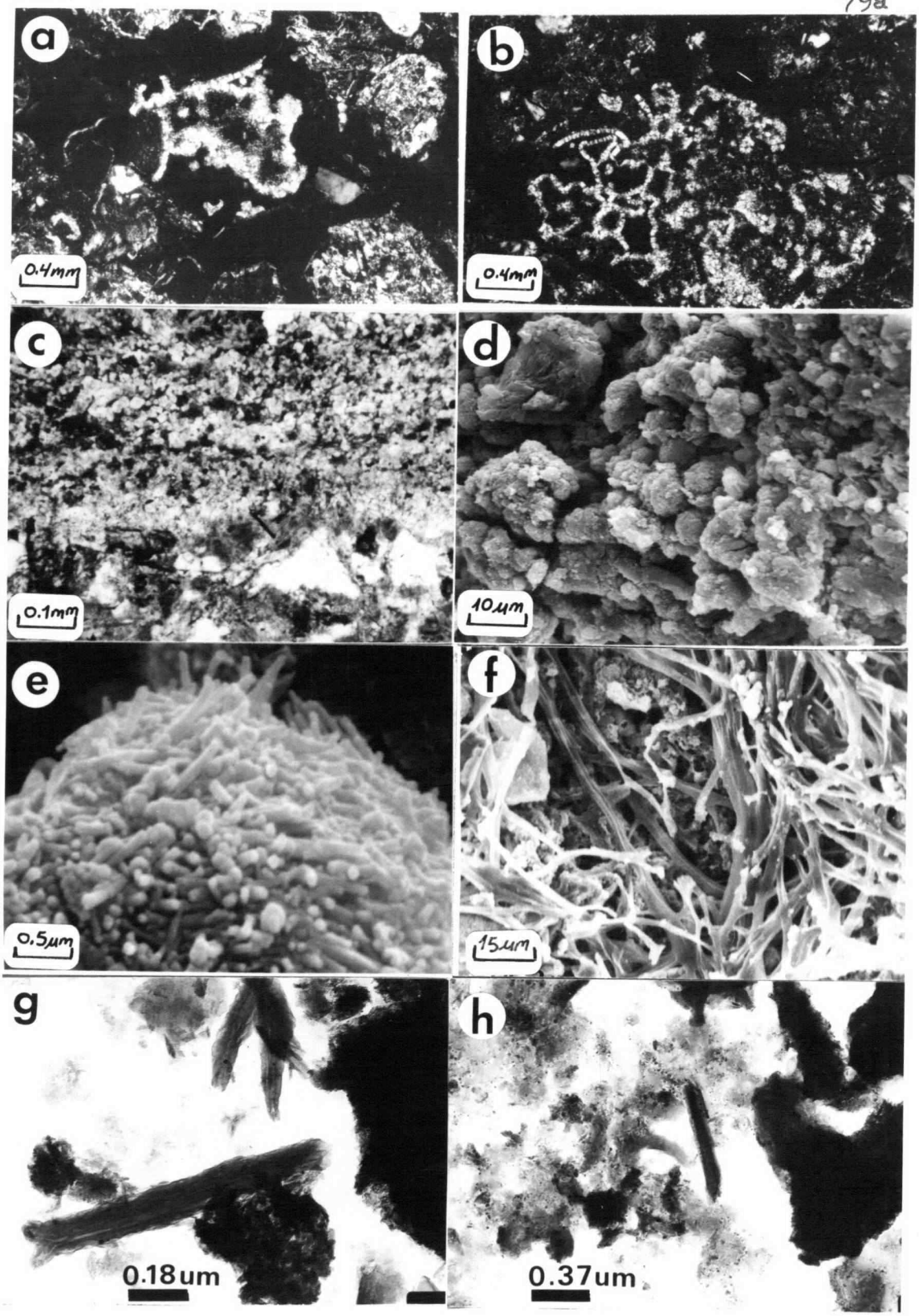
a
0.4mm
b
0.4mm
c
0.1mm
d
10μm
e
0.5μm
f
15μm
g
0.18um
h
0.37um

produced deposits characterized by gibbsite, kaolinite, hematite, and maghemite, where as basaltic saprolites from the Coast Range sites are dominated by smectite, hydrated halloysite, and goethite (Cocoran and Libbey, 1956; Glasmann and Simonson, 1982). Thus, while the Coast Range sites represent remnants of old geomorphic surfaces, the formation of smectite (or Al-hydroxy interlayered smectite at site BP) appears to be contemporaneous with the modern soil environment.

Gibbsite occurs in the 2C horizon of the soil at site OR (Figs. 8c and 9e), where it forms pseudomorphs after plagioclase, as amygdules, as replacement of palagonitic glass in altered basaltic sands, and as free-grain gibbsans (Plates 7a, b). The abundance of easily weatherable, vitrophyric basalt lithologies in the fluvial sands of the 2C horizon is one factor responsible for the genesis of gibbsite in this horizon. The high porosity of the sand, coupled with abundant rainfall and rapid through flow create strong leaching conditions favoring the formation of gibbsite. Complete alteration of basaltic clasts in the 3Eb horizon of this soil has produced chlorite (Fig. 8b). The weathering of grains in this horizon is complicated by a prior weathering cycle, since this horizon is part of a buried soil profile. The chlorite shows slight instability after the 550° heat treatment, which suggests it may have originated from near complete aluminum hydroxy interlayering of a smectite. Some mica also occurs, but its origin is tied to the alteration of metamorphic or sedimentary rock fragments in the sands of this horizon. Alteration of grains in the surface horizons of this soil has also led to the formation of chloritic intergrade, but it lacks the heat stability of the clay from the 3Eb (Fig. 8d). The stronger interlayering of the 3Eb horizon clay has probably been aided by alumina rich solution percolating down from the gibbsitic 2C horizon.

Zone 4

A further indication of the importance of the modern day weathering environment affecting basalt alteration occurs at sites H13 and BP. The thick weathering rinds occurring at these sites have several concentric shells separated by spheroidal fracture envelopes. The boundary between different shell layers shows the destruction of saprolitic structure with the development of granular zones. The granular zones are usually bounded by a thin zone of opaque iron oxide accumulation (Plate 7c). Tongues of light reddish brown material separating adjacent weathering crusts at site H13 also show granular morphology in thin section. Plates 7c, d, and e are SEM micrographs of a portion of the granular zone from a weathering crust at H13. Individual granules are composed of a dense agglomeration of tubular and spheroidal halloysite. X-ray diffraction and DTA analyses of material from the granular zone show strong indications of hydrated halloysite, as well as smectite and iron oxides (Figs. 8h, 9b, c, and d). These minerals were also observed by TEM analyses, which further suggested the presence of an amorphous gel phase (Plates 7g, h). The micromorphology of the granular zone gives no indication of an illuvial origin, since well oriented cutanic structure is lacking. It seems most probable that volume changes during the course of alteration created fissures through which solution movement is more rapid than in the microporous saprolite of the weathering crust. This creates conditions within the fissures favoring the formation of halloysite, either by direct precipitation from solution, or by alteration of smectitic saprolite exposed to the more leaching environment. The merging of the granular zone into the saprolite argues for the latter explanation. The precipitation of iron oxides about the granular zone

further indicates a difference in chemical microenvironment between these zones and the rest of the weathering crust. Thus, it appears that smectite is metastable with respect to halloysite along better drained, more oxidizing microzones within the weathering crust. The fact that the clay mineralogy of adjacent soil material from sites H13 (Glasmann and Simonson, 1982) and BP (Glasmann, unpub. data) strongly resembles that of the granular zones suggests that this granularization may be an initial phase in the formation of present day soil matrix from these basaltic saprolites.

Biotic factors also influence the present day weathering microenvironment. These factors have been largely ignored in past field studies of basalt alteration. Fungi were the most often observed organisms contributing to active disintegration of basalts in this study. Dense tufts of fungal hyphae occur in cavities in the weathering rinds at sites BP and H14 (Plate 7f), and often mycellia were observed penetrating fine cracks into the relatively fresh rock characterizing the zone 1 stage of alteration. The pronounced cavities wherein the fungal hyphae occur suggest that these organisms facilitate the dissolution of basalt and hinder the precipitation of void filling clay minerals. Studies of fungus-induced weathering in western Oregon soils have documented the occurrence of fungal exudates in soil solution extracts (Cromack et al., 1979). These are most often low molecular weight organic acids which are noted for their ability to complex Al and Fe. Dense fungal mats were shown to alter the chloritic character of soil colloids towards more smectite-like behavior by dissolving interlayer Al or Fe hydroxy sheets. Metabolically produced fungal acids accelerate mineral dissolution by lowering the pH of the soil solution and by

chelating dissolved metals, thereby favoring congruent dissolution (Graustein et al., 1977; Silverman and Munoz, 1970). Thus, biologically induced variations in the weathering microenvironment need to be considered along with passive microenvironmental factors such as lithology, precipitation, and internal drainage.

CONCLUSIONS

Alteration products of basalts from western Oregon soils include a variety of secondary minerals depending on local soil microenvironmental factors. Beidellite occurs as an initial alteration product in samples of Siletz River Basalt in the Oregon Coast Range where it forms pseudomorphs after plagioclase or augite. This smectite is metastable with respect to hydrated halloysite where the soil microenvironment is subject to more intense leaching. At drier locations having pronounced wetting and drying cycles, the neoformed beidellite converts to chloritic intergrade and dehydrated halloysite. Goethite occurs as the major crystalline iron oxide in these altered basalts, contrasting with the large amounts of hematite and maghemite noted in tropical weathering environments. Rapid desilication of glassy basaltic lithologies in coastal marine terrace sands has resulted in the formation of gibbsite in these Pleistocene deposits. Alteration of these compositionally immature sands causes extensive textural and mineralogical modification of the original material, often masking its geologic origin.

CHAPTER III

CLAY MINERAL GENESIS IN SOILS DEVELOPED FROM THE LATE EOCENE SPENCER FORMATION, OREGON

J. R. Glasmann and G. H. Simonson

Department of Soil Science

Oregon State University

CLAY MINERAL GENESIS IN SOILS DEVELOPED FROM THE LATE EOCENE SPENCER FORMATION, OREGON[1]

J. R. Glasmann and G. H. Simonson[2]

ABSTRACT

Clay mineral genesis was studied in soils developed from sandy beds of the late Eocene Spencer Formation which are exposed along the western margin of Willamette Valley, Oregon. Petrographic, scanning electron microscope (SEM), and X-ray diffraction techniques were used to characterize mineralogical changes originating during sandstone diagenesis, deep subaerial weathering, and pedogenic alteration. Montmorillonite formed during early sandstone diagenesis in conjunction with the development of quartz and feldspar overgrowths. The montmorillonite occurs as patchy clay films having delicate honeycomb morphology on detrital grain surfaces. Kaolinite formed either during a later stage of burial diagenesis, or in response to percolating ground waters, and occurs as scattered hexagonal-shaped plates or booklets in sandstone packing voids. Kaolinitization of feldspar occurs during subaerial weathering, resulting in pronounced textural and mineralogical changes upward in the weathering profile. Smectite also forms in the weathering profile by alteration of basic volcanic clasts. Non-crystalline materials often are associated with

---

[1]Oregon Agricultural Experiment Station Technical Paper No. _____.
Contribution of the Dept. of Soil Science. Received _____.

[2]Graduate research assistant and professor of soil science, respectively, Oregon State University, Corvallis, OR 97331.

altering primary minerals and form weak cements between adjacent sand grains. Authigenic clay films can be distinguished from illuviated clay (argillans) on the basis of their respective different SEM morphologies.

Additional index words: Weathering, montmorillonite, kaolinite, mica, amorphous material, sandstone diagenesis, feldspar alteration, argillan, scanning electron microscope, soil micromorphology.

INTRODUCTION

As part of a broad study of mineral genesis in western Oregon soils, soils were studied that developed in materials of different composition on geomorphic surfaces of different age and stability. Many of these soils occur on landscapes underlain by mafic igneous rock and have formed either directly from residuum or from colluvial materials of mafic composition. The results of clay mineral genesis studies in these soils have been reported elsewhere (Glasmann, 1982; Glasmann and Simonson, 1982a). Other landscapes in western Oregon are underlain by sedimentary rocks which often show great lithologic variability over a narrow geographic area. The genesis and morphology of foothill soils on the western margin of the Willamette Valley have been strongly influenced by variable sedimentary bedrock (Glasmann et al., 1980). The study of clay mineral genesis in these soils is complicated by the lithologic variability of the bedrock, as well as by the occurrence of one or more lithologic discontinuities within the soil profile which separate materials of different age and origin (Glasmann and Kling, 1980).

The purpose of this paper is to report the results of clay genesis studies in several foothill soils of the Willamette Valley, Oregon. The objectives of this study were to identify authigenic mineral phases in the soil profile and separate these phases from inherited and illuvial materials. A secondary objective was to assess the relative importance of allogenic, authigenic, and illuvial clay in affecting the morphological properties of the soils studied.

MATERIALS AND METHODS

Description of Study Area

The study area is part of an agricultural watershed in southern Polk County, Oregon. This watershed has been the site of intensive soil and geomorphic studies and detailed descriptions of soil-geomorphic relationships for this area have been published (Glasmann et al., 1980). The watershed is underlain by sedimentary rocks of the late Eocene Spencer Formation, which consists of interbedded feldspathic sandstone, siltstone and shale, with minor conglomerate and tuff (Hoover, 1963). The sands were derived in part from erosion of older sedimentary rocks exposed during initial uplift of the Oregon Coast Range (Tyee Formation) and were deposited in a near shore, alternating marine and fluvial environment (Schlicker, 1962).

The northern and eastern sections of the watershed are underlain predominantly by sandy beds of the Spencer Formation. A paleosol is often associated with these sediments, separating weathered Eocene-age materials from overlying Pleistocene sediments of the Willamette Formation (Glasmann and Kling, 1980). At higher elevations in the northern section of the watershed, deposition of the Willamette Formation did not occur and the soils are interpreted as relict paleosols (Glasmann et al., 1980). In order to simplify the study of clay mineral genesis in soils on the watershed, it was decided to initially focus attention on the formation of clay in relict paleosols overlying coarse textured beds of the Spencer Formation. Such beds were presumably deposited with little or no detrital clay in the marine environment (Schlicker, 1962) and, therefore, the presence of clay in these beds must either indicate authigenic formation or the introduction of foreign material.

Field and Laboratory Methods

Bulk and undistrubed soil samples were obtained from 4 soil pits in the northern and eastern sections of the watershed and stored in plastic containers. The soil pits were excavated by backhoe to a depth of approximately 3 m in order to gain exposure to the least weathered bedrock possible. Additional undisturbed samples were obtained from a deep borrow pit in Spencer sands located just south of the watershed. Calcite-cemented nodules were sampled from borrow pit sands and from deep excavations on the watershed for thin section analyses. These nodules formed shortly after sandstone deposition and protected their included sands from the effects of later alteration. As such, the nodules serve to establish a reference point from which compositional changes during alteration may be evaluated.

Bulk soil samples were subsampled for particle size and clay mineral analyses, following the procedures outlined in Kilmer and Alexander (1949) and Glasmann and Simonson (1982a), respectively. Undisturbed soil samples were initially examined with a binocular microscope to aid in selecting subsamples for scanning electron microscope (SEM) analyses. Fractured soil clods from the areas of interest were glued to metal stubs and coated with about 20-nm of gold in a vacuum evaporator prior to SEM analysis. Remaining undisturbed soil material was impregnated with resin and thin sections were prepared for petrographic examination. Point counts were made to determine species composition. Morphological terminology is from Brewer (1976). Further characterization of soil colloids was done by transmission electron microscopy, differential thermal analysis, and X-ray diffraction analyses (XRD).

RESULTS AND DISCUSSION

Characteristics of Unweathered Sandstone

Petrographic examination of calcite-cemented nodules from sandy beds of the Spencer Formation indicate that the sands as initially deposited were free of detrital clay. Moderately well to well sorted, subangular to subrounded fine-grain sands of quartz and plagioclase dominate, with lesser amounts of lithic clasts, muscovite, biotite, microcline, and heavy minerals. Modal analysis of 3 thin sections indicates the following average composition: 40% quartz (including chert and polycrystalline grains), 37% plagioclase (Ab_{70}-Ab_{50}), 10% lithics (extrusive and intrusive volcanics, lesser plutonic), 3-5% muscovite, 2% microcline, and lesser amounts of biotite, hornblende, augite, magnetite, and other heavy minerals. Compositional variation occurs from sample to sample, most noticeably in the percentage of lithic fragments and mica, which may range from 3-15% and 2-7%, respectively. Compositional variation is closely tied to changes in mean particle size, with the micaceous components more frequently occurring in fine to very fine sand fractions. The sands within the calcite-cemented nodules are corroded in appearance due to some replacement of grain margins by calcite, but otherwise appear fresh and unaltered. Minor altered plagioclase and the presence of lithic sands suggest that the sediment was rapidly eroded from steep terrain and deposited without much reworking after winnowing of finer particles (Folk, 1980). The relatively high concentration of mica indicates that the depositional environment was one of low to intermediate energy.

Diagenetic Alteration

Indurated sandstone is rare in the Spencer Formation (Hoover, 1963) and, because of the unconsolidated porous nature of the sediment, effects of weathering extend deep into surface exposures of the formation. For this reason, it is difficult to separate the effects of subaerial weathering from burial diagenesis without studying a number of samples from different depths. Thin sections of unconsolidated sands from the 3 m depth of 3 profiles in the northern section of the watershed show the presence of thin, patchy, pale yellowish-brown, simple free-grain argillans (terminology after Brewer, 1976) and thin reddish brown argillans on vertical and horizontal fracture surfaces. These thin, reddish-colored argillans extend down into the Spencer Formation from the overlying paleosol (Table 9) and are considered illuvial in origin, showing well oriented, laminar structure in thin section. However, conclusive evidence for an illuvial origin of the free-grain argillans could not be found from thin section analyses.

Scanning electron microscope analyses of deep C horizon and borrow pit sands suggest that the free-grain argillans formed during burial diagenesis of the sandstone. The diagenetic sequence apparently began with the formation of quartz and feldspar overgrowths which probably commenced shortly after burial of the sediment (Plates 8a, b, c, d). The microcrystalline nature of these overgrowths suggests that the sediments were only subjected to shallow burial (Pitman, 1972). Similar quartz surface textures were reported by Glasmann and Kling (1980) for Spencer sands from other areas of the watershed, but because of the harsh pretreatments used in that study, the occurrence of authigenic feldspar was not observed. Diagenetic feldspar overgrowths show rectangular morphology

Table 9. Morphology of 4 Willakenzie soils (Ultic Haploxeralfs) on Elkins Road Watershed.

Profile	Horizon	Depth	Color (moist)*	Texture*	Structure*	Boundary*	Other*
		--cm---					
E2H2	Ap	0-31	10YR 3/3 7.5YR 6/5	sil	2fgr	as	pH 5.5
	BAt	31-49	7.5YR 5/6	sil(-)	2m, fsbk	gs	1 n (7.5YR 4/4) pf; 2 mk (10YR 3/3) po. pH 5.4
	Bt1	49-69	10YR 4/6 w/7.5YR 6.8 in thin bands	sicl(-)	2msbk	cw	2 n (7.5YR 4/4) pf; 2 mk (10YR 3/3), po. pH 5.4
	Bt2	69-91	10YR 4/6 w/10YR 8/8 lamillae	sicl(-)	2msbk	cw	2 mk (7.5YR 4/4) pf; 2 mk (10YR 3/3), po. pH 5.4
	BCt	91-105	10YR 5/8 w/many 7.5YR 6/6, 2.5YR 3/4 variegations	sil	1vcabk	as	3 mk (7.5YR 4/4) pf, po. pH 5.4
	2Cr1	105-126	10YR 6/6 bands, 7.5YR 4/4 2.5YR 3/4	sil	m→lam[§]	cs	3 mk (7.5YR 4/4) ff (vert), po. pH 5.3
E2H3	Ap	0-24	10YR 3/3	sil	2 csbk→ 3 m, fsbk	aw	pH 5.4
	AB	24-42	7.5YR 4/4	sil	1 mpr→ 3 m, fsbk	cs	pH 5.3
	2BAt	42-56	7.5YR 4/4 7.5YR 4/6	sil(+)	1 mpr→ 3 msbk	cs	2n (7.5YR 4/4) pf, po. pH 5.3
	2Bt1	56-72	7.5YR 5/6	sicl(-)	1 mpr→3msbk	cw	3 mk, n(7.5TR 4/4) pf, po. pH 5.3
	2Bt2	72-105	7.5YR 5/4	sicl(-)	1 cpr→ 2 csbk→ 3 msbk	ai	3 k(7.5YR 4/4, 4/3) pf, po. pH 5.3

Table 9, cont.

Profile	Horizon	Depth	Color (moist)	Texture	Structure	Boundary	Other
		--cm---					
(E2H3, cont.)	2BCt	105-139	2.5YR 2/4 & 7.5YR 5/8 in thin (2-5 mm) laminae	sil	m→lam	cs	2 mk (7.5YR 4/4) ff, po. pH 5.2
	2Cr1	139-148	7.5YR 5/8, 5YR 4/6 7.5YR 4/4	sil	m→lam.	cs	2 mk, k (7.5YR 4/4) ff. pH 5.2
	2Cr2	148-195	7.5YR 5/8, 5YR 4/6, 10YR 5/6 var. in thin (1.3 mm) laminae	vfsl	m→lam		1 mk (7.5 YR 4/4) vert. fractures, po. pH 5.0
E2H5	Ap	0-22	10YR 3/3	sil	3f, msbk	as	pH 5.6
	BAt	22-34	7.5YR 5/6	sil	1mpr→3msbk	cw	2 mk 5YR 4/4 pf (vert. & hor.), po. pH 5.6
	Bt	34-50	7.5YR 5/6	sicl	1mpr→3msbk	ci	3k, mk 5YR 4/4 pf (vert & hor.), po. pH 5.6
	2BCt	50-68	7.5YR 5/8 & 10YR 6/3	sicl	1cpr→1cbsk	cs	3mk (5YR 4/6) pf (vert & hor.), po. pH 5.5
	2Cr1	68-80	10YR 5/4	sil	m→lam.	as	3mk (10YR 5/4) vert ff's. pH 5.4
	2Cr2	80-87	7.5YR 5/8 & 5YR 5/8 w/lesser 2.5YR 6/4 all in 2-12 mm hor. bands.	l	m	as	3npo (7.5YR 4/6), 3mk (10YR 5/4) ff. pH 5.4

Table 9, cont.

Profile	Horizon	Depth	Color (moist)	Texture	Structure	Boundary	Other
		--cm---					
(E2H5, cont.)	2Cr3	87-112	5YR 6/2, 2.5YR 5/4 7.5YR 5/8 in 0.1-5 cm laminae	sil	m w/tendency to part along hor. bedding planes, occas. (20-60 cm sep.) vert. ff	gs	2npo (7.5YR 4/6); 3mk (10YR 5/4) ff. pH 5.2
	2Cr4	112-200	5YR 6/2, 2.5YR 5/4 7.5YR 5/8 in 0.1-5 cm laminae	l	m	ps	occasional 1-5 mm thick "Fe-pan" (2.5YR 3/4) bands parallel to bedding. pH 5.2
E4T2	Ap	0-18	10YR 3/2	sil	2fsbk	as	pH 5.3
	A	18-50	10YR 3/3	sil(+)	2m, fsbk	cw	pH 5.5
	2BAt	50-66	10YR 5/4	sicl	2msbk	cw	3 mk (10YR 3/3) pf, po. pH 5.4
	2Bt	66-95	10YR 5/6	sic(-)	1cpr→2msbk	gw	3 k (10YR 4/4) pf, po. pH 5.4
	3BCt	95-117	5YR 4/6, 7.5 YR 5/8 variegated	cl(+)	1c, msbk	cw	3 k (10YR 4/4) pf, po; 2 mk (10YR 3/2) po. pH 5.4
	3C1	117-143	10YR 5/6, 5YR 5/8 2.5YR 7/4 variegated	l	m	as	highly wxd mod well rounded, mod spherical, well graded ss; 3 mk (10YR 4/4) pf. pH 5.6
	4C2	143-150	7.5YR 5/6, 10YR 6/4 variegated	sl	m	gs	wxd well-graded ss, 2 mk (10 YR 3/2) po. pH 5.5

*Symbols used are the same as given in Soil Survey Manual, USDA Agr. Handbook No. 18, p. 139-140. 1951.

§Arrow indicates structure which breaks to secondary structure indicated.

Plate 8. Scanning electron micrographs of Spencer Formation illustrating effects of burial diagenesis on surface morphologies of quartz and feldspar. (a) Feldspar showing etched surface. (b) Authigenic feldspar as overgrowths on surface of detrital feldspar grain. (c) Authigenic quartz on surfaces of detrital quartz sands and mica alteration (center). (d) Authigenic feldspar (left hand grain and protruding into packing void) and protruding into packing void) and initial quartz diagenesis (right).

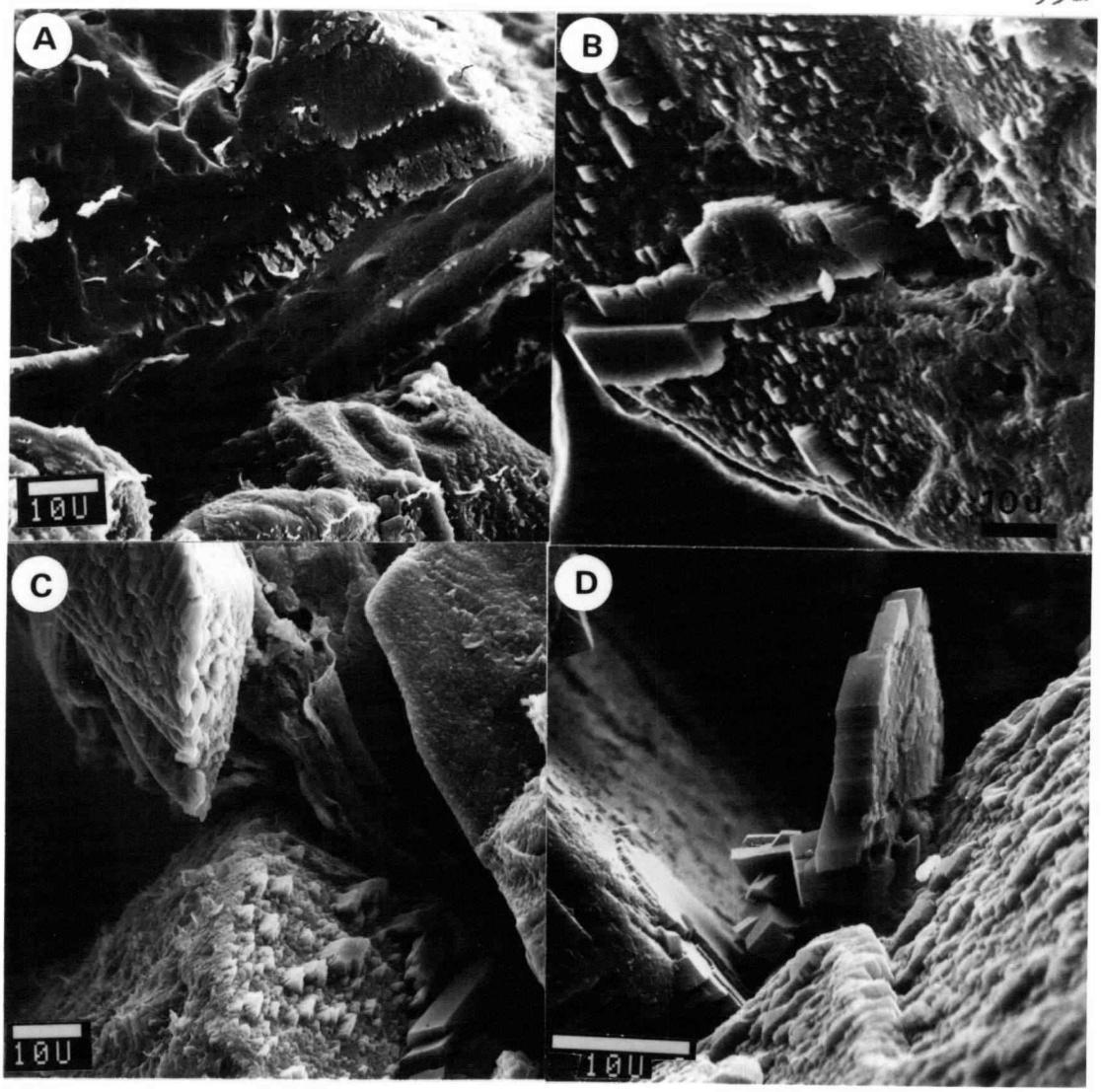
A
10U
B
10U
C
10U
D
10U

(Plates 8b and 8d, left corner) and complex twin forms (Plate 8d, center), and differ from the pyramidal morphology of incipient quartz overgrowths (Plate 8c, lower center; 8d, right corner). The growth of these microcrystalline quartz and feldspar overgrowths was accompanied by the formation of patchy clay films on grain surfaces (Plate 8c, lower left; Plates 9a, b, c). The clay films apparently inhibited the formation of quartz overgrowths on the clay coated surface of the quartz grain shown in Plate 8c.

High magnification images of the clay films show delicate honeycomb morphology (Plate 9c) characteristic of diagenetic montmorillonite (Wilson and Pitman, 1977). The predominance of montmorillonite is indicated in XRD patterns of the <2-μm material dispersed from these sands (Fig. 11a). The delicacy of the clay morphology seen by SEM is not characteristic of allogenic or illuvial clays, which typically show strong preferred orientation imposed by the platy nature of the particles (Wilson and Pittman, 1977; Plate 11, this article). The montmorillonite coatings on sand grains seen by SEM are analogous to the patchy, simple, free-grain argillans observed in thin sections of deep Cr horizon sands. Although the diagenetic origin of these clay films was not ascertainable from thin section analyses, the delicate honeycomb morphology observed by SEM strongly supports diagenetic formation.

Minor amounts of mica and kaolinite are also indicated by the diffractogram presented in Fig. 11a. Kaolin occurs in borrow pit sands as an alteration product of feldspar (Plates 9d, e) and as authigenic pore lining material (Plate 9f). In Plates 9d and e, kaolinite forms pseudomorphs after plagioclase, showing vermiform stacks having roughly pseudohexagonal morphology. The occurrence of kaolinite as discreet

Plate 9. Scanning electron micrographs illustrating diagenesis and subaerial alteration of Spencer sandstone. (a) Overview illustrating well-sorted, subangular sands having patchy simple freegrain argillans. (b) Diagenetic smectite coating detrital grain surfaces (right side) and altered plagioclase (left). (c) Honeycomb morphology of diagenetic smectite surface coatings. (d) Authigenic kaolinite produced from alteration of feldspar. (e) Vermicular morphology of authigenic kaolinite. (f) Diagenetic kaolinite in pores showing pseudohexagonal morphology and stacking of plates.

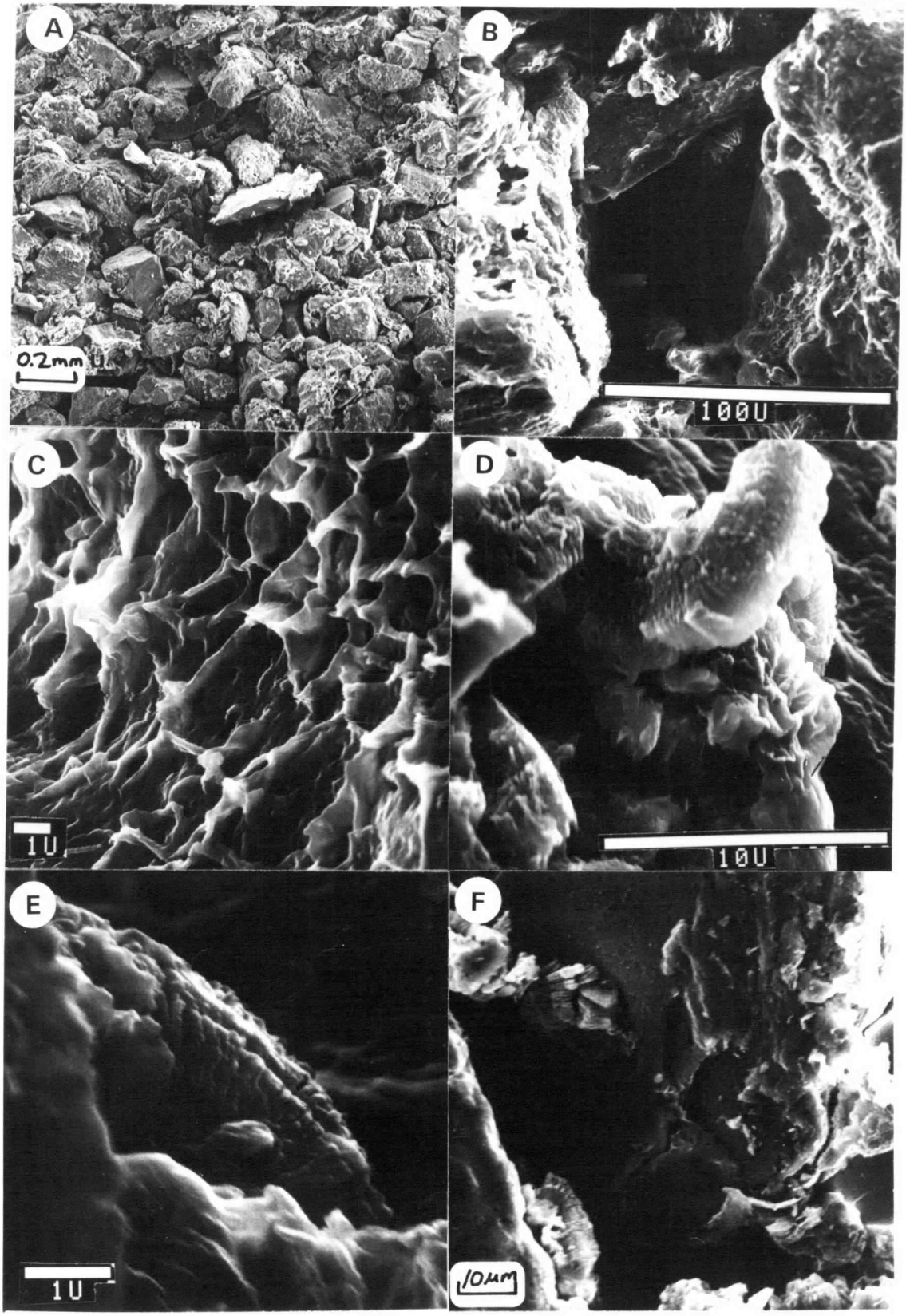
A
0.2mm
B
100U
C
1U
D
10U
E
1U
F
10µm

Figure 10. X-ray diffraction patterns of the <2-μm fraction of soils derived from Spencer sandstones. (a) Borrow pit, 5 m deep, showing smectite, minor mica and kaolinite. (b) Sample E2A14, 2C2, 200 cm deep, showing kaolinite, minor mica, and poorly crystalline smectite. (c) Sample E2H3, 2BCt, 140 cm deep, showing kaolinite, minor mica and chloritic intergrade. (d) Sample E2H3, 2Bt2, 60 cm deep, showing strong d_{001} for kaolinite, minor mica and chloritic intergrade. (e) Sample E2H3, 2BCt clay skins, 140 cm deep, showing predominance of smectite, with minor mica and kaolinite. Numbers 2, 4, and 7 refer to Mg-saturated ethylene glycol solvated, K-saturated 110°C dry air, and K-saturated 550°C dry air treatments, respectively. d-spacing in Angstroms.

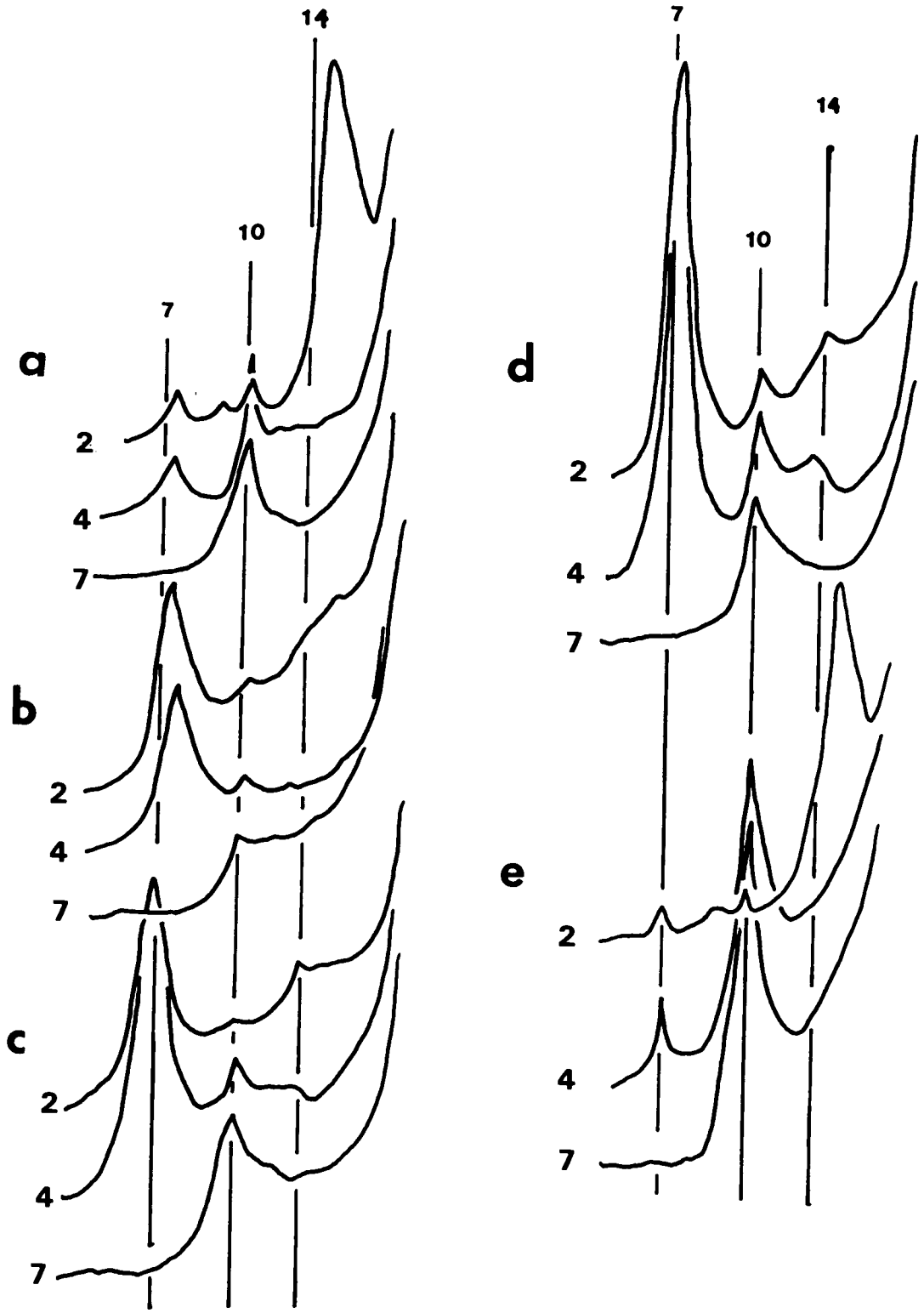
14
10
7
a
2
4
7
b
2
4
7
c
2
4
7
7
14
10
d
2
4
7
e
2
4
7

plates or books of plates lining packing voids in the sandstone (Plate 9f) probably indicates direct precipitation from percolating pore fluids. Pore lining kaolinite is present only in minor amounts and may have originated during the final stages of burial diagenesis as silica in the pore fluids became limiting for the formation of smectite. The growth of quartz overgrowths may have been a factor in reducing silica levels in pore fluids, creating conditions which favored kaolinite formation over montmorillonite. Kaolinitized feldspar increases dramatically upward in the weathering profile, and accounts for the increase in kaolinite d_{001} XRD intensities from samples progressively closer to the soil surface (Figs. 11b, c, d). This distribution pattern strongly suggests that the genesis of kaolinite from alteration of feldspar is related to subaerial weathering, and not to burial diagenesis. Soil solution chemical data presented by Glasmann and Simonson (1982b) further suggest that kaolinite is stable under present environmental conditions.

Subaerial Alteration

The presence of clay-size mica in Fig. 11 is probably due to diminution of sand-sized mica during chemical weathering. Mica flakes were bent and deformed around more competent grains during sediment compaction, resulting in some exfoliation and splitting along cleavage (Plate 10a). Continued exfoliation along the (100) planes occurs during surface weathering, leading to the formation of finer and finer mica particles (Plate 10a, note spalled flakes at bottom of large mica grain). Stripping of interlayer K probably occurs during subaerial weathering, producing charge imbalances which facilitate opening of the mica structure. Chemical alteration of mica is suggested by the formation of amorphous

Plate 10. Scanning electron micrographs of alteration of Spencer sandstone. (a) Alteration of mica; exfoliation and splitting leading to the production of finer mica particles. (b) Coating of mica surface by amorphous gel and rolling of altered surficial mica platelets. (c) Altered basalt clast showing remnants of plagioclase laths (left corner). (d) Initial alteration of feldspar characterized by rectangular etch pits and amorphous gel. (e) Amorphous material cementing grain contacts. (f) Desiccation of amorphous gel leads to the formation of fine filamentous morphologies seen in crack.

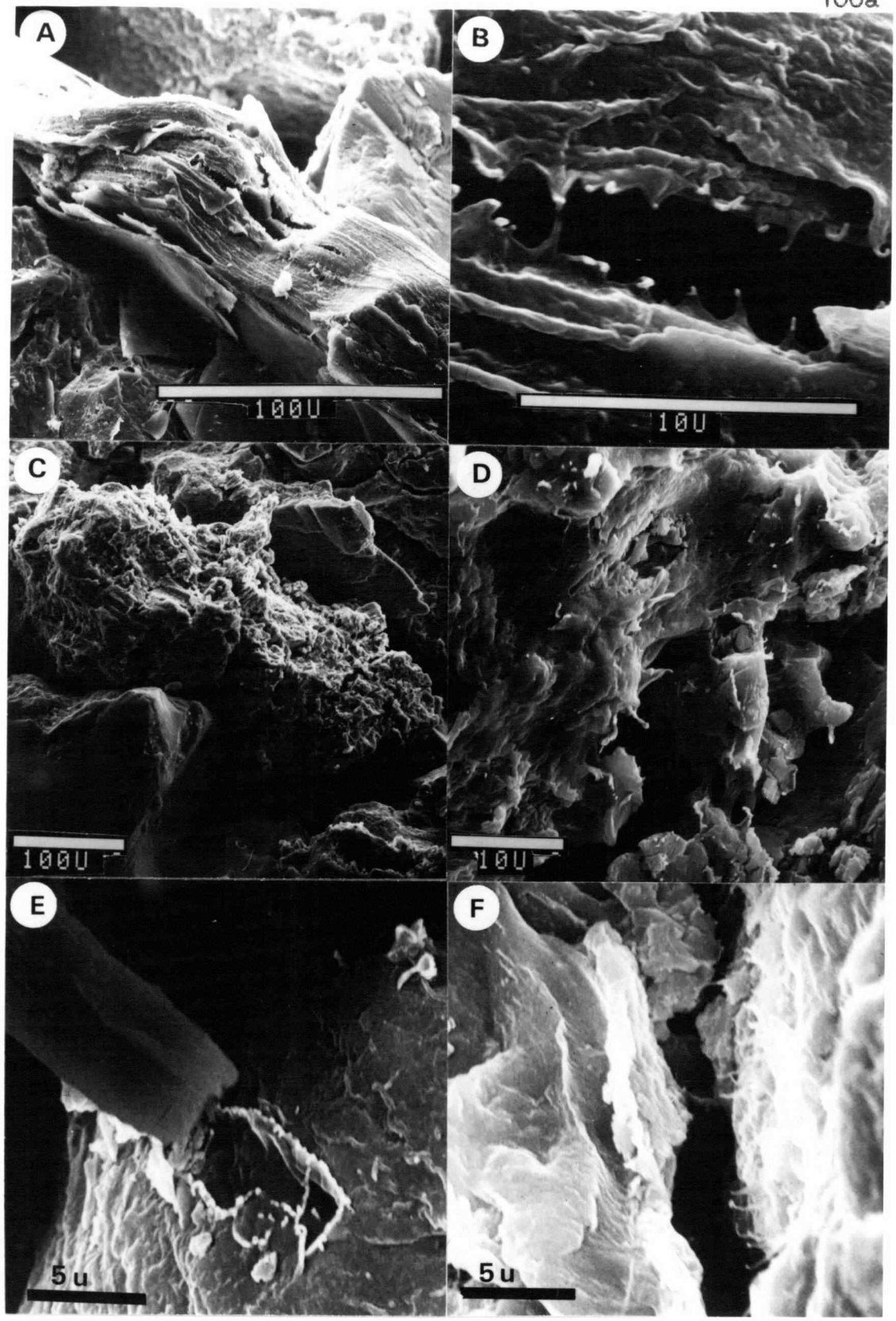
A
100U
B
10U
C
100U
D
10U
E
5u
F
5u

gel coatings on grain surfaces (Plate 10b) and by the rolled appearance of exposed mica sheets. Such rolling or curling of exposed plates may result from lattice stresses induced by the stripping of K along the edges of mica flakes. Tarzi and Protz (1978) studied the morphology of weathered soil micas and found that splitting and exfoliation along (100) planes were common, as well as the presence of amorphous surface coatings. They noted that the amorphous surface coatings can retard ion diffusion during weathering or cation exchange reactions, as well as cement adjacent soil particles.

Non-crystalline material occurs as a precursor to clay mineral formation during the alteration of feldspar in the Spencer Formation (Plate 10d) where it shows irregular or stretched gel-like morphology in SEM micrographs. The altered feldspar in Plate 10d shows the presence of rectangular etch pits (upper half of micrograph) and broad dissolution channels, some of which are bridged by amorphous gel (lower right of micrograph). The isotropic character of many weathered feldspar grains examined in thin section is consistent with the occurrence of an amorphous alteration phase. Other studies have shown that amorphous materials are commonly formed during the initial phase of feldspar alteration (Glasmann and Simonson, 1982a; Eswaran, 1979). Amorphous materials also form weak cements at points of contact between adjacent mineral grains as shown in Plate 10e. In this micrograph, physical distrubance of the specimen during mounting separated two adjacent grains revealing the outline of an amorphous cementing material at the original points of grain contact. These cements are unstable under the high vacuum conditions of the electron microscope and shrink with desiccation to produce delicate wispy fibers (Plate 10f). Gel shrinkage is probably the mechanism whereby

the jagged "teeth" formed around the opening in the mica illustrated in Plate 10b. Simple free-grain organo-sesquans observed by SEM in Bhir horizons of spodosols along the Oregon coast show similar gel fibres along desiccation cracks in the grain cutans (Glasmann, unpublished data).

Smectite, which forms patchy grain coatings during early burial diagenesis, also forms during the alteration of volcanic clasts in the surface weathering environment. Plate 10c illustrates an altered basalt clast from profile E2H5. The rectangular outlines of altered plagioclase phenocrysts are noticeable on the left corner of the grain and are due to remnants of more stable sodic zones in the original phenocryst. XRD analysis of altered lithic grains separated from Spencer sands indicates that the grains have altered to montmorillonite. The formation of montmorillonite is also suggested by the morphology of the material replacing altered calcic zones of feldspar phenocrysts and what was once glassy groundmass. These morphologies are similar to those presented by Glasmann and Simonson (1982a) for altered basalts in western Oregon. The decrease in alteration of lithic clasts with depth suggests that this alteration is related to surface weathering and not to burial diagenesis.

Pedogenic Alteration

In the lower part of the solum, sedimentary structure is replaced by insepic or skelsepic plasmic fabric as kaolinitic pseudomorphs break apart by plasmification and some of the clay is pressure oriented about skeletal grains. More clayey Bt horizons often show vo-masepic plasmic fabric and contain 3-5% papulic clay. The occurrence of well oriented papules suggests that restructuring of the soil fabric has occurred, isolating pieces of former argillans within ped interiors. The clay mineralogy of the paleosol is dominantly kaolinitic (Fig. 11c, d), with

lesser amounts of mica and hydroxy interlayered smectite (chloritic intergrade). Thick planar, channel, and vugh argillans constitute about 5% of the soil based on point counts of Bt horizon thin sections. Argillans separated from the soil with a microscalpel under a binocular microscope show dominance by smectite by XRD analysis (Fig. 11e). The difference in clay mineralogy between soil matrix and cutans is probably the result of concentration of illuviated fine clay in the cutans.

Scanning electron microscope analysis of the paleosol indicates that a major difference exists between the morphology of illuviation cutans (Plates 11a, b, c, d, e, f) and diagenetic clay films (Plates 9b, c, f). Illuviation cutans show strong laminated morphology (Plates 11c, d) which is especially evident on freshly fractured cutan surfaces (Plate 4c, upper right). This laminated morphology contrasts markedly with the delicate honeycomb morphology of diagenetic smectite clay films (Plate 9c) and the worm-like stacks or discreet booklets of authigenic kaolinite (Plate 9f). The contact between argillans and underlying ped surfaces is quite abrupt, but ped fabric at the point of contact may be variable, sometimes showing preferred orientation of platey mineral grains (plane neostirans, Plate 11d), and at other times showing a lack of preferred orientation in the soil matrix (Plate 11e). In contrast to the 1-2 μm size platey grains which dominate the soil matrix (Plates 11d, e), the argillans are composed of much smaller particles which could not be resolved even at high magnification (Plate 11f). Sesquioxide gel also coats some argillan surfaces, evidenced by thin, dark, isotropic surface layers in thin section. This amorphous coating probably hinders the ability of the SEM to resolve underlying crystalline clay components of the cutans.

Plate 11. Scanning electron micrographs of paleosol argillans in soils of Elkins Road Watershed. (a) Undulose, planar argillan. (b) Vugh argillan. (c) Well-laminated argillan showing abrupt contact with underlying ped. Ped composed largely of micron-sized platey particles, while individual clay particles in cutan are not discernible at this magnification. (b) Boundary of illuviation argillan and neostiran, showing stress orientation of kaolinite plates. (e) Argillan masking ped surface without indication of stress oriented soil fabric. (f) Close up of argillan showing coating by amorphous material. Fine laminated structure of illuviation cutans differs from honeycomb morphology of authigenic smectite free-grain cutans (Plate 9c).

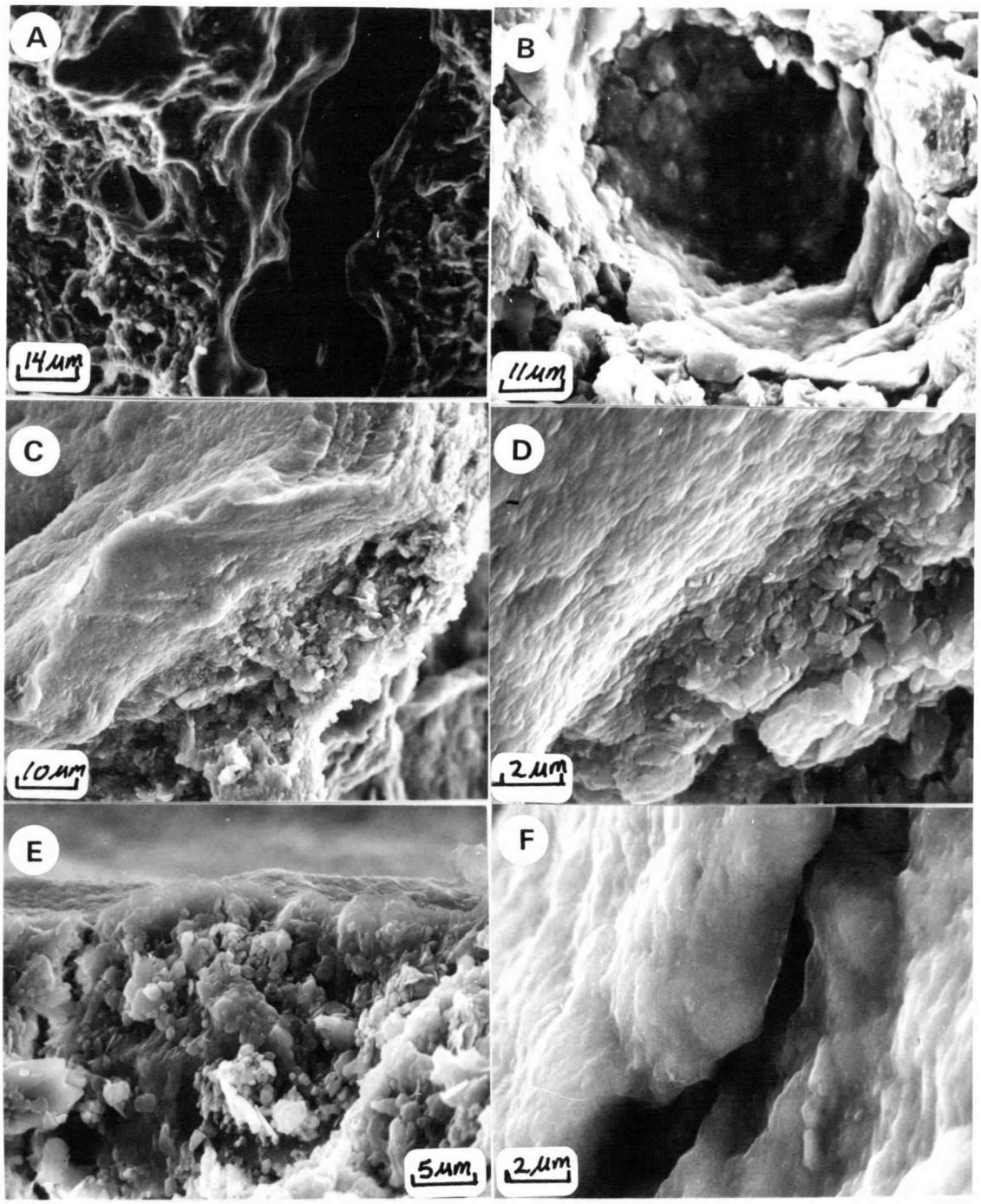
A
14 µm
B
11 µm
C
10 µm
D
2 µm
E
5 µm
F
2 µm

Argillans are absent in the late Pleistocene silty sediments which mantle the paleosol on the Brateng geomorphic surface on the watershed (Glasmann, et al., 1980). These silts, which occur in profile E4T2 (Table 9), were deposited during the final period of flooding from glacial Lake Missoula about 13,000 years ago (Glasmann and Kling, 1980) and show only the development of argillasepic plasmic fabric in most thin sections. It thus appears likely that the major episode of argillan formation in the soils studied predates deposition of late Pleistocene silts in the area and may be related to warmer, moister conditions that existed in the Willamette Valley during Pleistocene interglacial periods (Gelderman and Parsons, 1972; Balster and Parsons, 1969). However, well developed argillic horizons also occur in soils on more recent deposits in the Willamette Valley (Reckendorf and Parsons, 1966).

Significant changes in soil texture occur as a result of alteration of chemically unstable sands in soil profiles developed in the Spencer Formation (Tables 9 and 10). A difficulty was encountered in correlating field estimates of soil texture with laboratory particle size measurements. Laboratory particle size estimates were generally coarser than corresponding field estimations. Microscopic examination of sand separates show them to consist largely of undispersed soil fragments which break down with mild rubbing between the fingers to smaller particles.

Table 10 indicates a major textural break occurs at the 148 cm depth in profile E2H3. Thin sections of this horizon indicate that kaolinitized feldspar grains constitute about 25% of the total sand. These grains, when separated from the soil, shatter easily under slight physical pressure. The increase in fines and accompanying decrease in sand is due largely to the breakdown of altered lithic fragments and kaolinitized

Table 10. Particle size data for several soil profiles developed in coarse textured beds of Spencer formation.

Profile number	Horizon	Depth	Sand						Silt			Clay
			vcs	cs	ms	fs	vfs	Total s	csi	fsi	Total si	
		--cm--										
			Willakenzie (Ultic Haploxeralf, fine silty)									
E2H2	Ap	0-31	0.3	0.1	0.5	5.7	21.2	27.8	24.9	28.8	53.7	18.5
	BAt	31-49	0.3	0.1	0.6	5.0	18.7	24.7	21.3	28.5	49.8	25.5
	Bt1	49-69	0.4	0.5	0.4	4.4	17.8	23.5	20.4	28.6	49.0	27.5
	Bt2	69-91	0.3	0.3	0.3	3.5	17.1	21.5	20.6	28.9	49.5	29.0
	BCt	91-105	0.2	0.1	0.1	5.4	23.5	29.3	16.5	22.5	39.0	31.7
	2Cr1	105-126	0.5	0.3	0.2	1.3	16.3	18.6	23.9	33.7	57.6	23.8
	2Cr2	126-153	0.1	0.1	0.1	1.3	19.8	21.4	28.6	32.5	61.1	17.5
	3Cr3	153-208	0.1	0.1	0.1	2.7	23.1	26.1	24.3	32.7	57.0	16.9
			Willakenzie taxadjunct, fine (Ultic Haploxeralf, fine)									
E2H3	Ap	0-24	0.4	0.3	0.5	9.4	18.6	29.2	22.8	28.4	51.2	19.6
	AB	24-42	0.1	0.1	0.4	8.0	18.3	26.9	21.5	26.8	48.3	24.8
	2BAt	42-56	0.2	0.1	0.4	7.5	16.8	25.0	19.8	30.0	49.8	25.2
	2Bt1	56-72	0.2	0.2	0.3	5.9	17.1	23.7	17.8	23.9	41.7	34.6
	2Bt2	72-105	0.1	0.1	0.2	5.0	13.8	19.2	16.6	24.2	40.8	40.0
	2BCt	105-139	0.1	0.1	0.1	8.6	15.7	24.6	21.7	27.2	48.9	26.5
	2Cr1	139-148	0.1	0.2	0.4	11.3	15.8	27.7	21.8	27.1	48.9	23.4
	2Cr2	148-187	0.3	1.8	1.6	31.1	24.1	59.9	13.2	14.6	27.8	12.3
			Willakenzie taxadjunct, fine (Ultic Haploxeralf, fine)									
E4T2	A2	18-25	0.2	1.2	1.7	7.7	7.4	17.2	16.5	40.9	57.4	25.4
	AB	25-30	1.0	1.5	1.8	8.4	7.4	18.5	17.1	37.5	54.6	26.9
		30-40	0.5	1.3	1.8	8.3	7.9	19.8	17.8	37.5	55.3	24.9
		40-50	0.6	1.7	2.2	9.9	8.6	23.0	17.6	36.8	54.4	22.6
	2BAt	50-60	0.9	1.9	2.2	11.0	10.6	26.6	16.5	27.0	43.5	29.9
		60-66	2.0	2.4	2.7	11.9	10.3	29.3	14.7	25.8	40.5	30.2
	2Bt	66-76	2.9	2.8	2.6	10.9	9.3	28.5	12.4	21.2	33.6	37.9
	3BCt	95-105										
		105-117	1.2	4.5	4.8	14.5	9.2	34.2	11.6	21.3	32.9	32.9
	3C1	117-127	5.4	11.0	6.3	11.8	8.8	43.3	5.5	24.5	30.0	26.7
	3C2	127-137										
	3C3	137-143	3.7	8.1	6.3	13.5	10.4	42.0	13.5	21.1	34.6	23.4

plagioclase pseudomorphs during mechanical analysis of the soil. However, finer soil textures in the lower part of the solum result from the natural breakdown of kaolinitized plagioclase during plasmification and from illuvial clay. Textural changes induced by weathering and subsequent plasmification were observed in soils of the Western Cascades by Paeth, et al. (1971) and have been noted in soils developed in Pleistocene marine terrace sands along the Oregon coast (Glasmann and Simonson, 1982a). Given favorable chemical and physical conditions, rapid alteration of easily weatherable mineral grains can produce sharp textural discontinuities that may be mistaken for lithologic discontinuities without accompanying petrographic characterization.

CONCLUSIONS

Smectite forms as an initial product of burial diagenesis in sands of the Spencer Formation where it forms discontinuous simple freegrain argillans having honeycomb morphology by SEM. Additional smectite forms during surface alteration of unstable volcanic clasts that are part of the Spencer sands. Kaolinite formed during the final stages of burial diagenesis and shows characteristic pseudohexagonal plate morphology. Kaolinite also formed by surface weathering of the Spencer sands during paleosol development, and probably continues to form in the present weathering environment. Plasmification of highly weathered sedimentary rocks occurs in the paleosol where clay mobilization has produced thick, smectite-rich argillans showing well developed laminar structure. Illuvial clay accumulations may be distinguished from authigenic clay on the basis of differing SEM morphologies, even when thin section evidence is inconclusive. Significant soil textural changes result from the weathering of compositionally immature sands. Such changes need to be evaluated microscopically in order to insure proper interpretation of textural discontinuities.

CHAPTER IV

ALTERATION OF ANDESITE IN WET UNSTABLE SOILS OF OREGON'S WESTERN CASCADES

J. R. Glasmann

Department of Soil Science

Oregon State University

ALTERATION OF ANDESITE IN WET UNSTABLE SOILS OF OREGON'S WESTERN CASCADES[1]

J. R. Glasmann[2]

ABSTRACT

Alteration of products of andesite cobbles from wet soils formed in volcanic colluvial material were studied using petrographic, electron microcope, X-ray diffraction, and thermal techniques. Augite phenocrysts altered by congruent dissolution leaving voids which were subsequently filled with smectite. Plagioclase also altered to produce micrometer-size spheroidal aggregates of smectite. Halloysite was not observed within the altered cobbles, although it was abundant in the soil matrix. The formation of smectite in the altered cobbles was probably favored by the restrictive drainage of the microenvironment in combination with wet soil conditions.

Additional index words: Andesite alteration, smectite, clay mineral genesis, SEM, micromorphology, plagioclase, augite, halloysite.

---

[1]Technical Paper No. 6131, Oregon Agric. Exp. Stn., Corvallis, OR 97331. Contribution of the Dept. of Soil Science.

[2]Graduate research assistant, Dept. of Soil Science, Oregon State University.

INTRODUCTION

The bedrock geology of Oregon's Western Cascade Range is a complex of interbedded basaltic and andesitic lava flows, pyroclastic rocks, water-laid tuff, volcanic conglomerate, and ignimbrite (Peck et al., 1964; Baldwin, 1976). Recent studies have shown that a strong relationship exists between geology, geomorphology, clay mineralogy, and landscape stability in this region (Taskey et al., 1978; Taskey, 1978; Swanston and Swanson, 1976; Paeth et al., 1971; Youngberg et al., 1971). In evaluating the nature of the clay fraction of a number of soils formed in volcanic materials, Taskey et al. (1978) found that clay mineral associations and profile morphology could be used to characterize both stable and unstable land surfaces, as well as to distinguish between different types of mass movement. Numerous data were cataloged on the identity of the soil clay fraction in the Western Cascades, and genetic relationships were interpreted from analysis of major trends and associations of bulk soil mineralogy and site characteristics. In general, halloysite and noncrystalline aluminosilicate gels were associated with colluvium which mantled smectite-rich, altered pyroclastic rocks.

Much of the literature dealing with clay mineral genesis from volcanic materials has concentrated on basalt weathering in tropical environments (e.g., Eswaran, 1979; Eswaran and DeConinck, 1971; Siefferman and Milliot, 1969) or on the alteration of tephra (Kirkman, 1981; Dudas and Harward, 1975; Askenasy et al., 1973). These studies have shown that allophane, halloysite, kaolinite, and gibbsite are the dominant secondary minerals produced by weathering of such materials. Smectite has also been noted as an intermediate product or as a dominant secondary phase, depending on microenvironmental conditions, and mineral

transformations during near-surface rock weathering appear to be largely determined by soil microenvironmental factors with large-scale climatic factors acting as modifiers (Eswaran and DeConinck, 1971).

Genetic studies of the clay minerals in the soils of Oregon's Western Cascades are complicated by the great heterogeneity of soil parent materials. Steep slopes, high annual precipitation, short-range lithologic variability, and soil mass movement have resulted in complex volcanic colluvial deposits. The colluvium contains a mixture of basaltic and andesitic clasts, ignimbrite, altered pyroclastic materials, clayey weathering products, and Quaternary tephras. This paper describes the weathering of andesitic clasts in soils of colluvial origin in the Western Cascade Range of Oregon, characterizes the alteration products of the primary minerals in the andesites, and relates clay genesis to soil microenvironment.

MATERIALS AND METHODS

The study area is located in the Middle Santiam River drainage in the tributary drainage of Pyramid Creek (SW¼, NW¼, Sec. 19, T12S, R6E along Road 1234, at site MS-P-one of Taskey (1978)). The area receives on average 2000–2200 mm precipitation annually and has an average annual temperature of 10.3°C (Johnsgard, 1963). Deeply altered pyroclastic rocks of the Little Butte Volcanics underlie the watershed at intermediate elevations (Peck et al., 1964). The Sardine Formation, which consists primarily of basaltic and andesitic lava flows, outcrops at higher elevations. The soils at the sample site formed in colluvium containing subangular to subrounded basaltic and andesitic cobbles which overlies decomposed ash flow tuff. Varying amounts of volcanic ash are also

present in the soil. Taskey et al. (1978) found the bulk-soil clay mineralogy of the colluvium at this location to be dominated by hydrated halloysite and noncrystalline aluminosilicate gel, whereas the underlying ignimbrite is characterized by smectite alteration. The smectite-rich, altered ignimbrite supports a perched water table through much of the year, resulting in wet soils, even though the slope of the study area is near 70%.

Andesitic cobbles in various stages of decomposition were sampled from the A horizon of a wet, unstable soil (site MS-P-one f, Taskey, 1978) and sealed in plastic bags. The consistence of field-moist cobbles ranged from extremely firm to extremely hard, and the cobbles could readily be removed from the soil without breakage or loss of material. The andesite cobbles were subsampled while in field moist condition for clay mineral analysis after carefully removing adhering soil material. Subsamples were obtained by cutting or breaking off a portion of the rock, followed by gentle grinding of the rock fragments with a diamonite mortar and pestle. The ground material was dispersed in distilled water with agitation from a milkshake blender equipped with a rubber policeman instead of shearing blades. The <10-μm and clay (<2-μm) fractions were separated by centrifugation. The separates were saturated with Mg using 1 N $MgCl_2$ and freed of excess salt by three washings with distilled water. Subsamples of the Mg-saturated clay were saved in a moist state for transmission electron microscope (TEM) and differential thermal analysis (DTA) characterization. Portions of the Mg-saturated separates were used for the preparation of oriented clay films for X-ray diffraction (XRD) analysis using the paste method (Theisen and Harward, 1962). The remaining material was then saturated with K using 1 N KCl and distilled

water washing. Slides of this material were prepared for XRD analysis. The characterization treatments used for clay mineral identification were those prescribed by Harward et al. (1969) and Carstea et al. (1970).

TEM analysis of the <2-μm fraction was performed using a Philips EM 300 operated at 80-100 kV and 7 μa. A liquid nitrogen decontamination device was employed to help minimize possible sources of contamination. Samples were prepared by dropping a dilute clay suspension onto Formar-coated copper grids. Exposure of specimens to the electron beam was held to a minimum to avoid adverse effects of specimen-beam interaction (Jones and Uehara, 1973). DTA analyses of Mg-saturated clays equilibrated at 54% R.H. were done using a DuPont Model 900 Differential Thermal Analyzer.

The remaining undisturbed cobble material was further characterized by petrographic and scanning electron microscope (SEM) examination. Thin sections for petrographic study were prepared by impregnating slabs of air-dried cobbles with a polyester resin and sectioning by standard techniques. Descriptive terminology used in this study was that suggested by Stoops et al. (1979) for rock weathering and by Brewer (1976). Fracture surfaces of andesitic fragments for SEM observation were mounted on brass stubs and sputter coated with gold in a vacuum evaporator. A JEOL 35 or an International Scientific Instruments mini-SEM was used to analyze the specimens. The JEOL microscope was equipped with a Princeton Gamma Tech energy-dispersive X-ray elemental analyzer which permitted qualitative analyses of specimens. Elemental analyses, though subject to errors due to specimen topography and electron-capture volume, provided additional clues to aid in mineral identification by SEM. This combination

of thin section and SEM observations has proven extremely useful in studying the alteration of primary minerals in soil materials (Eswaran, 1979; Eswaran and DeConinck, 1971).

RESULTS AND DISCUSSION

The samples studied are weathered pilotaxitic porphyritic to glomeroporphyritic andesites (i.e., lath-shaped microlites show sub-parallel flow orientation and phenocrysts are sometimes gathered together in distinct clumps, Williams et al., 1954, p. 19, 23) with megaphenocrysts of plagioclase (An_{55-60}) and augite. None are completely saprolitic; i.e., they did not consist completely of pseudomorphic secondary minerals preserving original rock fabric (Eswaran and Wong Chaw Bin, 1978a). Individual cobbles contain primary phenocrysts showing a wide range of alteration, which provides an excellent opportunity to follow the weathering sequence from its initial through its more advanced stages.

Unweathered plagioclase phenocrysts are euhedral with distinctive albite and pericline twinning. They range in length from 0.3 to 4 mm, with an average size of 1.5 mm. The plagioclase crystals show normal and oscillatory zoning, having cores of labradorite (An_{55-60}) and rims of andesine composition (An_{45-50}). The final stage of feldspar crystallization produced microlites of andesine having moderate flow orientation. Augite phenocrysts are euhedral to subhedral in form and 0.5-2.0 mm in size. The groundmass consists of feldspar microlites, interstitial glass, and accessory magnetite.

Andesite alteration progresses from the rock's surface inward along transmineral porosity. Transmineral pores traverse the rock without following grain boundaries and may develop upon cooling of the parent

lavas or reflect tectonic shattering (Stoops et al., 1979). Thin section observation suggests that several processes are associated with the initial phase of alteration. The interstitial glass becomes discolored and shows the development of weakly anisotropic granular forms. This change is usually associated with pale, yellowish brown staining and reduced birefringence of feldspar microlites. Such groundmass alteration is most pronounced bordering transmineral pores and decreases rapidly away from the pore. Initial phenocryst alteration consists of pellicular congruent dissolution of augite and weak surface etching of plagioclase.

Plate 12a illustrates rock weathering which is associated with a transmineral pore system. The upper right corner of the micrograph shows a large plagioclase phenocryst bordered by a pore which trends diagonally across the photograph to the lower left corner. This pore intersects moldic porosity produced by complete congruent dissolution of augite. Hyaline material is present along portions of this porosity network. The cross polar view (Plate 12b) shows very fine grained, highly birefringent material bordering the intermineral pore along the plagioclase phenocryst, as well as thin, discontinuous clay films on the moldic pore walls. At this magnification it is difficult to tell whether these clay films represent authigenic accumulation of clay or infiltration of pedogenic clay into the porous andesite clasts, but subsequent observations show that such features are authigenic. The groundmass bordering the pore system shows the presence of weakly anisotropic granular forms in the interstitial glass and microlites with lowered birefringence, suggesting alteration of glass to clay. Phenocryst alteration in this micrograph ranges from slight dotted alteration of plagioclase to complete, pellicular congruent dissolution of augite.

Plate 12. (a) Photomicrograph showing dotted alteration of plagioclase, pellicular alteration of augite (upper left) and transmineral porosity; (b) X-polar view of Plate 12(a) showing cutanic material and smectite formation from feldspar; (c) Scanning electron micrograph of initial dissolution of feldspar; (d) Photomicrograph illustrating cavernous alteration of plagioclase showing andesine rim perforated by intramineral porosity and smectite pseudomorphs after plagioclase zonation; (e, f) Advanced dissolution of feldspar shown in scanning electron micrographs.

Plate 12

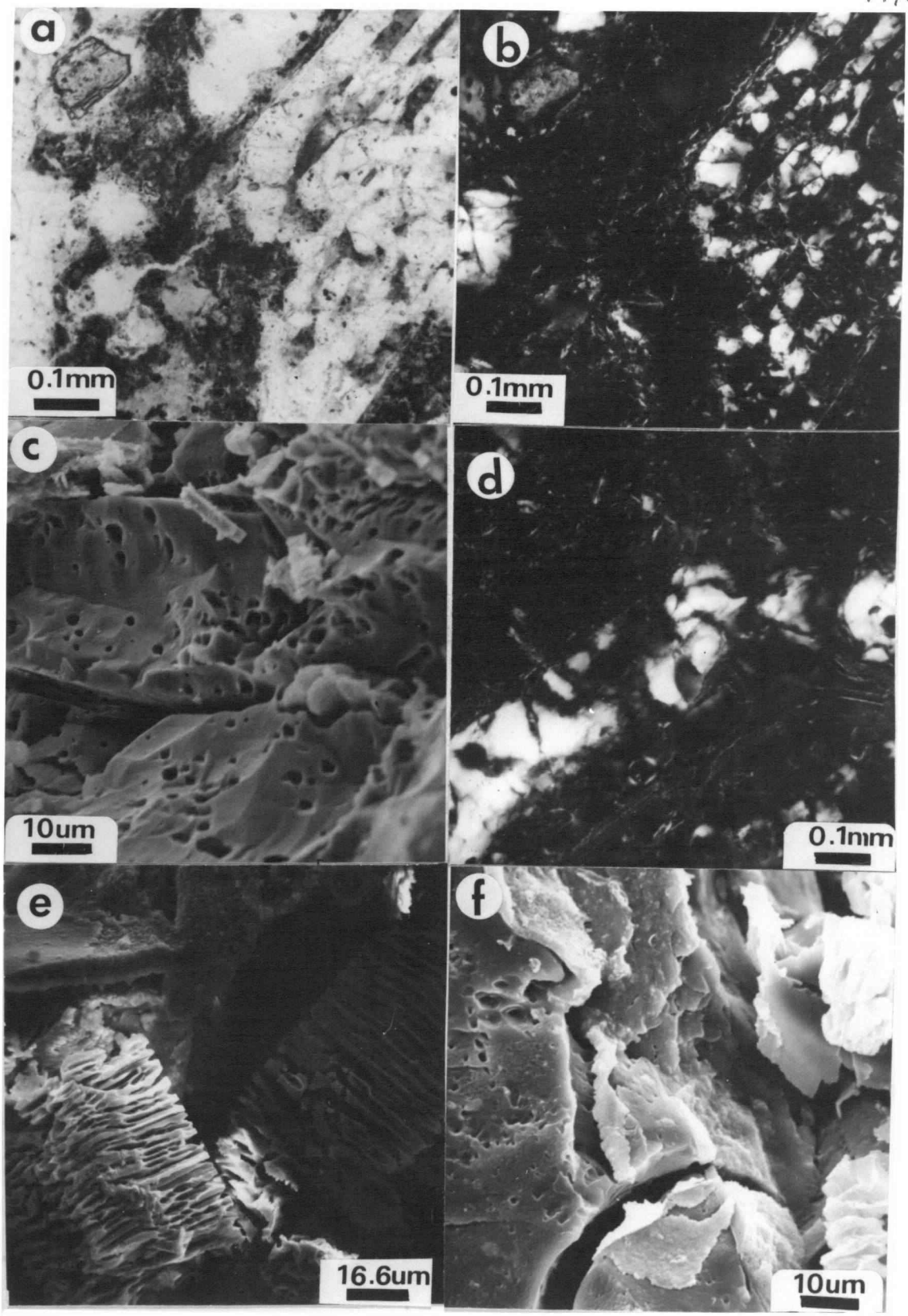

Plagioclase alteration begins with surface etching that eventually leads to the formation of intramineral porosity as the crystals are penetrated by a network of hairline cracks (Plates 12a, 12b, 12c, 12f). Propagation of these pores probably occurs along crystal dislocations or compositional zonations (Berner and Holdren, 1977; Wilson, 1975). Once the intramineral porosity penetrates the andesine-rich surface zone, complex dotted alteration of the labradoritic core zones occurs rapidly, resulting from the alteration of discrete zones of the host material (Stoops et al., 1979). Altering zones go through an isotropic, probably noncrystalline, phase prior to mineral dissolution and development of porosity, similar to the alteration sequence noted by Eswaran (1979). The resultant intramineral pores may or may not show lining with birefringent hyaline material. In more advanced stages of plagioclase alteration, the intramineral pores have broadened and coalesced to form a complex cavernous alteration pattern (Plates 12d and 13d). Plate 12d shows a plagioclase phenocryst whose interior labradoritic zones are completely altered, leaving a porous andesine rim and a central core containing zones of pseudomorphic secondary clay after the original feldspar zonation. The andesine rim and microlites commonly persist through this stage of alteration, although they are honeycombed by the development of etch porosity (Plates 12d, 12e, 12f).

Augite alteration shows a strong relationship to the proximity of transmineral porosity. Where such porosity intercepts augite phenocrysts, strong to complete pellicular dissolution has occurred. This is probably favored by rapid fluid movement through large pores which may connect to the outside soil solution and facilitate removal of dissolved constituents. However, a neighboring pyroxene surrounded by altered matrix devoid of

obvious secondary porosity may show only slight pellicular alteration (Plates 12a and 13a). The alteration of interstitial glass to clay (Plate 13a), shown below to be smectite (Figure 12), may restrict fluid movement by plugging secondary porosity. While the dominant pattern of augite alteration is pellicular, some large phenocrysts, which appear to have been shattered, show irregular linear dissolution leading to the formation of randomly oriented residues.

The initial dissolution of augite produces an intricately etched surface of sharp pinnacles (Plates 13a, 13b). The surface is clear of adhering contaminants, supporting the conclusion that augite alters by congruent dissolution. Advanced dissolution produces an extremely delicate honeycombed fabric that reflects the crystal structure of the parent pyroxene (Plate 13c). Similar etch textures for augite were reported by Rahmani (1973) and were observed in altered basalts and sedimentary rocks (Glasmann, unpublished data). However, the SEM morphology of altered augite noted in this study differs markedly from the knobby, irregular surfaces illustrated by Eswaran (1979) for tropically weathered basalts. Eswaran found that noncrystalline surface coatings and pseudomorphic goethite were common alteration products of augite. The differences in alteration products and morphology between the two studies probably are due to differences in host rock geochemistry (tholeiitic basalt vs. calc-alkaline andesite) and soil microenvironment (very high precipitation and very warm vs. saturated conditions and cool). The year-round wetness of the Cascade Range site apparently has a pronounced influence on augite alteration, favoring congruent over incongruent dissolution. Congruent dissolution of pyroxene is favored in an environment where oxygen is limiting and the formation of protective

Plate 13. Scanning electron micrographs of andesite alteration: (a) Augite dissolution and unaltered feldspar microlites in matrix of smectite; (b, c) Congruent dissolution of augite: (d) Cavernous alteration of plagioclase showing convoluted sheets of smectite; (e) Higher magnification view of Plate 13d showing rectangular etch pits (upper left) and fibrous smectite sheets (center and lower right); (f) Initial stage of smectite formation on feldspar surface.

Plate 13

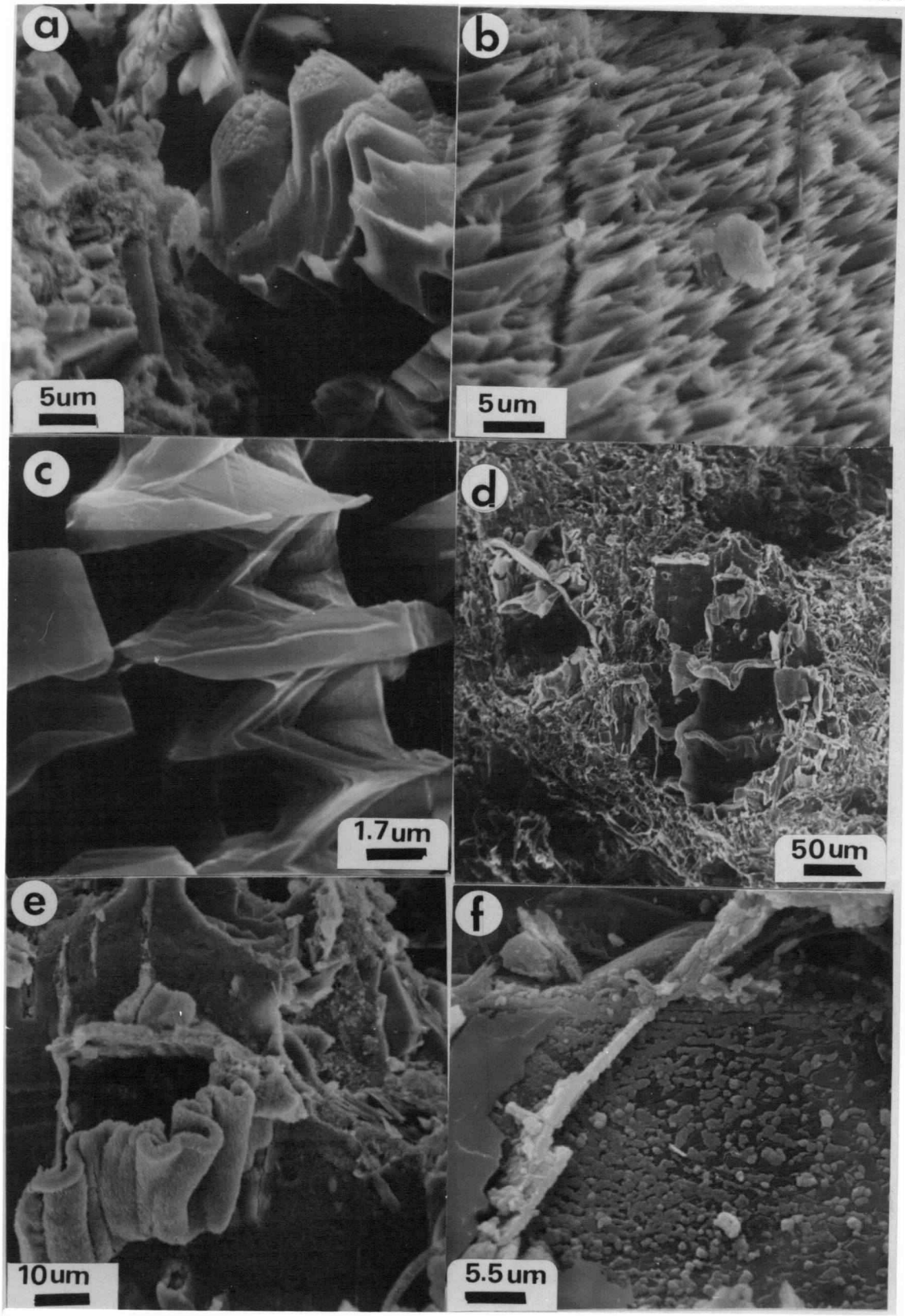

$Fe(OH)_3$ precipitates is hindered (Siever et al., 1979). Such an environment probably exists in the wet soils at the Pyramid Creek site.

The intermediate phase of andesite alteration is characterized by advanced phenocryst alteration and the precipitation of clay minerals within the secondary porosity network. Moldic secondary pores after augite (pores retaining the outline of the original phenocryst) are partially to completely filled with pale, yellowish brown to pale green fibrous clay. Feldspar phenocrysts show strong to complete complex cavernous alteration of labradoritic cores. Filling of internal cavernous voids by authigenic clay is incomplete, but this may be in part an artifact of thin section preparation. The extremely fine intramineral pores which cross the andesine rim and permit solution "mining" of the interior core restrict resin penetration during sample impregnation. Thus, it is possible that some of the pseudomorphic clay may be lost during thin section preparation. However, SEM observations suggest that secondary clay forms a delicate, complex, cross-linear alteration fabric which maintains high internal porosity (Plates 13d, 13e, and 14b). The clay in deformed intersecting sheets is probably produced by clay precipitation in intramineral pores which follow compositional zoning.

Close inspection of the clay films in secondary pores and channels reveals a two-stage development of authigenic clay. The first stage is characterized by the precipitation and growth of composite spherical forms on void walls or host grain surfaces (Plates 13f, 14a, 14b). The spheroids are about 1 μm in diameter and consist of a porous aggregate of much smaller particles (Plate 14a). The internal morphology of the spheroids consists of haphazard packing of extremely small plates, suggesting the possiblity of smectite (Wilson and Pittman, 1977).

Plate 14. Stages of smectite genesis in altered andesite: (a, b) Scanning electron micrographs showing initial formation of aggregate spheroids. (a) Spheroidal forms showing complex internal structure. (b) Development of sheet structure in smectite spheroids on grain surface. (c) Photomicrograph of fibrous smectite clay film lining a dissolution void showing multi-stage growth. Large plagioclase phenocryst on left. (d) Higher magnification of Plate 14c showing initial precipitation of granular smectite followed by fibrous growth. Void is in upper right corner. Growth has occurred from lower left to upper right, perpendicular to void wall. (e, f) Scanning electron micrographs of transformation of plagioclase to smectite, showing development of fibrous sheet structure.

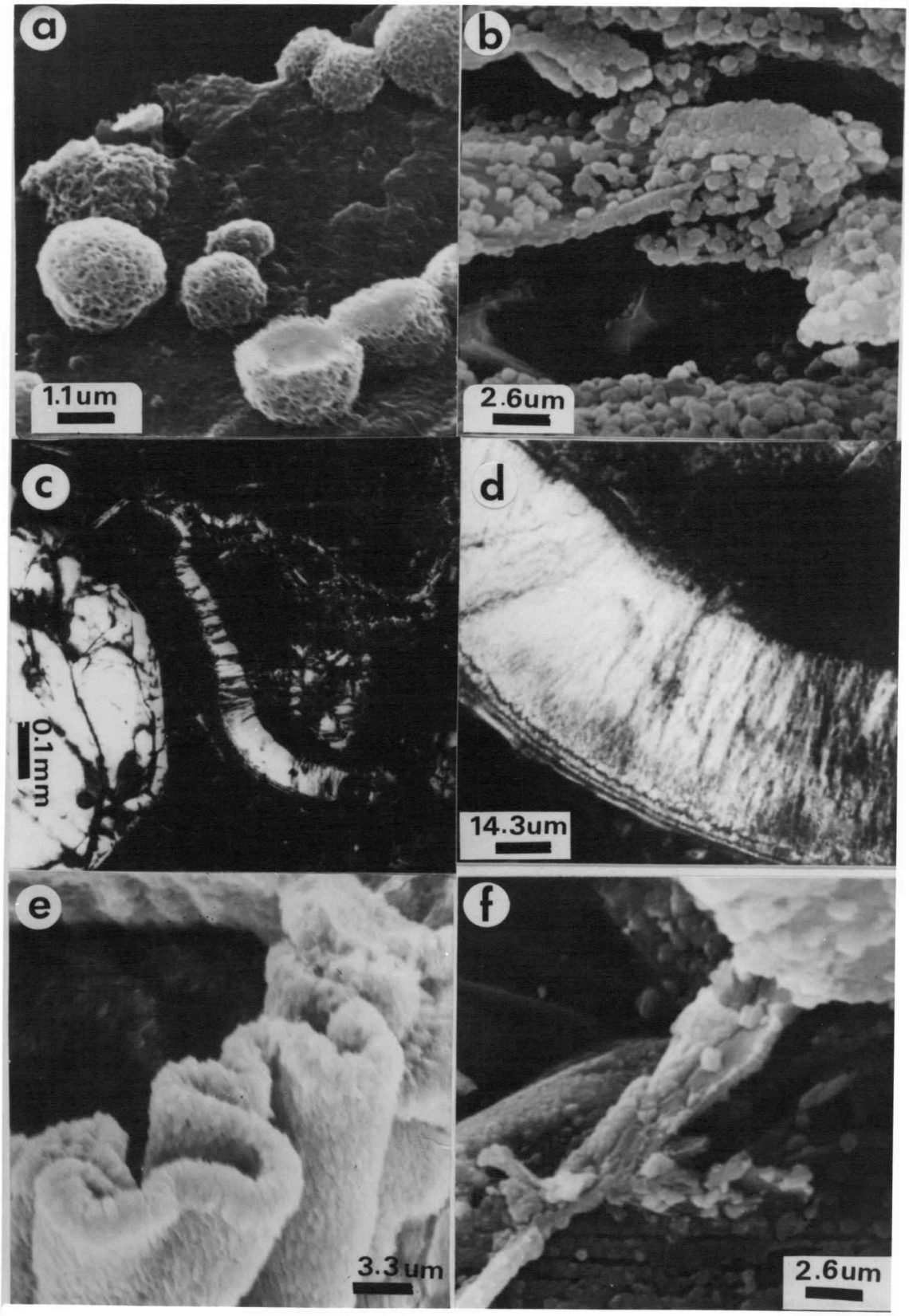
a
1.1um
b
2.6um
c
0.1mm
d
14.3um
e
3.3um
f
2.6um

Analyses by XRD and TEM (Figure 12 and Plate 15) confirm the presence of montmorillonite as the major authigenic phase of the weathered andesites. However, the occurrence of montmorillonite as spherical aggregates is heretofore unmentioned in the literature. Eswaran (1979) found similar spheroids in altered plagioclase which he termed "amorphous alumino-silicates". Eswaran's globular coatings were isotropic in thin section, in contrast to the anisotropic nature of the coatings observed in this study (Plates 12b, 14c, 14d). The aggregate spheroids probably grew from a "seed" precipitated onto a suitable substrate and then merged to form irregular sheet-like structures, representing the beginning of clay film formation (Plate 13f, upper right corner; Plate 14b). This initial stage of clay precipitation is sometimes difficult to recognize due to the very small size of the spheroids. Furthermore, they are weakly anisotropic unless organized into continuous sheets.

The second phase of clay authigenesis is characterized by pore filling by fibrous smectite. The two-phase sequence is illustrated in Plates 14c and 14d, which show a precipitation clay film partially filling a moldic dissolution pore. The clay film had at least three episodes of aggregate spheroid formation which led to the formation of continuous, overlapping sheets of clay displaying granular extinction (Plate 14d, lower left corner). Each sheet is about 1 μm thick, with the third layer showing a tendency towards fibrous growth habit. Following the precipitation of the aggregate spheroid sheets, more rapid growth of smectite occurred, producing interlocking cyrstals with fibrous growth habit which partially filled the void. The smectite fibers are oriented roughly perpendicular to void walls in contrast to the parallel orientation of pedologic clay films (or cutans, see Brewer, 1964, p. 206), and

commonly show convolute structure (Plates 13d, 13e, and 14e). Such convolution may be an artifact of sample preparation and reflects shrinkage of clay sheets on drying.

During advanced weathering, andesine microlites undergo extensive congruent dissolution and appear as delicate, honeycombed euhedral laths encased in a smectite matrix (Plate 12e). The absence of residual surface "armor" and the dominance of selective etching during feldspar alteration agrees with observations of Berner and Holdren (1977) and Wilson (1975). The alteration of plagioclase phenocrysts from the inside-out must be controlled by fluid movement through intramineral pores connecting the cavernous crystal interior to the outside environment. Fluid movement through such minute tortuous pores must be extremely slow, creating a very poorly drained microenvironment within the cavernous pore. Such a microenvironment favors the formation of smectite over other phyllosilicates (Borchardt, 1977).

None of the tubular forms of halloysite observed during plagioclase alteration in volcanic materials (Kirkman, 1981; Eswaran, 1979; Eswaran and DeConinck, 1971; Parham, 1969) or granites (Eswaran and Wong Chaw Bin, 1978c) were observed in this study. XRD analysis of altered andesites gave no indication of the presence of 1:1 phyllosilicates (Figures 12a, 12b) in either the <10-μm or clay fractions. XRD patterns characteristic of montmorillonite were obtained from the clay fraction. The possibility of halloysite is suggested in DTA patterns by an intermediate endotherm (Figure 12c), although such endotherms have also been reported for some smectites (MacKenzie, 1957). The low-temperature endotherm shows asymmetry characteristic of smectites saturated with divalent cations, and a weak high-temperature endotherm, at ∿860°C, further suggests smectite

Figure 11. (A) X-ray powder diffraction patterns of <2-μm fraction of altered andesite. Treatments: (a) Mg-saturation, 54% RH, (b) Mg-ethylene glycol, (c) Mg-glycerol, (d) K-saturation, 105°C, 0% RH, (e) K-saturation, 54% RH, (f) K-saturation, 300°C, 0% RH, (g) K-saturation, 550°C, 0% RH. (B) XRD of <10-μm fraction of altered andesite showing presence of smectite, augite, plagioclase. (a) Mg-saturation, 54% RH, (b) Mg-ethylene glycol. (C) Differential thermal analysis pattern of <2-μm fraction.

Figure 11

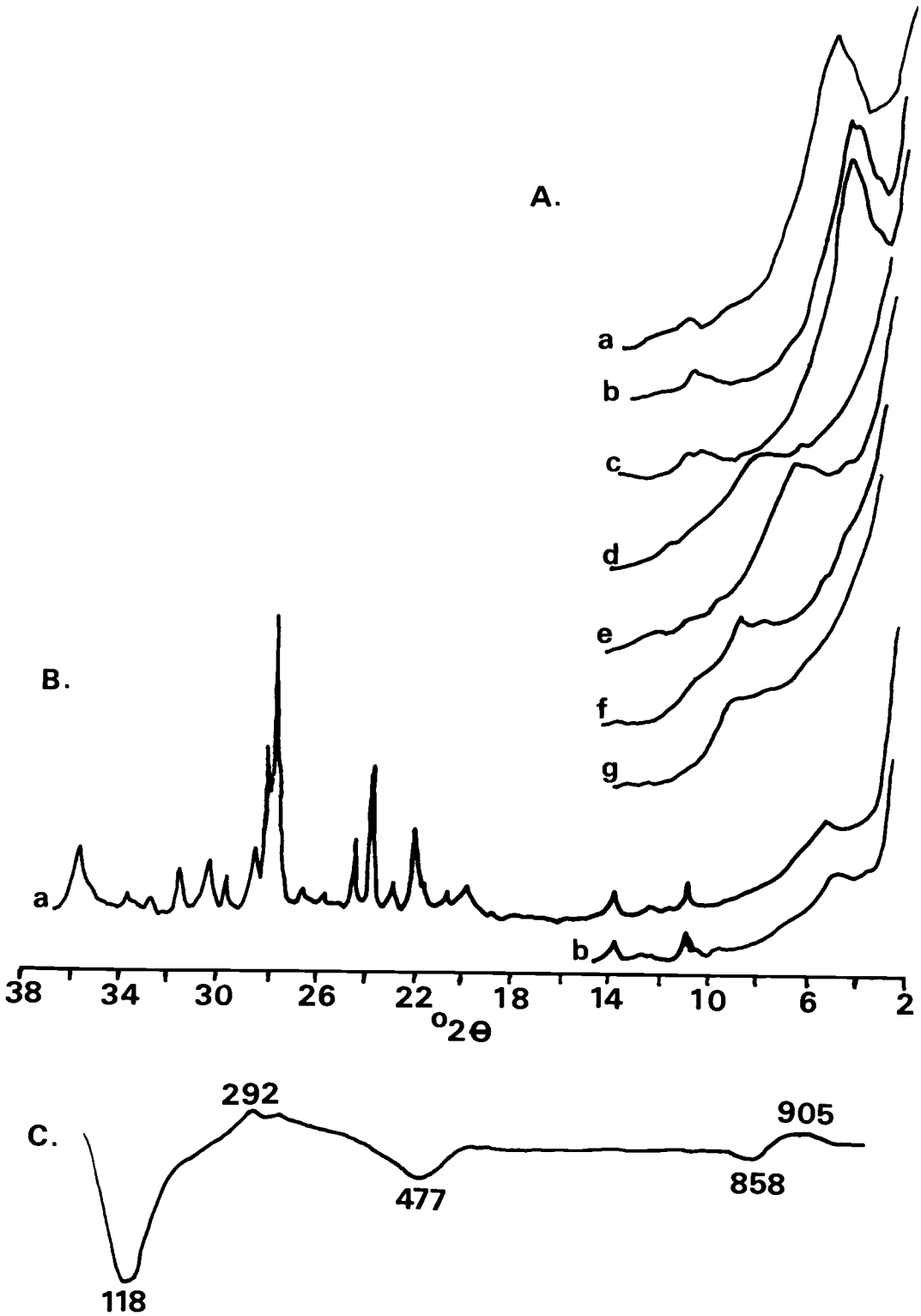

(Mackenzie, 1957). TEM provides the only positive indication of the presence of halloysite in the andesite samples. Trace amounts of spheroidal halloysite were observed (Plate 15c), although the mineralogy on the whole is dominated by smectite (Plates 15a and 15d). The halloysite spheres are much smaller (∿0.1 μm) than the aggregate spheroids observed by SEM (∿1 μm) and lack the complex floccular internal structure of the smectite bodies. The absence of halloysite XRD peaks is probably due to its occurrence in very small amounts and in very small particles. Delicate fragments of plagioclase (Plate 15b) probably reflect phenocrystic or microlitic fragments shattered during sample preparation.

Taskey et al. (1978) found hydrated halloysite and noncrystalline gel to be the dominant weathering products in upper horizons of wet colluvial soils in Oregon's Western Cascades. The occurrence of smectite in upper soil horizons was related to the incorporation of subsoil material from the Little Butte Volcanics into the colluvium. The predominant formation of smectite during alteration of andesitic cobbles in a wet soil from colluvium seems at first to contradict Taskey's observations (Taskey et al., 1978, Figures 3, 4). Several factors are probably responsible for the divergent mineralogy of the fine earth fraction vs. entrained, altered lithic fragments. First, the volcanic colluvium contains pyroclastic material in addition to clasts of andesite and basalt. The formation of hydrated halloysite and noncrystalline gel during alteration of tephra has been well documented (Kirkman, 1981; Dudas and Harward, 1975; Askenasy, 1973) and must be considered a likely source for the halloysite at Pyramid Creek. Second, differences in internal drainage between the soil material and the altered lithics create important differences in their respective chemical microenvironments.

Plate 15. Transmission electron micrograph of <2-μm fraction. (a) Montmorillonite. (b, d) Montmorillonite and plagioclase fragments. (c) Spheroidal halloysite and thin flakes of montmorillonite.

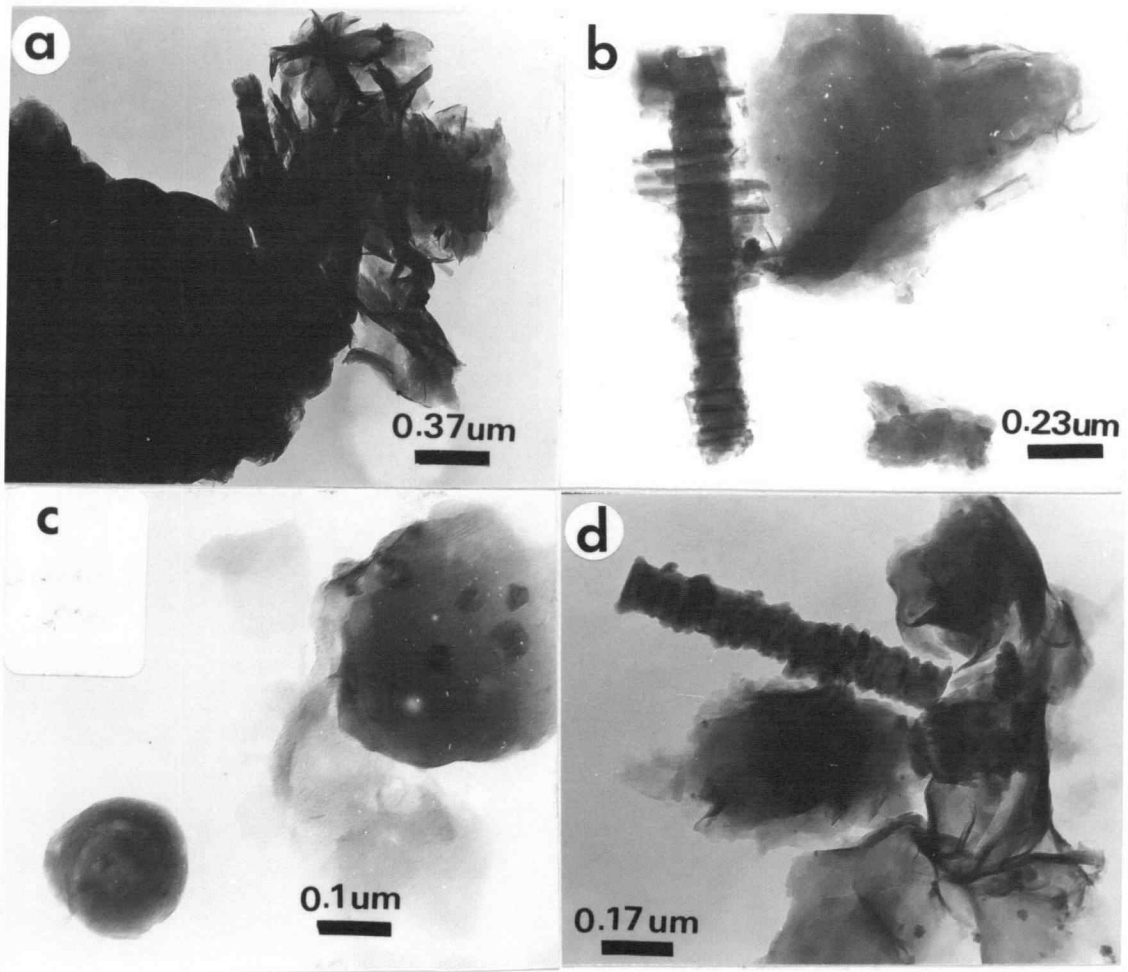
a
0.37um
b
0.23um
c
0.1um
d
0.17um

The weathered clasts contain different levels of microporosity which affect fluid movement between cobble and soil, as well as between individual weathering domains within the cobbles. Thus, stagnant conditions favoring retention of silica and cations probably exist on a microscale within the altering andesitic clasts, whereas the bulk soil lies in the framework of an overall leaching, though wet, environment. Smectite forms in the altering lithic fragments due to the favorable chemical microenvironment, whereas halloysite forms in the adjacent soil material. It may be possible that smectite is a precursor of the halloysite. As the cobbles decompose and alter to soil matrix, microdrainage conditions may change, causing silica and bases to be leached, favoring the transformation of smectite to halloysite. Halloysite has been observed in discrete zones in altered basaltic lithorelicts elsewhere in Oregon soils, although the initial mineral transformation of plagioclase produced smectite (Glasmann, unpublished data). This hypothesis requires further examination.

Taskey's methodology precluded the opportunity to study clay genesis on anything but a macroenvironmental scale which proved very useful in his broad study of clay mineral--landscape stability relationships. However, the present study shows that clay genesis in Western Cascade soils from colluvium is most closely tied to soil microenvironment, reaffirming conclusions reported in other recent studies of clay genesis (Gardner et al., 1981; Eswaran, 1979; Meliner and Velde, 1979; Eswaran and Wong Chaw Bin, 1978a, 1978b; Eswaran and DeConinck, 1971).

CONCLUSIONS

The study of andesite alteration in Oregon's Western Cascade Range noted the following mineralogical changes: (1) Augite alters by pellicular congruent dissolution producing moldic secondary porosity. This porosity is sequentially filled by precipitation of smectite. (2) Plagioclase phenocrysts alter initially by surface etching, leading to the development of microconduits through which dotted and complex cavernous alteration of crystal interiors is facilitated. Microlites alter by congruent dissolution. (3) Interstitial glass alters to smectite and may have a protective effect on crystal alteration by restricting fluid movement through the matrix. (4) Smectite genesis follows a two-stage sequence showing initial formation of aggregate spheroids on void walls followed by a later stage of fibrous smectite growth. The formation of smectite is favored by the restrictive drainage of the microenvironment of the altering andesitic clasts and the wet soil environment of the sample location. However, the bulk soil data (Taskey et al., 1978) did not show this effect.

EPILOGUE

The motivation for this study was found in the complex surface images of sand grains studied as part of another project (Glasmann and Kling, 1980). If quartz sands could show such complexity, yet be understood through study, then other soil components could also be probed to gain a broader understanding of soils as natural bodies. The first natural "bodies" to be studied were altered andesites (Chapter IV). Though simple enough to understand in thin section, SEM images required additional data to interpret the significance of authigenic forms. It was not until additional studies had been made of basalt and sandstone alteration that the clues to the micromorphologic puzzle began to emerge when similarities in modes of plagioclase and augite alteration between the various lithologies became apparent.

The alteration of primary minerals in soils and geologic deposits and the genesis of secondary mineral phases are determined by the nature of the weathering microenvironment. The great diversity of such microenvironments, which arises from a combination of geological, climatological, biological, hydrological, and other factors, results in the genesis of various solids or gels which are the basis of the "messy" real world of soils. Gel coatings are common in the western Oregon soils studied, forming thin films on cutans, on weathering mineral grains, cementing soil particles, and plugging voids. It is doubtful that the composition of such gels will ever be known, at least with present microanalytical techniques. Attempts were made to analyze such gels with an SEM EDX (Energy Dispersive X-ray spectrometer), but proved fruitless. The extremely small size and location of the gels in holes and as coatings makes such analyses impossible without interference from neighboring

materials. The gels are also unstable under prolonged electron beam exposure which results from the long counting times needed to chemically analyze weak signal emitters.

Much of the problem in relating soil solution chemical determinations to mineralogical processes in the soil arises from the influence of amorphous gels of unknown solubility and composition. Even with supposedly pure mineral systems, surface gel layers have been observed to form on mineral surfaces. There is a great need to study these amorphous materials by non-destructive analytical methods of the sort used in this study, to better understand fundamental soil properties important to soil management and land use. For example, aggregate stability could be studied microscopically and microchemically to try to gain a better understanding of the source of coherency. Plant-soil interactions, especially root-rhizosphere interactions, can be studied to better understand how plants modify their soil environment. Understanding the nature and characteristics of the soil solid and liquid components on a microscale will aid every aspect of soil science.

This study has been but a small effort to view the soil system as it really exists. It is hoped that the material presented will serve as a springboard to others who might seek to understand soils as a fundamental natural system.

REFERENCES CITED

American Public Health Association. 1976. Standard Methods for the Examination of Water and Waste Water. 14th ed. Washington, D.C. 1193 p.

Askenasy, P. E., J. B. Dixon, and T. R. McKee. 1973. Spheroidal halloysite in a Guatemalan soil. Soil Sci. Soc. Am. Proc. 37:799-803.

Baldwin, E. M. 1976. Geology of Oregon. Univ. Oregon Coop. Bookstore, Eugene, Oregon. 165 pp.

Baldwin, E. M. 1964. Geology of the Dallas and Valsetz quadrangles, Oregon. Oregon Dept. Geol. and Min. Ind. Bull. 35 (revised). 52 p.

Balster, C. A., and R. B. Parsons. 1969. Late Pleistocene stratigraphy, southern Willamette Valley, Oregon. Northwest Sci. 43:116-129.

Balster, C. A., and R. B. Parsons. 1968. Geomorphology and Soils, Willamette Valley, Oregon. Oregon Agric. Exp. Stn. Spec. Report no. 265. 31 pp.

Beckwith, R. S., and R. Reeve. 1963. Studies on soluble silica in soils. I. The sorption of silicic acid by soils and minerals. Aust. J. Soil Res. 1:157-168.

Berg, M. G., and E. H. Gardner. 1978. Methods of Soil Analysis Used in the Soil Testing Laboratory at Oregon State University. Oregon Agric. Exp. Stn. Spec. Report no. 321.

Berner, R. A., and G. R. Holdren, Jr. 1977. Mechanism of feldspar weathering: some observational evidence. Geology 5:369-372.

Borchardt, G. A. 1977. Montmorillonite and other smectite minerals. pp. 293-330. In J. B. Dixon and S. B. Weed (eds.) Minerals in Soil Environments. Soil Sci. Soc. Am., Madison, Wisconsin.

Brewer, R. 1976. Fabric and Mineral Analysis of Soils. Robert E. Krieger Pub. Co., Huntington, New York. 482 pp.

Bricker, O. P., A. E. Godfrey, and E. T. Cleaves. 1968. Mineral-water interaction during the chemical weathering of silicates. p. 128-142. In R. F. Gould (ed.) Trace Inorganics in Water, Adv. Chem. Series, 73.

Cady, J. C. 1960. Mineral occurrence in relation to soil profile differentiation. Int. Congr. Soil Sci. Trans. 7th (Madison, Wis.) 59:418-424.

Carstea, D. D., M. E. Harward, and E. G. Knox. 1970. Formation and stability of hydroxy-Mg interlayers in phyllosilicates. Clays & Clay Miner. 18:213-222.

Cocoran, R. G., and F. W. Libbey. 1956. Ferruginous bauxite deposits in the Salem Hills, Marion Co., Oregon. Oregon State Dept. Geol. Min. Ind. Bull. 46.

Coen, G. M., and R. W. Arnold. 1972. Clay mineral genesis of some New York Spodosols. Soil Sci. Soc. Am. Proc. 36:342-350.

Cromack, K., Jr., P. Sollins, W. C. Graustein, K. Speidel, A. W. Todd, G. Spycher, C. Y. Li, and R. L. Todd. 1979. Calcium oxalate accumulation and soil weathering in mats of the hypogeous fungus Hysterangium crassum. Soil Biol. Biochem. 11:463-468.

Curtin, D., and G. W. Smillie. 1981. Composition and origin of smectite in soils derived from basalt in Northern Ireland. Clays & Clay Miner. 29:277-284.

Davies, C. W. 1962. Ion Association. Butterworths, London.

Devore, G. W. 1959. The surface chemistry of feldspars as an influence on their decomposition products. p 26-41. In Proc. 6th Nat. Conf. Clays and Clay Minerals, Berkeley, Calif. Pergamon Press, London.

Dudas, M. J., and M. E. Harward. 1975. Weathering and authigenic halloysite in soil developed in Mazama ash. Soil Sci. Soc. Am. Proc. 39: 561-566.

Eswaran, H. 1979. The alteration of plagioclases and augites under differing pedo-environmental conditions. J. Soil Sci. 30:547-555.

Eswaran, H. 1972. Micromorphological indicators of pedogenesis in some tropical soils derived from basalts from Nicaragua. Geoderma 7:15-31.

Eswaran, H. 1968. Point-count analysis as applied to soil micromorphology. Pedologie 18:238-252.

Eswaran, H., and C. Sys. 1979. Argillic horizon in L.A.C. soils: formation and significance to classification. Pedologie 29:175-190.

Eswaran, H., A. van Wambeke, and F. H. Beinroth. 1979. A study of some highly weathered soils of Puerto Rico: micromorphological properties. Pedologie 29:139-162.

Eswaran, H., and Wong Chaw Bin. 1978a. A study of a deep weathering profile on granite in Peninsular Malaysia: I. Physiochemical and micromorphological properties. Soil Sci. Soc. Am. J. 42:144-149.

Eswaran, H., and Wong Chaw Bin. 1978b. A study of a deep weathering profile on granite in Peninsular Malaysia: II. Mineralogy of the clay, silt, and sand fractions. Soil Sci. Soc. Am. J. 42:149-153.

Eswaran, H., and Wong Chaw Bin. 1978c. A study of a deep weathering profile on granite in Peninsular Malaysia. III. Alteration of feldspars. Soil Sci. Soc. Am. J. 42:153-158.

Eswaran, H., and F. DeConinck. 1971. Clay mineral formations and transformations in basaltic soils in tropical environments. Pedologie 21:181-210.

Fisher, R. V. 1966. Rocks composed of volcanic fragments and their classification. Earth Sci. Rev. 1:287-298.

Flach, K. W., J. G. Cady, and W. D. Nettleton. 1968. Pedogenic alteration of highly weathered parent materials. Trans. Int. Congr. Soil Sci. 9th (Adelaide, Australia) IV:343-351.

Gardner, L. R., I. Kheoruenromne, and H. S. Chen. 1981. Geochemistry and mineralogy of an unusual diabase saprolite near Columbia, South Carolina. Clays & Clay Miner. 29:184-190.

Gelderman, F. W., and R. B. Parsons. 1972. Argixerolls on late Pleistocene surfaces in northwestern Oregon. Soil Sci. Soc. Am Proc. 36: 335-341.

Glasmann, J. R. 1982. Alteration of andesite in wet unstable soils of Oregon's Western Cascades. Clays & Clay Miner. (in press).

Glasmann, J. R., and G. H. Simonson. 1982a. Alteration of basalt in soils of western Oregon. Soil Sci. Soc. Am. J. (submitted).

Glasmann, J. R., and G. H. Simonson. 1982b. Clay genesis in soils developed from the late Eocene Spencer Formation. Oregon. Soil Sci. Soc. Am. J. (submitted).

Glasmann, J. R., and G. H. Simonson. 1982c. Interrelationships of clay mineralogy, soil solution chemistry, and landscape age in soils of western Oregon. Soil Sci. Soc. Am. J. (to be submitted)

Glasmann, J. R., and G. F. Kling. 1980. Origin of soil materials in foothill soils of Willamette Valley, Oregon. Soil Sci. Soc. Am. J. 44:123-130.

Glasmann, J. R., R. G. Brown, and G. F. Kling. 1980. Soil-geomorphic relationships in the western margin of the Willamette Valley, Oregon. Soil Sci. Soc. Am. J. 44:1045-1052.

Graustein, W. C., K. Cromack, Jr., and P. Sollins. 1977. Calcium oxalate: occurrence in soils and effect on nutrient and geochemical cycles. Science 198:1252-1254.

Hammermeister, D. 1978. Water and anion movement in selected soils of western Oregon. Unpub. Ph.D. Thesis, Oregon State University, Corvallis, Oregon.

Hansen, H. P. Postglacial forest succession, climate, and chronology in the Pacific Northwest. Trans. Am. Phil. Soc. 37:1-130.

Harr, R. D. 1977. Water flux in soil and subsoil on a steep forested slope. J. Hydrology 33:37-58.

Harward, M. E., Carstea, D. D., and Sayegh, A. H. 1969. Properties of vermiculites and smectities: Expansion and collapse. Clays & Clay Minerals 16:437-447.

Heusser, Calvin J. 1966. Pleistocene climatic variations in the western United States. In David T. Blumenstock (ed.) Pleistocene and post-Pleistocene climatic variations in the Pacific area: a symposium. Honolulu, Bishop Museum. 182 pp.

Hickman, J. S., M. L. Montgomery, and M. E. Harward. 1980. Diuron in runoff. Chpt. 13. In M. E. Harward, G. F. Kling, and J. D. Istok (eds.) Erosion, Sediment, and Water Quality in the High Winter Rainfall Zone of the Northwestern United States. Oregon Agric. Exp. Stn. Spec. Report no. 602.

Hoffmann, J., and J. Hower. 1979. Clay mineral assemblages as low grade metamorphic geothermometers: Application to the thrust faulted disturbed belt of Montana, U.S.A. p. 55-79. In P. A. Scholle and P. R. Schluger (eds) Aspects of Diagenesis. SEPM Spec. Pub. No. 26. Tulsa, Oklahoma.

Hoover, L. 1963. Geology of the Anlauf and Drain quadrangles, Douglas and Lane Counties, Oregon. U.S. Geol. Survey Bull. 1122-D.

Huang, P. M., and S. Y. Lee. 1969. Effects of drainage on weathering transformations of mineral colloids of some Canadian prairie soils. Proc. Int. Clay Conf., Tokyo, Japan. Paper 49, 1:541-551.

Johnsgard, G. A. 1963. Temperature and water balance for Oregon weather stations. Oregon Agric. Exp. Stn. Spec. Rep. no. 150. Corvallis, Oregon. 127 pp.

Jones, R. C., and G. Uehara. 1973. Amorphous coatings on mineral surfaces. Soil Sci. Soc. Am. Proc. 37:792-798.

Keller, W. D. 1970. Environmental aspects of clay minerals. J. Sediment. Petrol. 40:788-813.

Kilmer, V. S., and L. J. Alexander. 1949. Methods of making mineral analysis of soil. Soil Sci. 68:15-24.

Kirkman, J. H. 1981. Morphology and structure of halloysite in New Zealand tephras. Clays & Clay Minerals 29:1-9.

Kittrick, J. A. 1971. Montmorillonite equilibria and the weathering environment. Soil Sci. Soc. Am. Proc. 35:815-820.

Kittrick, J. A. 1969. Soil minerals in the Al_2O_3-SiO_2-H_2O system and a theory of their formation. Clays & Clay Miner. 17:157-167.

Knezevich, C. A. 1975. Soil Survey of Benton Co. Area, Oregon. USDA Soil Conserv. Serv., U.S. Government Printing Office, Washington, DC.

Lowrey, B. 1981. Hydrological parameters affecting overland flow in an agricultural watershed. Unpub. Ph.D. Thesis, Oregon State University, Corvallis, Oregon.

Lowrey, B., G. F. Kling, and J. A. Vomocil. 1981. Overland flow from sloping land: Effects of perched water tables and subsurface drains. Soil Sci. Soc. Am. J. (in press).

Mackenzie, R. C. (ed.) 1957. The Differential Thermal Investigation of Clays. Mineralogical Society, London. 456 pp.

MacLeod, N. S., and P. D. Snavely, Jr. 1973. Field trip no. 2. In J. D. Beaulieu (ed.) Geologic Field Trips in Northern Oregon and Southern Washington. Oregon Dept. Geol. Min. Ind. Bull. 77. Salem, Oregon.

McAleese, D. M., and W. A. Mitchell. 1958. Studies on the basaltic soils of Northern Ireland: IV. Mineralogical study of the clay separates (<2 μm). J. Soil Sci. 9:76-80.

Melinier, A., and B. Velde. 1979. Weathering mineral facies in altered granites: The importance of local small-scalequilibria. Mineral. Mag. 43:261-268.

Miller, W. R., and J. I. Drever. 1977. Chemical weathering and related controls on surface water chemistry in the Absaroka Mountains, Wyoming. Geochim. Cosmochim. Acta 41:1693-1702.

Mubarak, A., and R. A. Olsen. 1976. An improved technique for measuring soil pH. Soil Sci. Soc. Am. J. 40:880-882.

Paeth, R. C., M. E. Harward, E. G. Knox, and C. T. Dyrness. 1971. Factors affecting mass movement of four soils in the Western Cascades of Oregon. Soil Sci. Soc. Am Proc. 35:943-947.

Parham, W. E. 1969. Halloysite-rich tropical weathering products of Hong Kong. p. 403-416. In L. Heller (ed.) Vol. 1. Proc. Int. Clay Conf., Tokyo, Japan, 1969. Israel Univ. Press, Jerusalem.

Parsons, R. B., C. A. Balster, and A. O. Ness. 1970. Soil development and geomorphic surfaces, Willamette Valley, Oregon. Soil Sci. Soc. Am. Proc. 34:485-491.

Peck, D. L., A. B. Griggs, H. G. Schlicker, F. G. Wells, and H. M. Dole. 1964. Geology of the central and northern parts of the Western Cascade Range in Oregon. U.S. Geol. Surv. Prof. Pap. 449. 56 pp.

Pittman, E. D. 1972. Diagenesis of quartz in sandstone as revealed by scanning electron microscopy. J. Sediment. Petrol. 42:507-519.

Rahe, T. M. 1978. Movement of labeled Escherichia coli through western Oregon hillslope soils under conditions of saturated flow. Unpub. M.S. Thesis, Oregon State University, Corvallis, Oregon.

Rahmani, R. A. 1973. Grain surface etching features of some heavy minerals. J. Sed. Petrol. 43:882-888.

Reckendorf, F. F., and R. B. Parsons. 1966. Soil development over a hearth in Willamette Valley, Oregon. Northwest Sci. 40:46-55.

Rich, C. I. 1968. Hydroxy interlayers in expansible layer silicates. Clays & Clay Miner. 16:15-30.

Richards, S. J., L. S. Willardson, S. Davis, and J. R. Spencer. 1973. Tensiometers use in shallow ground-water studies. J. Irrig. Drain. Div., ASCE 99:457-464.

Rodgers, G. P., and H. D. Holland. 1979. Weathering products within microcracks in feldspars. Geology 7:278-280.

Schlicker, H. G. 1962. The occurrence of Spencer sandstone in the Yamhill Quadrangle. ORE Bin. 24(11):173-181.

Schwertmann, U., and R. M. Taylor. 1977. Iron oxides. p. 145-180. In J. B. Dixon and S. B. Weed (eds.) Minerals in Soil Environments. Soil Sci. Soc. Am. Pub., Madison, Wisc.

Sevink, J., and J. M. Verstraten. 1978. Neoformation of montmorillonite by post-depositional subsurface weathering in a slope deposit in central France. Earth Surf. Processes 3:23-29.

Siefferman, G., and G. Milliot. 1969. Equatorial and tropical weathering of recent basalts from Cameroun: allophane, halloysite, meta-halloysite, kaolinite, and gibbsite. p. 417-430. In L. Heller (ed.) Vol. 1, Proc. Int. Clay Conf., Tokyo, Japan, 1969. Israel Univ. Press, Jerusalem.

Siever, R., and N. Woodford. 1979. Dissolution kinetics and the weathering of mafic minerals. Geochim. Cosmochim. Acta 43:717-724.

Silverman, M. P., and E. F. Munoz. 1970. Fungal attack on rock: solubilization and altered infra-red spectra. Science 169:985-987.

Simmons, F. W., Jr. 1980. Nitrogen and phosphorus in runoff. Ch. 12. In M. E. Harward, G. F. Kling, and J. D. Istok (eds.) Erosion, Sediment, and Water Quality in the High Winter Rainfall Zone of the Northwestern United States. Oregon Agric. Exp. Stn. Spec. Report no. 602.

Singer, M., F. C. Ugolini, and J. Zachara. 1978. In situ study of podsolization on tephra and bedrock. Soil Sci. Soc. Am. J. 42:105-111.

Smith, J. 1957. A mineralogical study of weathering and soil formation from olivine basalt in Northern Ireland. J. Soil Sci. 8:225-239.

Snavely, P. D., Jr., N. S. MacLeod, and W. W. Rau. 1969. Geology of the Newport area, Oregon. The Ore Bin 31(2,3):25-71.

Snavely, P. D., Jr., N. S. MacLeod, and H. C. Wagner. 1968. Tholeiitic and alkalic basalts of the Eocene Siletz River Volcanics, Oregon Coast Range. Am. J. Sci. 266:454-481.

Stoops, G., H.-J. Altemüeller, F. B. A. Bisdom, J. Delvigne, V. V. Dobrovolsky, E. a. Fitzpatrick, G. Paneque, and J. Sleeman. 1979. Guidelines for description of mineral alteration in soil micromorphology. Pedologie 29:121-135.

Stumm, W., and J. J. Morgan. 1980. Aquatic Chemistry. Wiley-Interscience, New York.

Swanston, D. N., and F. J. Swanson. 1976. Timber harvesting, mass erosion, and steepland forest geomorphology in the Pacific Northwest. p. 199-221. In D. R. Coates (ed.) Geomorphology and Engineering. Dowden, Hutchinson, and Ross, Inc., Straoudsburg, Pennsylvania.

Tarzi, J. C., and R. Protz. 1978. Characterization of morphological features of soil micas using scanning electron microscopy. Clays & Clay Miner. 26:352-360.

Taskey, R. D. 1978. Relationships of clay mineralogy to landscape stability in western Oregon. Ph.D. Thesis, Oregon State University. Univ. Microfilms, Ann Arbor, Mich. (Mic. No. 7811993). (Diss. Abstr. 39:631). 223 pp.

Taskey, R. D., M. E. Harward, and C. T. Youngberg. 1978. Relationship of clay mineralogy to landscape stability.· p. 140-162. In C. T. Youngberg (ed) Forest Soils and Land Use. Proc. 5th North American Forest Soils Conf., Ft. Collins, Colo. Colorado State University, Ft. Collins, Colorado.

Theissen, A. A., and M. E. Harward. 1962. A paste method for preparation of slides for clay mineral identification by X-ray diffraction. Soil Sci. Soc. Am. Proc. 26:90-91.

Vokes, H. E., D. A. Myers, and L. Hoover. 1954. Geology of the west-central border area of the Willamette Valley, Oregon. USGS Oil and Gas Invest. Map OM 110.

Wada, K., T. Henmi, N. Yoshinaga, and S. H. Patterson. 1972. Imogolite and allophane formed in saprolite of basalt on Maui, Hawaii. Clays & Clay Miner. 20:375-380.

Weaver, R. M., M. L. Mackson, and J. K. Syers. 1971. Magnesium and silicon activities in matrix solutions of montmorillonite-containing soils in relation to clay mineral stability. Soil Sci. Soc. Am. Proc. 35:823-830.

Williams, H., F. J. Turner, and C. M. Gilbert. 1954. Petrography: An introduction to the study of rocks in thin sections. W. H. Freeman, San Francisco, California. 406 pp.

Wilson, M. D., and E. D. Pittman. 1977. Authigenic clays in sandstones: recognition and influence on reservoir properties and paleoenvironmental analysis. J. Sed. Petrol. 47:3-31.

Wilson, M. J. 1975. Chemical weathering of some primary rock-forming minerals. Soil Sci. 119:349-355.

Youngberg, C. T., M. E. Harward, G. H. Simonson, D. Rai, P. C. Klingeman, D. W. Larson, H. K. Phinney, and J. R. Bell. 1971. Hills Creek Reservoir turbidity study. Water Resources Research Institute Pub. WRRI-14, Dec. 1971, 35-51.